

Lyapunov-Based Graph Neural Networks for Adaptive Control of Multi-Agent Systems

Brandon C. Fallin, Cristian F. Nino, Omkar Sudhir Patil, Zachary I. Bell, and Warren E. Dixon

Abstract—Graph neural networks (GNNs) have a message-passing framework in which vector messages are exchanged between graph nodes and updated using feedforward layers. The inclusion of distributed message-passing in the GNN architecture makes them ideally suited for distributed control and coordination tasks. Existing results develop GNN-based controllers to address a variety of multi-agent control problems while compensating for modeling uncertainties in the systems. However, these results use GNNs that are pre-trained offline. This paper provides the first result on GNNs with stability-driven online weight updates to address the multi-agent target tracking problem. Specifically, new Lyapunov-based distributed GNN and graph attention network (GAT)-based controllers are developed to adaptively estimate unknown target dynamics and address the second-order target tracking problem. A Lyapunov-based stability analysis is provided to guarantee exponential convergence of the target state estimates and agent states to a neighborhood of the target state. Numerical simulations show a 20.8% and 48.1% position tracking error performance improvement by the GNN and GAT architectures over a baseline DNN architecture, respectively.

Index Terms—Graph neural networks, multi-agent systems, nonlinear control systems

I. INTRODUCTION

MULTI-agent systems often operate in uncertain environments which may include unknown, heterogeneous agent dynamics or unknown disturbances. To address these uncertainties, traditional machine learning approaches train neural networks (NNs) offline by minimizing a loss function over a pre-collected dataset and deploying the trained model to the system. However, the datasets required to train these models can be difficult to obtain, may not match the operating conditions of the environment, and do not adjust online to a mismatch between the pretrained data and actual data. Adaptive control can offer a powerful alternative by enabling real-time estimation of unknown model parameters with stability guarantees for the system.

Lyapunov-based adaptive update laws for NN-based controllers are well established for real-time learning for dynamical systems. Motivation exists to generalize such update laws

to online deep learning because of the improved approximation performance of deep NNs (DNNs) [1]. However, this generalization has been technically challenging because the unknown DNN weights are embedded in a nested cascade of nonlinear functions, preventing a structure that is suitable for Lyapunov-based analysis. The authors of [2] provided the first breakthrough to enable real-time learning methods for uncertain weights in all layers of DNNs by taking advantage of the compositional structure of the architecture. The Lyapunov-based DNN (Lb-DNN) approach developed in [2] for fully connected feedforward networks has been extended to incorporate a variety of deep learning architectures [3]–[9], enabling broad applications including: online approximation of unknown dynamics [10]–[13], herding agents with unknown interaction dynamics [14], control input determination using historical sensor data [15], safety constraint enforcement under uncertain dynamics [16], and development of end-to-end learning methods [17], [18].

Much of the multi-agent adaptive NN literature relies on single-layer NNs to compensate for unknown, heterogeneous agent dynamics [19]–[21]. Although NNs with a single hidden layer are capable of approximating general nonlinear functions over a compact domain, DNNs provide improved performance [1].

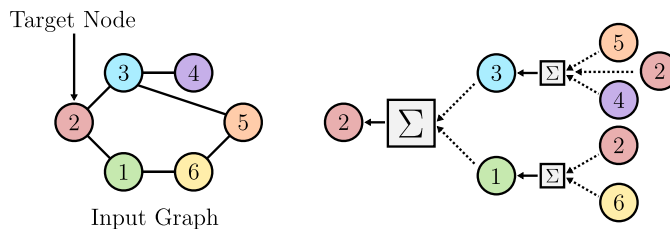


Fig. 1. Overview of the message-passing framework employed at each GNN layer in which nodes aggregate messages from their local neighborhoods. This figure shows a two-layer implementation of the message-passing model [22].

Traditional deep learning architectures have specific structural limitations: convolutional neural networks (CNNs) operate on grid-structured data like images, while recurrent neural networks (RNNs), long short-term memory (LSTM) blocks, and transformers process sequential data [22]–[24]. Initially conceived as a spatial analogue to RNNs [25], graph neural networks (GNNs) were developed to extend deep learning to graph-valued data.

As depicted in Fig. 1, GNNs operate through a message-passing framework where nodes exchange vector messages that are updated using feedforward NN layers. At every layer, the GNN aggregates outputs from each agent’s neighborhood,

Brandon C. Fallin, Cristian F. Nino, Omkar Sudhir Patil, and Warren E. Dixon are with the Department of Mechanical and Aerospace Engineering, University of Florida, Gainesville, FL 32611, USA. Email: {brandonfallin, cristian1928, patilomkarsudhir, wdixon}@ufl.edu.

Zachary I. Bell is with the Munitions Directorate, Air Force Research Laboratory, Eglin AFB, FL 32542 USA. Email: zachary.bell.10@us.af.mil.

This research is supported in part by AFOSR grant FA9550-19-1-0169. Any opinions, findings and conclusions or recommendations expressed in this material are those of the author(s) and do not necessarily reflect the views of the sponsoring agency.

multiplies by the layer weights, and produces an update using an elementwise activation function. The traditional GNN architecture can also be augmented with an attention mechanism to form the graph attention network (GAT) architecture [26]. The attention mechanism enables each node to rank the importance of messages from its neighbors. Leveraging attention is particularly useful in applications where some nodes are more informative than others [22]. Unlike traditional NNs, GNNs efficiently process and share information across networked agents, making them ideally suited for distributed tasks among multiple agents.

GNNs have been used extensively in the offline learning literature for a variety of applications, including (i) node classification, which aggregates information from neighboring nodes to sort graph nodes into distinct categories [27], (ii) graph classification, which combines local node features into global graph representations [28], and (iii) link prediction, which uses graph-valued data to determine likely future connections in settings like social media networks and online shopping platforms [29]. Only recently have GNNs received attention in the multi-agent literature, where they have been used to develop decentralized controllers [30], perform coordinated path planning [31], [32] and perimeter defense [33], facilitate deep reinforcement learning [34], and classify data from distributed sensor networks [35]. Moreover, GNNs have been used to solve the multi-robot decentralized tracking problem through an imitation learning framework [36]. In [36], the robots must jointly select actions to maximize target tracking performance with local communications. The GNN in [36] was trained on an action set of a state-of-the-art expert target tracking algorithm offline, and its performance was shown to generalize for large networks of robots. This method differs from the application of GNNs in our work, in which we do not require offline training, and update GNN parameters in real-time. These works show the promise of the GNN architecture when controlling complex, distributed systems. We build on these applications by providing stability guarantees for a new GNN-based adaptive controller.

Many results have leveraged feedforward NNs to solve the distributed target tracking problem, in which multiple agents are tasked with monitoring, engaging with, or intercepting a target [37]–[40]. However, none have used graph-theoretic learning methods to enhance the NN’s ability to approximate the target dynamics. Most notably, [40] considered the use of deep neural networks (DNNs) updated in real-time to achieve a target tracking objective with unknown target dynamics and partial state feedback. This objective was accomplished by developing an adaptive update law for each agent’s DNN and a distributed observer employing the DNN estimate to learn the unknown state of the target. Despite its contribution to distributed estimation capabilities of multi-agent systems, this work did not leverage the underlying communication topology of the graph to inform its DNN estimate. By not leveraging the underlying communication graph, the target tracking performance can be limited because of the lack of additional state information from network neighbors in the DNN forward pass.

In this work, we explore the application of a construc-

tively developed real-time, Lyapunov-based update law to the weights of the GNN architecture and evaluate its performance when applied to the target tracking problem. We note that the GNN can be applied to a variety of multi-agent control problems including average consensus with unknown agent dynamics, distributed state estimation of an uncertain target using networked agents, or decentralized sensor fusion for multi-agent systems. This work represents the first ever application of a GNN trained in real-time, where its weight adaptation law is derived from Lyapunov-based methods. We then augment the classical GNN architecture with attention, allowing each layer of the GNN to rank the importance of its neighbors updates. The attention augmentation results in the GAT architecture, and we develop a Lyapunov-based update law for the attention weights in real-time. These stability-driven adaptation laws allow for the developed architectures to adapt to system uncertainties without offline training requirements; however, offline training can be used to set the initial conditions for each agent’s weights. A Lyapunov-based stability analysis for the target tracking problem is performed to prove exponential convergence of the target state estimates and agent states to a neighborhood of the target state. New bounds are developed for the eigenvalues of the graph interaction matrix which allow gain conditions to be derived in a decentralized manner, without knowledge of the global communication topology. Additionally, a novel distributed weight adaptation law is developed which ensures exponential convergence of the GNN weights to a neighborhood of the ideal values.

The analytical results were empirically validated by numerical simulations which showed a 20.8% and a 48.1% position tracking error performance improvement by the GNN and GAT architectures over a baseline DNN architecture, respectively. This improvement was shown for a network of 6 agents with a path communication graph, where 3 agents were linked to the target. These results suggest that GNN and GAT architectures are particularly valuable for real-world distributed systems where achieving full network connectivity is challenging due to hardware constraints.

II. PRELIMINARIES

A. Notation

Let \mathbb{R} and \mathbb{Z} denote the sets of reals and integers, respectively. For $x \in \mathbb{R}$, let $\mathbb{R}_{\geq x} \triangleq [x, \infty)$ and $\mathbb{Z}_{\geq x} \triangleq \mathbb{R}_{\geq x} \cap \mathbb{Z}$. Let \mathbf{h}_i represent the i^{th} standard basis in \mathbb{R}^N , where the standard basis is made up of vectors that have one entry equal to 1 and the remaining $N - 1$ entries equal to 0. The $p \times p$ identity matrix, and the $p \times 1$ column vector of ones are denoted by I_p and $\mathbb{1}_p$, respectively. The $p \times 1$ column vector of zeros is denoted by $\mathbf{0}_p$. The enumeration operator $[\cdot]$ is defined as $[N] \triangleq \{1, 2, \dots, N\}$. A norm $\|\cdot\|$ is submultiplicative if for any two matrices $A \in \mathbb{R}^{m \times n}$ and $B \in \mathbb{R}^{n \times p}$, it satisfies $\|AB\| \leq \|A\|\|B\|$. The first partial derivative of a matrix $A \in \mathbb{R}^n$ with respect to a vector $B \in \mathbb{R}^m$ is expressed in column convention as $\nabla_B A \in \mathbb{R}^{n \times m}$. The Kronecker product of $A \in \mathbb{R}^{m \times n}$ and $B \in \mathbb{R}^{o \times p}$ is denoted by $A \otimes B \in \mathbb{R}^{m \circ \times n \circ}$. The concatenation operator of $A \in \mathbb{R}^{m \times n}$ and $B \in \mathbb{R}^{o \times n}$ is

denoted by $A \oplus B \in \mathbb{R}^{(m+o) \times n}$. Given a positive integer N and collection $\{x_i\}_{i \in [N]}$, let $[x_i]_{i \in [N]} \triangleq [x_1, x_2, \dots, x_N] \in \mathbb{R}^{m \times N}$ for $x_i \in \mathbb{R}^m$. For a set $\mathcal{S} \subset \mathbb{Z}$, let $x_{j:j \in \mathcal{S}}$ denote the tuple $(x_{k_1}, x_{k_2}, \dots, x_{k_{|\mathcal{S}|}})$, where $k_1 < k_2 < \dots < k_{|\mathcal{S}|}$ are the elements of \mathcal{S} in ascending order. The interior of a set \mathcal{S} is denoted by $\text{int}(\mathcal{S})$.

The Kronecker delta is denoted by $\delta_{a,b}$, where $\delta_{a,b} = 1$ if $a = b$ and $\delta_{a,b} = 0$ otherwise. For a set A and an input x , the indicator function is denoted by $\mathbf{1}_A(x)$, where $\mathbf{1}_A(x) = 1$ if $x \in A$, and $\mathbf{1}_A(x) = 0$ otherwise. For $x \in \mathbb{R}^m$, let $\text{diag}(\cdot)$ denote the diagonalization operator which assigns the i^{th} value of x to the i^{th} entry in an output $m \times m$ matrix for all $i \in [m]$. Similarly, let $\text{blkdiag}(\cdot)$ denote the block diagonalization operator. For $A \in \mathbb{R}^{m \times n}$ and $B \in \mathbb{R}^{o \times p}$,

$$\text{blkdiag}(A, B) \triangleq \begin{bmatrix} A & \mathbf{0}_{m \times p} \\ \mathbf{0}_{o \times n} & B \end{bmatrix},$$

where $\mathbf{0}_{m \times p} \in \mathbb{R}^{m \times p}$ is the $m \times p$ matrix of zeros and $\text{blkdiag}(A, B) \in \mathbb{R}^{(m+o) \times (n+p)}$. Given $A \in \mathbb{R}^{m \times n}$ with columns $[a_i]_{i \in [n]}^{\top} \subset \mathbb{R}^b$, $\text{vec}(A) \triangleq [a_1^{\top}, a_2^{\top}, \dots, a_n^{\top}]^{\top} \in \mathbb{R}^{mn}$. Given any $A \in \mathbb{R}^{m \times n}$, $B \in \mathbb{R}^{n \times o}$, $C \in \mathbb{R}^{o \times p}$, the vectorization operator satisfies the property

$$\text{vec}(ABC) = (C^{\top} \otimes A) \text{vec}(B). \quad (1)$$

Differentiating $\text{vec}(ABC)$ on both sides with respect to $\text{vec}(B)$ yields

$$\frac{\partial}{\partial \text{vec}(B)} \text{vec}(ABC) = (C^{\top} \otimes A). \quad (2)$$

Equations (1) and (2) are proved in [41, Proposition 7.1.9]. Additionally, for $A(x), B(x) \in \mathbb{R}^m$ such that $A(x), B(x)$ are differentiable,

$$\frac{\partial}{\partial x} (A(x) \oplus B(x)) = \left(\frac{\partial}{\partial x} A(x) \oplus \frac{\partial}{\partial x} B(x) \right). \quad (3)$$

Equation (3) is proved in the Appendix. Let $\text{proj}(a, b, c) : \mathbb{R}^n \times \mathbb{R}^n \times \mathbb{R} \rightarrow \mathbb{R}^n$ denote the projection operator defined in [42, Appendix E], where for a smooth, convex function $\mathcal{P} : \mathbb{R}^n \rightarrow \mathbb{R}$, a convex set $\Pi \triangleq \{b \in \mathbb{R}^n : \mathcal{P}(b) \leq c\}$, and a user-defined symmetric and positive definite gain matrix $\Gamma \in \mathbb{R}^{n \times n}$,

$$\text{proj}(a, b, c) \triangleq \begin{cases} a, & b \in \overset{\circ}{\Pi} \text{ or} \\ & \nabla_b \mathcal{P}^{\top} a \leq 0, \\ \left(I_n - \min \left\{ 1, \frac{\mathcal{P}(b)}{c} \right\} \right) & b \in \Pi \setminus \overset{\circ}{\Pi} \text{ and} \\ \cdot \Gamma \frac{\nabla_b \mathcal{P} \nabla_b \mathcal{P}^{\top}}{\nabla_b \mathcal{P}^{\top} \Gamma \nabla_b \mathcal{P}} a, & \nabla_b \mathcal{P}^{\top} a > 0. \end{cases} \quad (4)$$

B. Graphs

For $N \in \mathbb{Z}_{\geq 0}$, let $G \triangleq (V, E)$ be a static and undirected graph with node set $V \triangleq [N]$ and edge set $E \subseteq V \times V$. The edge $(i, j) \in E$ if and only if the node i can send information to node j . In this work, G is undirected, so $(i, j) \in E$ if and only if $(j, i) \in E$. Let $A \triangleq [a_{ij}] \in \mathbb{R}^{N \times N}$ denote the adjacency matrix of G , where $a_{ij} = \mathbf{1}_E(i, j)$ and $a_{ii} = 0$ for all $i \in V$. An undirected graph is connected if and only if

there exists a sequence of edges in E between any two nodes in V . The neighborhood of node i is denoted by \mathcal{N}_i , where $\mathcal{N}_i \triangleq \{j \in V : (j, i) \in E\}$. The augmented neighborhood of node i is denoted by $\tilde{\mathcal{N}}_i$, where $\tilde{\mathcal{N}}_i \triangleq \mathcal{N}_i \cup \{i\}$. We denote node i 's k -hop neighborhood as \mathcal{N}_i^k . Additionally, we denote the augmented k -hop neighborhood of node i as $\tilde{\mathcal{N}}_i^k \triangleq \{i\} \cup \mathcal{N}_i^k$. The degree matrix of G is denoted by $D \triangleq \text{diag}(A\mathbf{1})$. The Laplacian matrix of G is denoted by $\mathcal{L}_G \triangleq D - A \in \mathbb{R}^{N \times N}$. In this work, we focus on a class of communication networks where information flows through all nodes, which occurs when the graph G is connected.

The set of permutations on $[N]$ is denoted by S_N . For a graph G and a permutation S_N , we define the graph permutation operation as $p * G$, where $p \in S_N$. Two graphs are isomorphic if they represent the exact same graph structure, differing only in the ordering of their nodes in their corresponding adjacency matrices [22]. Formally, two graphs G_1 and G_2 are isomorphic if they have the same number of nodes and there exists a permutation such that $G_1 = p * G_2$ [43].

III. GRAPH NEURAL NETWORK ARCHITECTURES

In this section, we explore two deep GNN architectures. We begin with the traditional GNN. Then, we investigate the GAT architecture which incorporates attention weights to compare the importance of neighboring nodes' features at each layer. We derive closed-form expressions for the first partial derivatives of k -layer GNN and GAT architectures with respect to their weight vectors. Calculating the first partial derivative of each architecture with respect to their layer weights allows us to train the network in real-time using a novel Lyapunov-based weight update law.

A. Graph Neural Network

The GNN architecture employs a message-passing framework in which nodes exchange and update vector-valued messages using feedforward layers. These messages are the outputs of each GNN layer calculated at the node level. The GNN processes an input graph G with a set of node features to generate node embeddings, which are the outputs of the final GNN layer at each node. In this framework, each node's output in a layer is informed by its previous layer output and messages received from neighboring nodes. We use superscripts to denote layer-specific elements. For example, $W_i^{(j)}$ denotes the i^{th} node's weights for the j^{th} GNN layer. Subscripts indicate the specific node where an embedding or function is applied.

Let the activation function for the j^{th} GNN layer at node i be denoted by $\sigma^{(j)}(\cdot)$, where $\sigma(\cdot)$ is an element-wise smooth, bounded nonlinearity with bounded first and second derivatives appended with 1 to allow for biases such that for $x \in \mathbb{R}^m$, $\sigma(x) \triangleq [\sigma(x_0), \dots, \sigma(x_m), 1]^{\top}$. Let the output of layer j for node i of the GNN be denoted by $\phi_i^{(j)}$. Let the aggregation function for the j^{th} GNN layer at node i be denoted by $\sum_{m \in \mathcal{N}_i} \phi_m^{(j-1)}$. Additionally, let $d^{(j)}$ represent the number of features at the j^{th} layer of the GNN for $j = 0, \dots, k$, where j denotes the layer index. Let $d^{(\text{in})}$ denote the dimension of the GNN input at the base layer of each node. Let $d^{(\text{out})}$ denote

TABLE I
PARTIAL DERIVATIVES OF THE GNN AND GAT ARCHITECTURES WITH RESPECT TO $\text{vec}(W_i^{(j)})$ AND $a_i^{(j)}$, RESPECTIVELY. DEFINITIONS OF THE TERMS $\varphi_m^{(\ell)}$, $\Lambda_m^{(\ell)}$, AND $\zeta_m^{(\ell)}$ ARE ESTABLISHED IN TABLE III.

	GNN	GAT
Partial derivative of ϕ_i with respect to $\text{vec}(W_i^{(j)})$ for $j = 0, \dots, k-1$	$\frac{\partial \phi_i}{\partial \text{vec}(W_i^{(j)})} = W_i^{(k)\top} \varphi_i^{(k-1)}$	$\frac{\partial \phi_i}{\partial \text{vec}(W_i^{(j)})} = W_i^{(k)\top} \Lambda_i^{(k-1)}$
Partial derivative of ϕ_i with respect to $a_i^{(j)}$ for $j = 0, \dots, k-1$	N/A	$\frac{\partial \phi_i}{\partial a_i^{(j)}} = W_i^{(k)\top} \zeta_i^{(k-1)}$

the output dimension of the output layer of each node. Let $d^{(j)} = d^{(in)} + 1$ when $j = -1$ and $d^{(j)} = d^{(out)}$ when $j = k$. Then, the message-passing update for the j^{th} layer of the i^{th} node is expressed as

$$\phi_i^{(j)} = \sigma^{(j)} \left(W_i^{(j)\top} \sum_{m \in \mathcal{N}_i} \phi_m^{(j-1)} \right), \quad (5)$$

where $W_i^{(j)} \in \mathbb{R}^{(d^{(j-1)}+1) \times d^{(j)}}$. We modify the framework of the original GNN models proposed in [25] and [44] by allowing each node to have distinct layer weights. While synchronized layer weights at each node may be desirable for some applications, allowing each node to have distinct layer weights enables distributed weight updates at each node of the GNN. Next, we define the GNN architecture for an arbitrary number of layers.

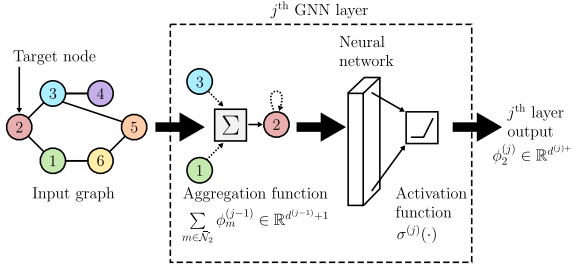


Fig. 2. Model of a single node's forward pass for the j^{th} layer of the GNN architecture. The output of the previous layer is aggregated over the neighborhood of the target node. The aggregated output is passed into a NN. The output of the NN is the input to the j^{th} layer activation function. The activation function also appends a bias. The activated output serves as an input for the next GNN layer [45].

Let $\bar{\kappa}_i$ denote the i^{th} node's input augmented with a bias term such that $\bar{\kappa}_i \triangleq [\kappa_i^\top, 1]^\top \in \mathbb{R}^{d^{(in)}+1}$. Let $\bar{\kappa} \triangleq [\bar{\kappa}_i]_{i \in V} \in \mathbb{R}^{(d^{(in)}+1) \times N}$. To distinguish between agent indices in cascading layers, we let $m^{(j)}$ denote an arbitrary index corresponding to the j^{th} layer, where $m^{(j)} \in V$. Then, we let $\mathbf{m}^{(j)}$ denote $m^{(j)} \in V$. Let $\phi^{(j)} \triangleq [\phi_i^{(j)}, \dots, \phi_n^{(j)}] = [\phi_i^{(j)}]_{\mathbf{m}^{(j)}} \in \mathbb{R}^{(d^{(j-1)}+1) \times N}$. Let $\bar{A} \in \mathbb{R}^{N \times N}$ represent the adjacency matrix with self loops, and $\bar{A}_i \in \mathbb{R}^{1 \times N}$ represent the i^{th} row of the adjacency matrix. The message-passing GNN architecture in (5) with k layers can be expressed as

$$\phi_i^{(j)} \triangleq \begin{cases} \sigma^{(j)}(W_i^{(j)\top} \bar{\kappa} \bar{A}_i^\top), & j = 0, \\ \sigma^{(j)}(W_i^{(j)\top} \phi^{(j-1)} \bar{A}_i^\top), & j = 1, \dots, k-1, \\ W_i^{(j)\top} \phi_i^{(j-1)}, & j = k. \end{cases} \quad (6)$$

Algorithm 1 GNN Message-Passing Algorithm

Input: Graph $G = (V, E)$, number of layers k , agent input $\kappa_i \in \mathbb{R}^{d^{(in)}}$ for all $i \in V$, adjacency matrix $A \in \mathbb{R}^{|V| \times |V|}$
Output: Agent GNN output $\phi_i^{(k)} \in \mathbb{R}^{d^{(out)}}$ for all $i \in V$
Initialize:
for each agent $i \in V$ **do** in parallel:
 Set $\bar{\kappa}_i = [\kappa_i^\top, 1]^\top$
 Initialize local dictionaries:
 D_i^A : Local adjacency vector
 D_i^O : Activated layer outputs
 D_i^W : Weight matrices
end for
1: **for** each layer $\ell = 0, \dots, k$ **do**:
2: **for** each agent $i \in V$ **do** in parallel:
3: **if** $\ell \neq k$:
4: Aggregate: $z_i^{(\ell)} = \phi^{(\ell-1)} \bar{A}_i^\top$
5: Update: $\phi_i^{(\ell)} = \sigma^{(\ell)}(W_i^{(\ell)\top} z_i^{(\ell)})$
6: **else**:
7: Update: $\phi_i^{(\ell)} = W_i^{(\ell)\top} \phi_i^{(\ell-1)}$
8: **end if**
9: Store in local dictionaries:
10: $D_i^O[(i, \ell)] = \phi_i^{(\ell)}$
11: $D_i^W[(i, \ell)] = W_i^{(\ell)}$
12: **end for**
13: **for** each agent $i \in V$ **do** in parallel:
14: **for** each neighbor $j \in \mathcal{N}_i$ **do**:
15: Exchange and update dictionaries:
16: $D_i^A \leftarrow D_i^A \cup D_j^A$
17: $D_i^O \leftarrow D_i^O \cup D_j^O$
18: $D_i^W \leftarrow D_i^W \cup D_j^W$
19: **end for**
20: **end for**
21: **end for**

For an input $y^{(j)} \in \mathbb{R}^m$, the partial derivative $\frac{\partial \sigma^{(j)}}{\partial y^{(j)}} : \mathbb{R}^{d^{(j)}} \rightarrow \mathbb{R}^{(d^{(j)}+1) \times d^{(j)}}$ of the activation function vector at the j^{th} layer with respect to its input is given as $[\sigma'^{(j)}(y_1) \mathbf{h}_1, \dots, \sigma'^{(j)}(y_{d^{(j)}}) \mathbf{h}_{d^{(j)}}]^\top \in \mathbb{R}^{(d^{(j)}+1) \times d^{(j)}}$, where \mathbf{h}_i is the i^{th} standard basis in $\mathbb{R}^{d^{(j)}}$ and $\mathbf{0}_{d^{(j)}}$ is the zero vector in $\mathbb{R}^{d^{(j)}}$. The algorithm for the forward pass of the message-passing GNN in (6) is given in Algorithm 1. In Algorithm 1, the \cup operator denotes dictionary merging, where unique values are appended to the existing dictionary.

The vector of weights for the GNN at node i is defined as

$\theta_i \in \mathbb{R}^{p_{\text{GNN}}}$, where

$$\theta_i \triangleq \left[\text{vec}(W_i^{(0)})^\top, \dots, \text{vec}(W_i^{(k)})^\top \right]^\top, \quad (7)$$

and $p_{\text{GNN}} \triangleq \sum_{j=0}^k (d^{(j)})(d^{(j-1)} + 1)$. We now compute the first partial derivative of the GNN architecture for node i in (6) with respect to (7).

Lemma 1. *For each node $i \in V$, the first partial derivative of the GNN architecture at node i in (6) with respect to (7) is*

$$\nabla_{\theta_i} \phi_i \triangleq \left[\frac{\partial \phi_i}{\partial \text{vec}(W_i^{(0)})}^\top, \dots, \frac{\partial \phi_i}{\partial \text{vec}(W_i^{(k)})}^\top \right]^\top, \quad (8)$$

where $\nabla_{\theta_i} \phi_i \in \mathbb{R}^{d^{(\text{out})} \times p_{\text{GNN}}}$ and the partial derivatives of ϕ_i with respect to $\text{vec}(W_i^{(\ell)})$ for all $\ell = 0, \dots, k$ is defined in Table I.

Proof: See the Appendix. ■

B. Graph Attention Network

We refine the capabilities of the GNN architecture in (6) by augmenting the input layer with an attention mechanism. Using attention, each node ranks the importance of messages from its neighbors. Adding attention to a GNN is a powerful strategy to increase its expressive abilities. Attention is especially useful in applications where some of a node's neighbors may be more informative than others [22]. The i^{th} node's attention mechanism at layer j is $\mathcal{M}_i^{(j)} : \mathbb{R}^{d^{(j)}} \times \mathbb{R}^{d^{(j)}} \rightarrow \mathbb{R}$. The attention mechanism computes attention coefficients $c_{i,\ell}^{(j)} \triangleq \mathcal{M}_i^{(j)}(W_i^{(j)\top} \phi_i^{(j-1)}, W_i^{(j)\top} \phi_\ell^{(j-1)})$ indicating the importance of node ℓ 's features to node i . These coefficients are calculated for all $\ell \in \bar{N}_i$. The attention coefficients are explicitly calculated as $c_{i,\ell}^{(j)} = a_i^{(j)\top} ((W_i^{(j)\top} \phi_i^{(j-1)}) \oplus (W_i^{(j)\top} \phi_\ell^{(j-1)}))$, where $a_i^{(j)} \in \mathbb{R}^{2d^{(j)}}$ is the i^{th} node's vector of attention weights at layer j . Let $\mathbf{c}_i^{(j)} \triangleq [c_{i,m^{(j)}}^{(j)}]_{\mathbf{m}^{(j)}}$, where $\mathbf{c}_i^{(j)} \in \mathbb{R}^{1 \times N}$. The coefficients are then normalized using the softmax function $\beta_{i,\ell}^{(j)} \in \mathbb{R}$, where

$$\beta_{i,\ell}^{(j)} \triangleq \frac{\exp(c_{i,\ell}^{(j)})}{\exp(\mathbf{c}_i^{(j)}) \bar{A}_i^\top}. \quad (9)$$

Any activation that maps a vector $\mathbf{c}_i^{(j)} \in \mathbb{R}^{1 \times N}$ to a vector $\beta_i^{(j)}$ such that $\|\beta_i^{(j)}\|_1 = 1$ is a valid activation function for the attention weights. The softmax function is used because it is differentiable and maps attention weights to a valid probability distribution. Let $\mathbf{B}_i^{(j)} \triangleq [\phi_i^{(j-1)} \beta_{i,1}^{(j)}, \dots, \phi_N^{(j-1)} \beta_{i,N}^{(j)}] = [\phi_{m^{(j)}}^{(j-1)} \beta_{i,m^{(j)}}^{(j)}]_{\mathbf{m}^{(j)}}$, where $\mathbf{B}_i^{(j)} \in \mathbb{R}^{(d^{(j-1)}+1) \times N}$. If $j = 0$, then $\mathbf{B}_i^{(0)} = [\bar{\kappa}_{m^{(0)}} \beta_{i,m^{(0)}}^{(0)}]_{\mathbf{m}^{(0)}}$. We combine the attention mechanism with the GNN architecture in (6) to yield the GAT architecture with k layers, expressed as

$$\phi_i^{(j)} \triangleq \begin{cases} \sigma^{(j)}(W_i^{(j)\top} \mathbf{B}_i^{(j-1)} \bar{A}_i^\top), & j = 0, \dots, k-1, \\ W_i^{(j)\top} \phi_i^{(j-1)}, & j = k. \end{cases} \quad (10)$$

We define the vector of layer weights for the i^{th} node of the GAT as $\mathcal{W}_i \in \mathbb{R}^{p_{\text{GNN}}}$, where $\mathcal{W}_i \triangleq [\text{vec}(W_i^{(0)})^\top, \dots, \text{vec}(W_i^{(k)})^\top]^\top$. Additionally, we define the

vector of attention weights for the i^{th} node of the GAT as $\mathcal{Z}_i \in \mathbb{R}^{p_{\text{ATT}}}$, where $\mathcal{Z}_i \triangleq [a_i^{(0)\top}, \dots, a_i^{(k-1)\top}]^\top$ and $p_{\text{ATT}} \triangleq \sum_{j=0}^{k-1} 2d^{(j)}$. Then, the total vector of weights for node i of the GAT is denoted by $\theta_i \in \mathbb{R}^{p_{\text{GAT}}}$, where

$$\theta_i \triangleq [\mathcal{W}_i^\top, \mathcal{Z}_i^\top]^\top, \quad (11)$$

and $p_{\text{GAT}} \triangleq p_{\text{GNN}} + p_{\text{ATT}}$. We now compute the first partial derivative of the GAT architecture in (6) with respect to θ_i .

Lemma 2. *For each node $i \in V$, the first partial derivative of the GAT architecture at node i in (10) with respect to (11) is*

$$\nabla_{\theta_i} \phi_i = \left[\frac{\partial \phi_i}{\partial \mathcal{W}_i}^\top, \frac{\partial \phi_i}{\partial \mathcal{Z}_i}^\top \right]^\top, \quad (12)$$

where $\nabla_{\theta_i} \phi_i \in \mathbb{R}^{d^{(\text{out})} \times p_{\text{GAT}}}$. The partial derivative of ϕ_i with respect to $\text{vec}(W_i^{(\ell)})$ for $\ell = 0, \dots, k$ and the partial derivative of ϕ_i with respect to $a_i^{(\ell)}$ for $\ell = 0, \dots, k-1$ are defined in Table I. ■

Proof: See the Appendix. ■

C. Approximation Capabilities of Graph Neural Networks

In this section, we establish the function approximation capabilities of the GNN architectures in (6) and (10). Let \mathcal{G}_N denote the space of undirected graphs with N nodes. Let $F \in \mathbb{R}^{N^m}$ denote the ensemble feature vector of the graph, where each node has features in \mathbb{R}^m . A function $f : \mathcal{G}_N \times \mathbb{R}^{N^m} \rightarrow \mathbb{R}^{N^\ell}$ on a graph G is invariant if $f(p * G, p * F) = f(G, F)$ for every permutation $p \in S_N$, every $G \in \mathcal{G}_N$, and every $F \in \mathbb{R}^{N^m}$. Practical examples of invariant functions on graphs include graph-level statistics such as the number of nodes or the graph diameter. A function $f : \mathcal{G}_N \times \mathbb{R}^{N^m} \rightarrow \mathbb{R}^{N^\ell}$ is equivariant if $f(p * G, p * F) = p * f(G, F)$ for every permutation $p \in S_N$, every $G \in \mathcal{G}_N$, and every $F \in \mathbb{R}^{N^m}$ [43]. Examples of equivariant functions on graphs include message-passing updates or continuous functions of a node's features evaluated at that node. In this work, we approximate equivariant functions of the graph using a GNN. Next, we discuss limitations of the GNN's discriminatory ability in relation to the Weisfeiler-Leman test.

The 1-Weisfeiler-Leman (1-WL) test is a graph isomorphism heuristic that iteratively refines node labels based on neighborhood information. The 1-WL's test ability to distinguish graph structures has been shown to be equivalent to the discriminative ability of the GNN architecture. In practice, the 1-WL test is carried out by assigning initial labels to the nodes of the graph and iteratively updating each node's label by aggregating and hashing the neighboring labels [22]. This process is repeated until the label assignments do not change, or a fixed number of iterations are reached. The discriminatory ability of the WL test is generalized through the k -WL test, with its discriminatory ability increasing as k grows. The message-passing GNN in (6) universally approximates equivariant functions on a graph less separating than the 2-WL test [43]. Next, we establish the universal function approximation ability of GNNs.

Let \mathcal{F} be a set of functions f defined on a set X . The equivalence relation $\text{eq}(\mathcal{F})$ defined by \mathcal{F} on X states that

for any $x, x' \in X$, $(x, x') \in \text{eq}(\mathcal{F})$ if and only if for all $f \in \mathcal{F}$, $f(x) = f(x')$. For a function f , we write $\text{eq}(f)$. Given two sets of functions \mathcal{F} and \mathcal{E} , we say that \mathcal{F} is more separating than \mathcal{E} if $\text{eq}(\mathcal{F}) \subseteq \text{eq}(\mathcal{E})$ [43]. The discriminatory power for the message-passing GNN Φ in (6) is expressed as $\text{eq}(\Phi) = \text{eq}(2 \cdot \text{WL}_E)$, where $k \cdot \text{WL}_E$ denotes the k -WL test for equivariant functions defined in [43].

Let $\mathcal{C}_E(X, Y)$ denote the set of continuous, equivariant functions from X to Y . The closure of a class of functions \mathcal{F} by the uniform norm is denoted by $\text{cl}(\mathcal{F})$. The universal function approximation theorem for GNNs is defined as follows.

Lemma 3. [43, Theorem 4] *Let $\Omega \subseteq G \times F$ be a compact set. Then, for the set of GNNs \mathcal{K} , we have*

$$\text{cl}(\mathcal{K}) = \{f \in \mathcal{C}_E(\Omega, \mathbb{R}^{N\ell}) : \text{eq}(2 \cdot \text{WL}_E) \subseteq \text{eq}(f)\}.$$

Lemma 3 shows that \mathcal{K} is dense in $\mathcal{C}_E(\Omega, \mathbb{R}^{N\ell})$ by the Stone-Weierstrass theorem, which states that if an algebra \mathcal{A} of real continuous function separates points, then \mathcal{A} is dense in the set of continuous functions on a compact set. This outcome allows us to use the Lyapunov-based GNN (Lb-GNN) to universally approximate equivariant functions on the graph of agents that are less separating than the 2-WL test.

IV. PROBLEM FORMULATION

In this section, we apply the GNN architectures described in Section III to the problem of target tracking with unknown target dynamics and unknown agent interaction dynamics. While we specifically address the target tracking problem, we note that the GNN is a general architecture that can be applied to a variety of multi-agent control problems, including average consensus with unknown agent dynamics, distributed state estimation of an uncertain target using networked agents, and sensor fusion for multi-agent systems.

A. System Dynamics and Network Topology

Let $Q_0 \triangleq [q_0^\top, \dot{q}_0^\top]^\top \in \mathbb{R}^{2n}$, where $q_0, \dot{q}_0 \in \mathbb{R}^n$ represent the target agent's unknown position and velocity. Consider target dynamics denoted by

$$\ddot{q}_0 = f(Q_0), \quad (13)$$

where $f(\cdot) : \mathbb{R}^{2n} \rightarrow \mathbb{R}^n$ is an unknown function and $\ddot{q}_0 \in \mathbb{R}^n$ represents the target agent's unknown acceleration.

Assumption 1. [40, Assumption 1] The target's position and velocity q_0 and \dot{q}_0 are bounded such that $\|q_0(t)\| \leq \bar{q}_0 \in \mathbb{R}_{\geq 0}$ and $\|\dot{q}_0(t)\| \leq \bar{\dot{q}}_0$ for all $t \in [t_0, \infty)$, where $\bar{q}_0, \bar{\dot{q}}_0$ are known.

Assumption 2. [40, Assumption 2] The unknown drift dynamics of the target modeled by $f(Q_0)$ in (13) are Lipschitz continuous on the set $\mathcal{Y}_{1,i}$. The Lipschitz constant defined on the set $\mathcal{Y}_{1,i}$ has a known upper bound denoted by L . The set $\mathcal{Y}_{1,i}$ is defined as

$$\mathcal{Y}_{1,i} \triangleq \{v_{1,i} \in \mathbb{R}^{2n} : \|v_{1,i}\| \leq 2(\bar{q}_0 + \bar{\dot{q}}_0) + c_\zeta(2 + \alpha_1)\}, \quad (14)$$

where $\alpha_1 \in \mathbb{R}_{> 0}$ is a user-selected constant, and $c_\zeta \in \mathbb{R}_{> 0}$ is a known bounding constant.

Consider a network of N agents indexed by V , modeled by the connected and undirected graph $G = (V, E)$. Let $Q_i \triangleq [q_i^\top, \dot{q}_i^\top]^\top \in \mathbb{R}^{2n}$, where $q_i, \dot{q}_i \in \mathbb{R}^n$ represent agent i 's known position and velocity. Let $R_i \triangleq [1_{\mathcal{N}_i}(m)Q_m^\top]_{m \in V}^\top \in \mathbb{R}^{2nN}$, where $1_{\mathcal{N}_i}(m)$ is the indicator function that returns 1 if $m \in \mathcal{N}_i$ and 0 otherwise. Agent i 's dynamics are given by

$$\ddot{q}_i = h(R_i) + u_i, \quad (15)$$

where $h(R_i) : \mathbb{R}^{2nN} \rightarrow \mathbb{R}^n$ is an unknown, continuous function, $\ddot{q}_i \in \mathbb{R}^n$ denote agent i 's unknown acceleration and $u_i \in \mathbb{R}^n$ denotes agent i 's control input. The function $h(\cdot)$ denotes unknown interaction dynamics between agent i and its neighboring agents.

B. Objective

The primary objective of this work is to drive each agent to the target by using only relative position and relative velocity measurements made between agents in the network, and relative position and velocity measurements with respect to the target if the agent and the target are connected.

Assumption 3. [46, Assumption 5] Let $b_i \in \{0, 1\}$ denote a binary indicator of agent i 's ability to take relative position and velocity measurements with respect to the target. Each agent i can measure (i) the target's relative position, $q_0 - q_i$, and relative velocity, $\dot{q}_0 - \dot{q}_i$, with respect to its own position and velocity if $b_i = 1$, and (ii) neighboring agents' relative position, $q_j - q_i$, and relative velocity, $\dot{q}_j - \dot{q}_i$, with respect to its own position and velocity if agent $j \in \mathcal{N}_i$. We assume that $b_i = 1$ for at least one $i \in V$.

To quantify the GNN target tracking objective, we define a position tracking error as

$$e_i \triangleq q_0 - q_i, \quad (16)$$

where $e_i \in \mathbb{R}^n$ for all $i \in V$. The signal e_i is measurable if $b_i = 1$. The target dynamics in (13) are unknown, so we develop a distributed observer which leverages online learning techniques to estimate $f(\cdot)$. To this end, we define the state estimation error as

$$\tilde{q}_i \triangleq q_0 - \hat{q}_{0,i}, \quad (17)$$

where $\tilde{q}_i \in \mathbb{R}^n$ for all $i \in V$, and $\hat{q}_{0,i}, \dot{\hat{q}}_{0,i} \in \mathbb{R}^n$ denote agent i 's estimate of the target agent's position and velocity, respectively. Additionally, we define the state estimation regulation error as

$$\hat{e}_i \triangleq \hat{q}_{0,i} - q_i, \quad (18)$$

where $\hat{e}_i \in \mathbb{R}^n$ for all $i \in V$. The state estimation regulation error signal \hat{e}_i is measurable by all agents. The state estimation error in (17) can be calculated locally if $b_i = 1$, where $\tilde{q}_i = e_i - \hat{e}_i$. An auxiliary state estimation error is defined as

$$r_{1,i} \triangleq \dot{\tilde{q}}_i + \alpha_1 \tilde{q}_i, \quad (19)$$

where $r_{1,i} \in \mathbb{R}^n$ for all $i \in V$ and $\alpha_1 \in \mathbb{R}_{\geq 0}$ denotes a user-selected constant. Similarly, an auxiliary state estimation regulation error is defined as

$$r_{2,i} \triangleq \dot{\hat{e}}_i + \alpha_2 \hat{e}_i, \quad (20)$$

where $r_{2,i} \in \mathbb{R}^n$ for all $i \in V$ and $\alpha_2 \in \mathbb{R}_{>0}$ denotes a user-selected constant. The structure of (19) and (20) are motivated by the subsequent stability analysis in Theorem 1 which indicates that the boundedness and convergence of \tilde{q}_i and \hat{e}_i can be determined from the boundedness and convergence of $r_{1,i}$ and $r_{2,i}$, respectively. As a result, the following error system development, control design, and stability analysis are focused on the boundedness and convergence of $r_{1,i}$ and $r_{2,i}$.

Taking the time derivative of (19) yields

$$\dot{r}_{1,i} = f(Q_0) - \ddot{q}_{0,i} + \alpha_1 (r_{1,i} - \alpha_1 \tilde{q}_i). \quad (21)$$

In (21), the input to the unknown function $f(\cdot)$ is Q_0 , which is unknown to all agents. Therefore, directly learning $f(Q_0)$ is not feasible. To facilitate indirect learning, we inject a reconstructible signal into (21), which yields

$$\dot{r}_{1,i} = \tilde{f}_i + f(\hat{Q}_{0,i}) - \ddot{q}_{0,i} + \alpha_1 (r_{1,i} - \alpha_1 \tilde{q}_i), \quad (22)$$

where $\hat{Q}_{0,i} \triangleq [\hat{q}_{0,i}^\top, \hat{q}_{0,i}^\top]^\top \in \mathbb{R}^{2n}$ represents agent i 's estimate of the target's position and velocity, respectively, and $\tilde{f}_i \triangleq f(Q_0) - f(\hat{Q}_{0,i})$. We use a deep Lb-GNN Φ_1 to approximate $f(\hat{Q}_{0,i})$ at each node, where $\Phi_1 \triangleq [\phi_{1,i}^\top]_{i \in V}^\top \in \mathbb{R}^{nN}$. Similarly, the time derivative of (20) yields

$$\dot{r}_{2,i} = \ddot{q}_{0,i} - h(R_i) - u_i + \alpha_2 (r_{2,i} - \alpha_2 \hat{e}_i). \quad (23)$$

We use a deep Lb-GNN Φ_2 to approximate the unknown agent interaction dynamics $h(R_i)$ at each node, where $\Phi_2 \triangleq [\phi_{2,i}^\top]_{i \in V}^\top \in \mathbb{R}^{nN}$. The observer is designed based on (22) and the controller is designed based on (23). In the following section, we design the distributed controller, observer, and adaptive update laws.

V. CONTROL SYNTHESIS

A. Observer Design

To develop the observer, we leverage the universal function approximation properties of GNNs established in Lemma 3, allowing us to represent the unknown function $f(\hat{Q}_{0,i})$ at all nodes with a deep Lb-GNN Φ_1 . Each node of a k -layer Lb-GNN is a function of its $(k-1)$ -hop neighbors' ideal weight values, $\theta_{j:j \in \mathcal{N}_i^{k-1}}^*$ and its k -hop neighbors' Lb-GNN inputs, $\hat{Q}_{0,j:j \in \mathcal{N}_i^k}$. Node i 's component of the Lb-GNN Φ_1 is denoted by $\phi_{1,i}(\hat{Q}_{0,i}, \hat{Q}_{0,j:j \in \mathcal{N}_i^k}, \theta_{1,i}^*, \theta_{1,j:j \in \mathcal{N}_i^{k-1}}^*)$. For notational simplicity, we omit the arguments of the Lb-GNN and let $\phi_{1,i} \triangleq \phi_{1,i}(\hat{Q}_{0,i}, \hat{Q}_{0,j:j \in \mathcal{N}_i^k}, \theta_{1,i}^*, \theta_{1,j:j \in \mathcal{N}_i^{k-1}}^*)$ and $\phi_{i,1}^* \triangleq \phi_{1,i}(\hat{Q}_{0,i}, \hat{Q}_{0,j:j \in \mathcal{N}_i^k}, \theta_{1,i}^*, \theta_{1,j:j \in \mathcal{N}_i^{k-1}}^*)$.

Let $\hat{Q}_0 \triangleq [\hat{Q}_{0,i}^\top]_{i \in V}^\top \in \mathbb{R}^{2nN}$. We use a deep Lb-GNN to approximate the ensemble function $F(\hat{Q}_0) \triangleq [f(\hat{Q}_{0,1})^\top, \dots, f(\hat{Q}_{0,N})^\top]^\top \in \mathbb{R}^{nN}$. Lemma 3 holds if (i) the graph-valued function being approximated by the Lb-GNN is less separating than the 2-WL test, and (ii) the input space of the graph valued function $F(\hat{Q}_0)$ is compact. The function $F(\hat{Q}_0)$ is an equivariant function of the graph G . The outputs of the function $F(\hat{Q}_0)$ are solely a function of each node's features. Therefore, this function is less separating than the 2-WL test. We subsequently prove that the input space of $F(\hat{Q}_0)$ is compact in the Lyapunov stability analysis in Theorem 1.

Next, we define the set Ω_1 as

$$\Omega_1 \triangleq G \times \mathcal{Y}_1, \quad (24)$$

where

$$\mathcal{Y}_1 \triangleq \{v_1 \in \mathbb{R}^{2nN} : v_{1,i} \in \mathcal{Y}_{1,i} \text{ for all } i \in V\}, \quad (25)$$

and $v_1 \triangleq [v_{1,i}^\top]_{i \in V}^\top$. Let the loss function for the GNN Φ_1 be defined as $\mathcal{L}_1 : \mathbb{R}^{pN} \rightarrow \mathbb{R}_{\geq 0}$

$$\mathcal{L}_1(\theta_1) \triangleq \int_{\Omega_1} \left(\|F(\hat{Q}_0) - \Phi_1\|^2 + \sigma \|\theta_1\|^2 \right) d\mu(\hat{Q}_0), \quad (26)$$

for all $i \in V$, where μ denotes the Lebesgue measure, $\sigma \in \mathbb{R}_{>0}$ denotes a regularizing constant, and the term $\sigma \|\theta_1\|^2$ represents L_2 regularization (also popularly known as ridge regression in the machine learning community) [47, Sec. 7.1.1]. Let $\mathcal{U}_1 \subset \mathbb{R}^{pN}$ denote a user-selected compact, convex parameter search space with a smooth boundary, satisfying $\mathbf{0}_{pN} \in \text{int}(\mathcal{U}_1)$. Additionally, define $\bar{\theta}_1 \triangleq \max_{\theta \in \mathcal{U}_1} \|\theta\|$.

The objective is to identify the vector of ideal GNN parameters $\theta_1^* \in \mathcal{U}_1$ defined as¹

$$\theta_1^* \triangleq \arg \min_{\theta \in \mathcal{U}_1} \mathcal{L}_1(\theta_1), \quad (27)$$

Remark 1. Notice that the universal function approximation property of GNNs was not invoked in the definition of θ_1^* . The universal function approximation theorem for GNNs established in Lemma 3 states that the function space of GNNs is dense in $C_E(\Omega_1, \mathbb{R}^{nN})$. Let $\varepsilon_1 : \Omega_1 \rightarrow \mathbb{R}^{nN}$ denote an unknown function representing the function approximation error that can be bounded as $\sup_{G \times \hat{Q}_0 \in \Omega_1} \|\varepsilon_1\| \leq \bar{\varepsilon}_1$. Therefore, $\int_{\Omega_1} \|F(\hat{Q}_0) - \Phi_1\|^2 d\mu(\hat{Q}_0) < \varepsilon_1^2 \mu(\Omega_1)$. As a result, for any prescribed $\bar{\varepsilon}_1 \in \mathbb{R}$, there exists a GNN Φ_1 such that there exist weights $\theta_1 \in \mathbb{R}^{pN}$ which satisfy $\sup_{G \times \hat{Q}_0 \in \Omega_1} \|F(\hat{Q}_0) - \Phi_1(\hat{Q}_0, \theta_1)\| \leq \bar{\varepsilon}_1$. However, determining a search space \mathcal{U}_1 for an arbitrary $\bar{\varepsilon}_1$ remains an open challenge. Therefore, we allow \mathcal{U}_1 to be arbitrarily selected in the above analysis, at the expense of guarantees on the approximation accuracy.

Denote the i^{th} component of ε_1 as $\varepsilon_{1,i} \in \mathbb{R}^n$ for all $i \in V$, where $\varepsilon_1 = [\varepsilon_{1,i}^\top]_{i \in V}^\top$. Each agent models the target agent's unknown drift dynamics as

$$f(\hat{Q}_{0,i}) = \phi_{1,i}^* + \varepsilon_{1,i}. \quad (28)$$

Substituting (28) into (22) yields

$$\dot{r}_{1,i} = \tilde{f}_i + \phi_{1,i}^* + \varepsilon_{1,i} - \ddot{q}_{0,i} + \alpha_1 (r_{1,i} - \alpha_1 \tilde{q}_i). \quad (29)$$

We perform a first-order Taylor approximation of $\phi_{1,i}^*$, noting that each node of a k -layer GNN is a function of its $(k-1)$ -hop neighbors' ideal weight values, $\theta_{1,j}^*$, where $j \in \mathcal{N}_i^{k-1}$.

¹Although using a bounded search space can restrict the optimality of the identified parameters to be local instead of global, it allows the subsequent development to be analyzed from a convex optimization perspective, which otherwise would be non-convex due to the nested NIP structure of the GNN architecture in (6). Specifically, due to the strict convexity of the regularizing term $\sigma \|\theta_1\|^2$ in (26), there exists $\sigma \in \mathbb{R}_{>0}$ which ensures $\mathcal{L}_1(\theta_1)$ is convex for all $\theta_1 \in \mathcal{U}_1$. Additionally, the regularizing term has other advantages such as mitigation of overfitting [47, Sec. 7.1.1]. However, selecting very high values of σ can be counterproductive as it can obscure the contribution of the $\|F(\hat{Q}_0) - \Phi_1\|^2$ term to the loss function while also causing underfitting [47, Sec. 7.1.1]; therefore, there is a tradeoff between selecting low vs. high values of σ .

Therefore, we perform a Taylor expansion about each of these ideal weights. Define the parameter estimation error for each node of the GNN, $\tilde{\theta}_{1,i}$, as

$$\tilde{\theta}_{1,i} \triangleq \theta_{1,i}^* - \hat{\theta}_{1,i}. \quad (30)$$

Similarly to $\phi_{1,i}^*$, we let $\hat{\phi}_{1,i} \triangleq \phi_{1,i}(\hat{Q}_{0,i}, \hat{Q}_{0,j:j \in \mathcal{N}_i^k}, \hat{\theta}_{1,i}, \hat{\theta}_{1,j:j \in \mathcal{N}_i^{k-1}})$. Then, the first-order Taylor approximation of $\phi_{1,i}(\hat{Q}_{0,i}, \hat{Q}_{0,j:j \in \mathcal{N}_i^k}, \theta_{1,i}^*, \theta_{1,j:j \in \mathcal{N}_i^{k-1}}^*)$ about the point $(\hat{Q}_{0,i}, \hat{Q}_{0,j}, \hat{\theta}_{1,i}, \hat{\theta}_{1,j:j \in \mathcal{N}_i^{k-1}})$ yields

$$\phi_{1,i}^* = \hat{\phi}_{1,i} + \sum_{j \in \mathcal{N}_i^{k-1}} \nabla_{\hat{\theta}_{1,j}} \hat{\phi}_{1,i} \tilde{\theta}_{1,j} + \sum_{j \in \mathcal{N}_i^{k-1}} T_{1,j}, \quad (31)$$

where $T_{1,j}$ denotes the first Lagrange remainder, which accounts for the error introduced by truncating the Taylor approximation after the first-order term. Let $\tilde{\theta}_{1,j} \triangleq \hat{\theta}_{1,j} + s_m(\tilde{\theta}_{1,j})\tilde{\theta}_{1,j}$, where $s_m(\tilde{\theta}_{1,j}) : \mathbb{R}^p \rightarrow [0, 1]$ for all $m \in [n]$. By [48, Theorem 15.29], the remainder term $T_{1,j} \in \mathbb{R}^n$ can be expressed as $T_{1,j} = \frac{1}{2}[T_{1,j}(s_1), \dots, T_{1,j}(s_n)]^\top$, where $T_{1,j}(s_m) \in \mathbb{R}$ is defined as $T_{1,j}(s_m) \triangleq \tilde{\theta}_{1,j}^\top \nabla_{\hat{\theta}_{1,j}}^2 \phi_{1,i}(\hat{Q}_{0,i}, \hat{Q}_{0,j:j \in \mathcal{N}_i^k}, \hat{\theta}_{1,j}, \hat{\theta}_{1,\ell:\ell \in \mathcal{N}_i^{k-1} \setminus j})\tilde{\theta}_{1,j}$ for all $m \in [n]$, and $\nabla_{\hat{\theta}_{1,j}}^2 \phi_{1,i}(\hat{Q}_{0,i}, \hat{Q}_{0,j:j \in \mathcal{N}_i^k}, \hat{\theta}_{1,j}, \hat{\theta}_{1,\ell:\ell \in \mathcal{N}_i^{k-1} \setminus j}) \in \mathbb{R}^{n \times p \times p}$ denotes the second partial derivative of $\hat{\phi}_{1,i}$ with respect to $\hat{\theta}_{1,j}$.

Substituting (31) into (29) gives

$$\begin{aligned} \dot{r}_{1,i} &= \tilde{f}_i + \hat{\phi}_{1,i} + \sum_{j \in \mathcal{N}_i^{k-1}} \nabla_{\hat{\theta}_{1,j}} \hat{\phi}_{1,i} \tilde{\theta}_{1,j} \\ &+ \sum_{j \in \mathcal{N}_i^{k-1}} T_{1,j} + \varepsilon_{1,i} - \tilde{q}_{0,i} + \alpha_1 (r_{1,i} - \alpha_1 \tilde{q}_i). \end{aligned} \quad (32)$$

Based on (32), the distributed observer is designed as

$$\begin{aligned} \ddot{\hat{q}}_{0,i} &= \hat{\phi}_{1,i} + \sum_{j \in \mathcal{N}_i^{k-1}} \nabla_{\hat{\theta}_{1,j}} \hat{\phi}_{1,i} (\hat{\theta}_i - \hat{\theta}_j) \\ &+ k_1 \left(b_i \tilde{q}_i + \sum_{j \in \mathcal{N}_i} (\dot{\hat{q}}_{0,j} - \dot{\hat{q}}_{0,i}) \right) \\ &+ \alpha_1 \sum_{j \in \mathcal{N}_i} (\hat{q}_{0,j} - \hat{q}_{0,i}) + \alpha_1 b_i \tilde{q}_i, \end{aligned} \quad (33)$$

where b_i ensures that the signals \tilde{q}_i and \hat{q}_i are only implemented by agents who are connected to the target. Substituting (33) into (32) yields

$$\begin{aligned} \dot{r}_{1,i} &= \tilde{f}_i + \sum_{j \in \mathcal{N}_i^{k-1}} \nabla_{\hat{\theta}_{1,j}} \hat{\phi}_{1,i} \tilde{\theta}_{1,j} + \alpha_1 (r_{1,i} - \alpha_1 \tilde{q}_i) \\ &+ \chi_{1,i} + \varepsilon_{1,i} - k_1 \left(\sum_{j \in \mathcal{N}_i} (\dot{\hat{q}}_{0,j} - \dot{\hat{q}}_{0,i}) + b_i \tilde{q}_i \right) \\ &+ \alpha_1 \sum_{j \in \mathcal{N}_i} (\hat{q}_{0,j} - \hat{q}_{0,i}) + \alpha_1 b_i \tilde{q}_i, \end{aligned} \quad (34)$$

where $\chi_{1,i} \triangleq \sum_{j \in \mathcal{N}_i^{k-1}} T_{1,j} + \sum_{j \in \mathcal{N}_i^{k-1}} \nabla_{\hat{\theta}_{1,j}} \hat{\phi}_{1,i} (\theta_{1,j}^* - \hat{\theta}_{1,i})$. The graph interaction matrix is defined as

$$\mathcal{H} \triangleq (\mathcal{L}_G + \mathcal{B}) \otimes I_n, \quad (35)$$

where $\mathcal{B} \triangleq \text{diag}(b_1, \dots, b_N) \in \mathbb{R}^{N \times N}$, $\mathcal{H} \in \mathbb{R}^{nN \times nN}$, and \mathcal{L}_G is the graph Laplacian.

Remark 2. Assumption 3 states that $b_i = 1$ for at least one $b_i \in \{c_1, \dots, c_N\}$. Additionally, the communication graph G is connected. Thus, the graph interaction matrix \mathcal{H} defined in (35) is symmetric and positive definite [49, Corollary 4.33].

Define $\tilde{r}_1 \triangleq [\tilde{r}_{1,i}^\top]_{i \in V}^\top \in \mathbb{R}^{nN}$. Then, the ensemble auxiliary state estimation error dynamics are

$$\dot{\tilde{r}}_1 = \tilde{F} + \nabla_{\hat{\theta}_1} \hat{\Phi}_1 \tilde{\theta}_1 + \chi_1 + \varepsilon_1 - k_1 \mathcal{H} \tilde{r}_1 + \alpha_1 (r_1 - \alpha_1 \tilde{q}), \quad (36)$$

where $\tilde{F} \triangleq [\tilde{f}_i^\top]_{i \in V}^\top \in \mathbb{R}^{nN}$, $\tilde{q} \triangleq [\tilde{q}_i^\top]_{i \in V}^\top \in \mathbb{R}^{nN}$, and $\nabla_{\hat{\theta}_1} \hat{\Phi}_1 \triangleq \text{blkdiag}(\sum_{j \in \mathcal{N}_1^{k-1}} \nabla_{\hat{\theta}_{1,j}} \hat{\phi}_{1,1}, \dots, \sum_{j \in \mathcal{N}_N^{k-1}} \nabla_{\hat{\theta}_{1,j}} \hat{\phi}_{1,N})$.

We note that $\nabla_{\hat{\theta}_1} \hat{\Phi}_1 \in \mathbb{R}^{nN \times pN}$. Additionally, $\tilde{\theta}_1 \triangleq [\tilde{\theta}_{1,i}^\top]_{i \in V}^\top \in \mathbb{R}^{pN}$, $\chi_1 \triangleq [\chi_{1,i}^\top]_{i \in V}^\top \in \mathbb{R}^{nN}$, and $r_1 \triangleq [r_{1,i}^\top]_{i \in V}^\top \in \mathbb{R}^{nN}$. In the following subsection, we develop a distributed control law.

B. Controller Design

Let $R \triangleq [R_i^\top]_{i \in V}^\top \in \mathbb{R}^{2nN}$. We invoke the universal function approximation theorem for GNNs to approximate the ensemble function $H(R) \triangleq [h(R_1)^\top, \dots, h(R_N)^\top]^\top \in \mathbb{R}^{nN}$. The function $H(R)$ is an equivariant function of the graph whose outputs are solely a function of the 1-hop neighborhood of each node. This function is less separating than the 2-WL test. We subsequently prove that the input space of $H(R)$ is compact in the Lyapunov stability analysis in Theorem 1.

Define the set Ω_2 as

$$\Omega_2 \triangleq G \times \mathcal{Y}_2, \quad (37)$$

where $\mathcal{Y}_{2,i} \triangleq \{\tilde{v}_{2,i} \in \mathbb{R}^{2nN} : \|\tilde{v}_{2,i}\| \leq N(\bar{q}_0 + \bar{q}_0 + c_\zeta(3 + \alpha_1 + \alpha_2))\}$, and $\mathcal{Y}_2 \triangleq \{\tilde{v}_2 \in \mathbb{R}^{2nN} : \tilde{v}_{2,i} \in \mathcal{Y}_{2,i} \text{ for all } i \in V\}$, where $\tilde{v}_2 \triangleq [\tilde{v}_{2,i}^\top]_{i \in V}^\top$. Let $\theta_2 \triangleq [\theta_{2,i}^\top]_{i \in V}^\top$. As in Subsection V-A, let the loss function for the GNN Φ_2 at node i be defined as $\mathcal{L}_2 : \mathbb{R}^{pN} \rightarrow \mathbb{R}_{\geq 0}$

$$\mathcal{L}_2(\theta_2) \triangleq \int_{\Omega_2} (\|H(R) - \Phi_2\|^2 + \sigma \|\theta_2\|^2) d\mu(R), \quad (38)$$

where μ denotes the Lebesgue measure, $\sigma \in \mathbb{R}_{>0}$ denotes a regularizing constant, the term $\sigma \|\theta_2\|^2$ represents L_2 regularization. Let $\mathcal{U}_2 \subset \mathbb{R}^{pN}$ denote a user-selected compact, convex parameter search space with a smooth boundary, satisfying $\mathbf{0}_{pN} \in \text{int}(\mathcal{U}_2)$. Additionally, define $\bar{\theta}_2 \triangleq \max_{\theta \in \mathcal{U}_2} \|\theta\|$. We denote the ideal parameters of the GNN Φ_2 as $\theta_2^* \in \mathcal{U}_2$, where

$$\theta_2^* \triangleq \arg \min_{\theta \in \mathcal{U}_2} \mathcal{L}_2(\theta_2). \quad (39)$$

For clarity in the subsequent analysis, it is desirable that the solutions θ_1^* and θ_2^* to (27) and (39), respectively, be unique. To this end, the following assumption is made.

Assumption 4. The loss functions \mathcal{L}_1 and \mathcal{L}_2 are strictly convex over the sets \mathcal{U}_1 and \mathcal{U}_2 , respectively.

Let $\bar{\theta} \triangleq \max\{\bar{\theta}_1, \bar{\theta}_2\}$. Additionally, we let $\varepsilon_2 : \Omega_2 \rightarrow \mathbb{R}^{nN}$ denote an unknown function representing the function approximation error that can be bounded as $\sup_{G \times R \in \Omega_2} \|\varepsilon_2\| \leq \bar{\varepsilon}_2$. Denote the i^{th} component of ε_2 as $\varepsilon_{2,i} \in \mathbb{R}^n$ for all $i \in V$, where $\varepsilon_2 = [\varepsilon_{2,i}^T]_{i \in V}^T$. We denote node i 's component of the deep Lb-GNN Φ_2 as $\phi_{2,i}^* \triangleq \phi_{2,i}(R_i, R_{j:j \in \mathcal{N}_i^k}, \theta_{2,i}^*, \theta_{2,j:j \in \mathcal{N}_i^{k-1}}^*)$. Then, each agent models their unknown drift dynamics as

$$h(R_i) = \phi_{2,i}^* + \varepsilon_{2,i}. \quad (40)$$

Substituting (40) into (23) yields

$$\dot{r}_{2,i} = \ddot{q}_{0,i} - \phi_{2,i}^* - \varepsilon_{2,i} - u_i + \alpha_2 (r_{2,i} - \alpha_2 \hat{e}_i). \quad (41)$$

We perform a first-order Taylor approximation of $\phi_{2,i}(R_i, R_{j:j \in \mathcal{N}_i^k}, \theta_{2,i}^*, \theta_{2,j:j \in \mathcal{N}_i^{k-1}}^*)$ about the point $(R_i, R_{j:j \in \mathcal{N}_i^k}, \hat{\theta}_{2,i}, \hat{\theta}_{2,j:j \in \mathcal{N}_i^{k-1}})$ to find

$$\phi_{2,i}^* = \hat{\phi}_{2,i} + \sum_{j \in \mathcal{N}_i^{k-1}} \nabla_{\hat{\theta}_{2,j}} \hat{\phi}_{2,i} \tilde{\theta}_{2,j} + \sum_{j \in \mathcal{N}_i^{k-1}} T_{2,j}, \quad (42)$$

where $T_{2,j}$ denotes the first Lagrange remainder. Substituting (42) into (41) gives

$$\begin{aligned} \dot{r}_{2,i} = & \ddot{q}_{0,i} - \hat{\phi}_{2,i} - \sum_{j \in \mathcal{N}_i^k} \nabla_{\hat{\theta}_{2,j}} \hat{\phi}_{2,i} \tilde{\theta}_{2,j} \\ & - \sum_{j \in \mathcal{N}_i^{k-1}} T_{2,j} - \varepsilon_{2,i} - u_i + \alpha_2 (r_{2,i} - \alpha_2 \hat{e}_i), \end{aligned} \quad (43)$$

where the parameter estimation error for each node of the GNN, $\hat{\theta}_{2,i}$, is defined as

$$\hat{\theta}_{2,i} \triangleq \theta_{2,i}^* - \hat{\theta}_{2,i}. \quad (44)$$

Motivated by the structure of (43), the distributed controller is designed as

$$\begin{aligned} u_i = & \ddot{q}_{0,i} - \hat{\phi}_{2,i} - \sum_{j \in \mathcal{N}_i^{k-1}} \nabla_{\hat{\theta}_{2,j}} \hat{\phi}_{2,i} (\hat{\theta}_{2,i} - \hat{\theta}_{2,j}) \\ & + k_2 (\dot{\hat{e}}_i + \alpha_2 \hat{e}_i) \end{aligned} \quad (45)$$

where $k_2 \in \mathbb{R}_{>0}$ is a user-defined constant. Substituting (45) into (43) gives

$$\begin{aligned} \dot{r}_{2,i} = & - \sum_{j \in \mathcal{N}_i^{k-1}} \nabla_{\hat{\theta}_{2,j}} \hat{\phi}_{2,i} \tilde{\theta}_{2,i} - \chi_{2,i} \\ & - \varepsilon_{2,i} - (k_2 - \alpha_2) r_{2,i} - \alpha_2^2 \hat{e}_i, \end{aligned} \quad (46)$$

and $\chi_{2,i} \triangleq \sum_{j \in \mathcal{N}_i^{k-1}} T_{2,j} + \sum_{j \in \mathcal{N}_i^{k-1}} \nabla_{\hat{\theta}_{2,j}} \hat{\phi}_{2,i} (\theta_{2,j}^* - \theta_{1,j}^*)$. Define $\dot{r}_2 \triangleq [\dot{r}_{2,i}^T]_{i \in V}^T \in \mathbb{R}^{nN}$. The ensemble auxiliary state estimation regulation error dynamics are

$$\dot{r}_2 = -\nabla_{\hat{\theta}_2} \hat{\Phi}_2 \tilde{\theta}_2 - \chi_2 - \varepsilon_2 - (k_2 - \alpha_2) r_2 - \alpha_2^2 \hat{e}, \quad (47)$$

where $\tilde{\theta}_2 \triangleq [\tilde{\theta}_{2,i}^T]_{i \in V}^T \in \mathbb{R}^{pN}$, $\chi_2 \triangleq [\chi_{2,i}^T]_{i \in V}^T \in \mathbb{R}^{nN}$, $r_2 \triangleq [r_{2,i}^T]_{i \in V}^T \in \mathbb{R}^{nN}$, $\nabla_{\hat{\theta}_2} \hat{\Phi}_2 \triangleq \text{blkdiag}(\sum_{j \in \mathcal{N}_1^{k-1}} \nabla_{\hat{\theta}_{2,j}} \hat{\phi}_{2,1}, \dots, \sum_{j \in \mathcal{N}_N^{k-1}} \nabla_{\hat{\theta}_{2,j}} \hat{\phi}_{2,N}) \in \mathbb{R}^{nN \times pN}$, and $\hat{e} \triangleq [\hat{e}_i^T]_{i \in V}^T \in \mathbb{R}^{nN}$. In the following subsection, we develop Lyapunov-based adaptive update laws for the deep Lb-GNNs Φ_1 and Φ_2 .

C. Adaptive Update Law Design

Based on the subsequent stability analysis, we first design the distributed adaptive update law for the observer's deep Lb-GNN weights using the projection operator defined in (4), where

$$\hat{\theta}_{1,i} = \text{proj}(\aleph_{1,i}, \hat{\theta}_{1,i}, \bar{\theta}), \quad (48)$$

and

$$\begin{aligned} \aleph_{1,i} \triangleq & \Gamma_{1,i} \left(-k_3 \left(\sum_{j \in \mathcal{N}_i} (\hat{\theta}_{1,i} - \hat{\theta}_{1,j}) + \hat{\theta}_{1,i} \right) \right. \\ & + \sum_{j \in \mathcal{N}_i^{k-1}} \nabla_{\hat{\theta}_{1,j}} \hat{\phi}_{1,i}^T \left(\sum_{j \in \mathcal{N}_i} (\dot{\hat{q}}_{0,j} - \dot{\hat{q}}_{0,i}) \right. \\ & \left. \left. + b_i \dot{\hat{q}}_i + \alpha_1 \sum_{j \in \mathcal{N}_i} (\hat{q}_{0,j} - \hat{q}_{0,i}) + \alpha_1 b_i \tilde{q}_i \right) \right), \end{aligned} \quad (49)$$

where $k_3 \in \mathbb{R}_{>0}$ is a user-defined gain, $\Gamma_{1,i} \in \mathbb{R}^{p \times p}$ is a symmetric, positive-definite, user-defined gain, $\nabla_{\hat{\theta}_{1,j}} \hat{\phi}_{1,i}$ denotes the first partial derivative of the selected architecture $\hat{\phi}_{1,i}$ with respect to the vector of weights $\hat{\theta}_{1,j}^2$, $\bar{\theta} \in \mathbb{R}^p$ is the upper bound of the Lb-GNN weights, and p denotes the total number of weights for the selected GNN architecture (e.g. for the GAT architecture, $p = p_{\text{GAT}}$, where $p_{\text{GAT}} = \sum_{j=0}^{k-1} 2d^{(j)} + \sum_{j=0}^k (d^{(j)})(d^{(j-1)} + 1)$). The partial derivative of the selected architecture with respect to the vector of weights in (48) is multiplied by an implementable form of $r_{1,i}$ defined in (19), which each agent aims to minimize. Let $\hat{\theta}_1 \triangleq [\hat{\theta}_{1,i}^T]_{i \in V}^T \in \mathbb{R}^{pN}$. The ensemble update law for the weights of the observer's deep Lb-GNN is

$$\dot{\hat{\theta}}_1 = \left[\text{proj}(\aleph_{1,1}, \hat{\theta}_{1,1}, \bar{\theta}), \dots, \text{proj}(\aleph_{1,N}, \hat{\theta}_{1,N}, \bar{\theta}) \right]^T. \quad (50)$$

Similarly, we design the distributed adaptive update law for the controller's Lb-GNN using the projection operator defined in (4), where

$$\hat{\theta}_{2,i} = \text{proj}(\aleph_{2,i}, \hat{\theta}_{2,i}, \bar{\theta}), \quad (51)$$

and

$$\begin{aligned} \aleph_{2,i} \triangleq & \Gamma_{2,i} \left(-k_4 \left(\sum_{j \in \mathcal{N}_i} (\hat{\theta}_{2,i} - \hat{\theta}_{2,j}) + \hat{\theta}_{2,i} \right) \right. \\ & \left. - \sum_{j \in \mathcal{N}_i^{k-1}} \nabla_{\hat{\theta}_{2,j}} \hat{\phi}_{2,i}^T (\dot{\hat{e}}_i + \alpha_2 \hat{e}_i) \right), \end{aligned} \quad (52)$$

where $k_4 \in \mathbb{R}_{>0}$ is a user-defined gain, $\Gamma_{2,i} \in \mathbb{R}^{p \times p}$ is a symmetric, positive-definite, user-defined gain, and $\nabla_{\hat{\theta}_{2,j}} \hat{\phi}_{2,i}$ denotes the first partial derivative of the selected architecture $\hat{\phi}_{2,i}$ with respect to the vector of weights $\hat{\theta}_{2,j}$. The partial derivative of the selected architecture with respect to the vector of weights in (51) is multiplied by $r_{2,i}$ defined in (20), which each agent seeks to minimize. Let $\hat{\theta}_2 \triangleq [\hat{\theta}_{2,i}^T]_{i \in V}^T \in \mathbb{R}^{pN}$.

²The adaptive update law in (48) can be generalized for any NN architecture for which a closed form of the first partial derivative of $\hat{\phi}_{1,i}$ with respect to its weight vector $\hat{\theta}_{1,i}$ has been calculated, including the GNN and GAT architectures whose first partial derivatives with respect to their respective vectors of weights were explicitly calculated in Section III.

The ensemble update law for the weights of the controller's Lb-GNN is

$$\dot{\hat{\theta}}_2 = \left[\text{proj}(\mathfrak{N}_{2,1}, \hat{\theta}_{2,1}, \bar{\theta})^\top, \dots, \text{proj}(\mathfrak{N}_{2,N}, \hat{\theta}_{2,N}, \bar{\theta})^\top \right]^\top. \quad (53)$$

In the following subsection, we perform a stability analysis for the ensemble system.

VI. STABILITY ANALYSIS

Define the concatenated state vector $\zeta : \mathbb{R}_{\geq 0} \rightarrow \mathbb{R}^{N(4n+2p)}$ as $\zeta \triangleq [\tilde{q}^\top, \hat{e}^\top, r_1^\top, r_2^\top, \hat{\theta}_1^\top, \hat{\theta}_2^\top]^\top$. Let $\Gamma_1 \triangleq \text{blkdiag}(\Gamma_{1,1}, \dots, \Gamma_{1,N}) \in \mathbb{R}^{pN \times pN}$, $\Gamma_2 \triangleq \text{blkdiag}(\Gamma_{2,1}, \dots, \Gamma_{2,N}) \in \mathbb{R}^{pN \times pN}$, and $P \triangleq \text{blkdiag}(I_{2nN}, \mathcal{H}, I_{nN}, \Gamma_1^{-1}, \Gamma_2^{-1}) \in \mathbb{R}^{N(4n+2p) \times N(4n+2p)}$. By the definitions of Γ_1 and Γ_2 and Remark 2, the P matrix is positive definite and symmetric. Using (36), (47), (50), and (53) yields

$$\dot{\zeta} = \begin{bmatrix} r_1 - \alpha_1 \tilde{q} \\ r_2 - \alpha_2 \hat{e} \\ \tilde{F} + \nabla_{\hat{\theta}_1} \hat{\Phi}_1 \hat{\theta}_1 + \chi_1 + \varepsilon_1 - k_1 \mathcal{H} r_1 + \alpha_1 (r_1 - \alpha_1 \tilde{q}) \\ -\nabla_{\hat{\theta}_2} \hat{\Phi}_2 \hat{\theta}_2 - \chi_2 - \varepsilon_2 - (k_2 - \alpha_2) r_2 - \alpha_2 \hat{e} \\ -[\text{proj}(\mathfrak{N}_{1,1}, \bar{\theta})^\top, \dots, \text{proj}(\mathfrak{N}_{1,N}, \bar{\theta})^\top]^\top \\ -[\text{proj}(\mathfrak{N}_{2,1}, \bar{\theta})^\top, \dots, \text{proj}(\mathfrak{N}_{2,N}, \bar{\theta})^\top]^\top \end{bmatrix}. \quad (54)$$

We consider a candidate Lyapunov function defined as

$$V \triangleq \frac{1}{2} \zeta^\top P \zeta, \quad (55)$$

where $V : \mathbb{R}^{N(4n+2p)} \rightarrow \mathbb{R}_{\geq 0}$. Let

$$\lambda_1 \triangleq \frac{1}{2} \min \left\{ 1, \lambda_{\min}(\mathcal{H}), \frac{1}{\lambda_{\max}(\Gamma_1)}, \frac{1}{\lambda_{\max}(\Gamma_2)} \right\}, \quad (56)$$

and

$$\lambda_2 \triangleq \frac{1}{2} \max \left\{ 1, \lambda_{\max}(\mathcal{H}), \frac{1}{\lambda_{\min}(\Gamma_1)}, \frac{1}{\lambda_{\min}(\Gamma_2)} \right\}. \quad (57)$$

Then, by the Rayleigh-Ritz Theorem, (55) satisfies the inequality

$$\lambda_1 \|\zeta\|^2 \leq V(\zeta) \leq \lambda_2 \|\zeta\|^2. \quad (58)$$

Let $\underline{\lambda}_{\mathcal{H}} \triangleq \lambda_{\min}(\mathcal{H})$, and $\bar{\lambda}_{\mathcal{H}} \triangleq \lambda_{\max}(\mathcal{H})$. The quantities $\underline{\lambda}_{\mathcal{H}}$ and $\bar{\lambda}_{\mathcal{H}}$ can only be computed if knowledge of the global communication architecture is obtained *a priori*. Requiring knowledge of the network's inter-agent communication topology is undesirable when implementing a decentralized control protocol because the control gains must be sufficiently selected to ensure stability in comparison to these values. To mitigate the need for complete knowledge of the communication graph in the gain conditions for each agent, we develop bounds on $\underline{\lambda}_{\mathcal{H}}$ and $\bar{\lambda}_{\mathcal{H}}$ only in terms of the number of agents in the network. The developed bounds allow agents to certify that their gains are sufficiently large in a decentralized manner using knowledge of the number of agents in the network. For large networks, it may be difficult to know the exact number of agents, but it is reasonable to use a conservative upper bound to satisfy the sufficient gain conditions.

Lemma 4. *The minimum eigenvalue of \mathcal{H} , defined in (35) and denoted by $\underline{\lambda}_{\mathcal{H}}$ is equivalent to*

$$\underline{\lambda}_{\mathcal{H}} = 2 \left(1 + \cos \left(\frac{2N\pi}{2N+1} \right) \right),$$

and the maximum eigenvalue of \mathcal{H} , denoted by $\bar{\lambda}_{\mathcal{H}}$, is upper-bounded as $\bar{\lambda}_{\mathcal{H}} \leq N+1$.

Proof: See the Appendix. \blacksquare

For the subsequent stability analysis to hold, gain conditions must be sequentially established to satisfy sufficient inequalities. Let $\epsilon_1, \epsilon_2, \epsilon_3 \in \mathbb{R}_{>0}$ denote user-selected positive constants, and define $\lambda_3 \in \mathbb{R}_{>0}$ as

$$\lambda_3 \triangleq \min \left\{ \alpha_1 - \frac{(1 + \alpha_1^2 \bar{\lambda}_{\mathcal{H}})}{2\epsilon_1} - \frac{NL\bar{\lambda}_{\mathcal{H}}(1 + \alpha_1)}{2\epsilon_3}, \right. \\ \alpha_2 - \frac{(1 + \alpha_2^2)\epsilon_2}{2}, \frac{k_1 \underline{\lambda}_{\mathcal{H}}^2}{2} - \alpha_1 \bar{\lambda}_{\mathcal{H}} - \frac{(1 + \alpha_1^2 \bar{\lambda}_{\mathcal{H}})\epsilon_1}{2} \\ \left. - \frac{NL\bar{\lambda}_{\mathcal{H}}(1 + \alpha_1)\epsilon_3}{2} - NL\bar{\lambda}_{\mathcal{H}}, \right. \\ \left. \frac{k_2}{2} - \alpha_2 - \frac{(1 + \alpha_2^2)}{2\epsilon_2}, \frac{k_3}{2}, \frac{k_4}{2} \right\}. \quad (59)$$

To ensure the positivity of λ_3 , the following sufficient gain conditions are established. First, select $\alpha_1 > 0$. Then, select the positive constant ϵ_3 as

$$\epsilon_3 > NL\bar{\lambda}_{\mathcal{H}} \left(\frac{1}{2\alpha_1} + \frac{1}{2} \right). \quad (60)$$

Next, let the positive constant ϵ_1 be selected as

$$\epsilon_1 > \frac{1 + \alpha_1^2 \bar{\lambda}_{\mathcal{H}}}{2\alpha_1 - \frac{NL\bar{\lambda}_{\mathcal{H}}(1 + \alpha_1)}{\epsilon_3}}. \quad (61)$$

Selection of ϵ_3 and ϵ_1 according to the sufficient conditions in (60) and (61) ensures that $\alpha_1 - \frac{(1 + \alpha_1^2 \bar{\lambda}_{\mathcal{H}})}{2\epsilon_1} - \frac{NL\bar{\lambda}_{\mathcal{H}}(1 + \alpha_1)}{2\epsilon_3} > 0$. Next, select $\alpha_2 > 0$. Then, select the positive constant ϵ_2 as

$$\frac{2\alpha_2}{(1 + \alpha_2^2)} > \epsilon_2. \quad (62)$$

Selection of ϵ_2 and α_2 according to the sufficient condition in (62) ensures that $\alpha_2 - \frac{(1 + \alpha_2^2)\epsilon_2}{2} > 0$. Lastly, sufficient gain conditions for the observer gain k_1 defined in (33) and the controller gain k_2 defined in (46) are

$$k_1 > \frac{\bar{\lambda}_{\mathcal{H}}}{\underline{\lambda}_{\mathcal{H}}^2} (2\alpha_1 + \alpha_1^2 \epsilon_1 + NL(2 + \epsilon_3 + \alpha_1 \epsilon_3)) + \frac{\epsilon_1}{\underline{\lambda}_{\mathcal{H}}^2}, \quad (63)$$

and

$$k_2 > 2\alpha_2 + \frac{(1 + \alpha_2^2)}{\epsilon_2}, \quad (64)$$

ensuring that $\frac{k_1 \underline{\lambda}_{\mathcal{H}}^2}{2} - \alpha_1 \bar{\lambda}_{\mathcal{H}} - \frac{(1 + \alpha_1^2 \bar{\lambda}_{\mathcal{H}})\epsilon_1}{2} - \frac{NL\bar{\lambda}_{\mathcal{H}}(1 + \alpha_1)\epsilon_3}{2} - NL\bar{\lambda}_{\mathcal{H}} > 0$ and $\frac{k_2}{2} - \alpha_2 - \frac{(1 + \alpha_2^2)}{2\epsilon_2} > 0$ hold, respectively. Next, we establish bounds for the first Lagrange remainder of the GNNs Φ_1 and Φ_2 .

Lemma 5. *The z^{th} component of the y^{th} GNN's first Lagrange remainder $T_{y,z}$ can be upper-bounded as*

$$\|T_{y,z}\| \leq \rho(\|\kappa\|) \left\| \tilde{\theta}_{y,z} \right\|^2,$$

where $\rho : \mathbb{R}_{\geq 0} \rightarrow \mathbb{R}_{\geq 0}$ is a strictly increasing polynomial that is quadratic in the norm of the ensemble GNN input $\|\kappa\|$.

Proof: See the Appendix. \blacksquare

Lemma 6. The z^{th} component of the y^{th} GAT's first Lagrange remainder $T_{y,z}$ can be upper-bounded as

$$\|T_{y,z}\| \leq \rho(\|\kappa\|) \|\tilde{\theta}_{y,z}\|^2,$$

where $\rho: \mathbb{R}_{\geq 0} \rightarrow \mathbb{R}_{\geq 0}$ is a strictly increasing polynomial of degree $2k$ in terms of the norm of the ensemble GAT input $\|\kappa\|$, where k is the number of GAT layers.

Proof: See the Appendix. \blacksquare

To facilitate the subsequent stability analysis, we define $v \in \mathbb{R}_{>0}$ as

$$v \triangleq \frac{\bar{\lambda}_{\mathcal{H}}^2 \bar{\epsilon}_1^2}{2\bar{\lambda}_{\mathcal{H}}^2 k_1} + \frac{\bar{\epsilon}_2^2}{2k_2} + \left(\frac{k_3}{2} + \frac{k_4}{2}\right) \bar{\theta}^2 + \frac{N}{2\epsilon_4} (1 + \bar{\lambda}_{\mathcal{H}}). \quad (65)$$

Lemma 3 established that the universal function approximation property of GNNs for node-level tasks only holds over a compact domain. Therefore, the inputs of the GNNs Φ_1 and Φ_2 must lie on compact domains for all $t \in \mathbb{R}_{\geq 0}$ such that Lemma 3 holds. We enforce this condition by proving that $\hat{Q}_{0,i} \in \mathcal{Y}_{1,i}$ and $R_i \in \mathcal{Y}_{2,i}$ for all $t \in \mathbb{R}_{\geq 0}$. This is achieved by yielding a stability result which constrains ζ to a compact domain. Let $\rho: \mathbb{R}_{\geq 0} \rightarrow \mathbb{R}_{\geq 0}$ denote a strictly increasing function and define $\bar{\rho}(\cdot) \triangleq \rho(\cdot) - \rho(0)$, where $\bar{\rho}$ is strictly increasing and invertible. Then, consider the compact domain

$$\mathcal{D} \triangleq \left\{ z \in \mathbb{R}^{N(4n+2p)} : \|z\| \leq \bar{\rho}^{-1}(\lambda_3 - \lambda_4 - \rho(0)) \right\}, \quad (66)$$

where $\lambda_4 \in \mathbb{R}_{>0}$ is a user-defined constant and $\mathcal{D} \subset \mathbb{R}^{N(4n+2p)}$. Define $c_{\zeta} \in \mathbb{R}_{>0}$ as $c_{\zeta} \triangleq \bar{\rho}^{-1}(\lambda_3 - \lambda_4 - \rho(0))$. It follows that if $\zeta \in \mathcal{D}$, then the input to the GNN Φ_1 at node i can be bounded as $\|\hat{Q}_{0,i}\| \leq (\alpha_1 + 2)c_{\zeta} + \bar{q}_0 + \bar{q}_0$, and the input to the GNN Φ_2 at node i can be bounded as $\|R_i\| \leq N((3 + \alpha_1 + \alpha_2)c_{\zeta} + \bar{q}_0 + \bar{q}_0)$. Therefore, $\zeta \in \mathcal{D}$ implies $G \times \hat{Q}_0 \in \Omega_1$ and $G \times R \in \Omega_2$.

Since the solution $t \mapsto \zeta(t)$ is continuous³, there exists a time interval $\mathcal{I} \triangleq [t_0, t_1]$ for $t_1 > t_0$ such that $\zeta(t) \in \mathcal{D}$ for all $t \in \mathcal{I}$. It follows that $G \times \hat{Q}_0(t) \in \Omega_1$ and $G \times R(t) \in \Omega_2$ for all $t \in \mathcal{I}$. Therefore, the universal function approximation property of GNNs described in Lemma 3 holds for the GNNs Φ_1 and Φ_2 on the interval $[t_0, t_1]$. In the subsequent stability analysis, we analyze the convergence properties of the solutions and also establish that \mathcal{I} can be extended to $[t_0, \infty)$.

To this end, we define the set of initial conditions as

$$\mathcal{S} \triangleq \left\{ z \in \mathbb{R}^{N(4n+2p)} : \|z\| < \sqrt{\frac{\lambda_1}{\lambda_2} \bar{\rho}^{-1}(\lambda_3 - \lambda_4 - \rho(0))} - \sqrt{\frac{v}{\lambda_4}} \right\}, \quad (67)$$

where $\mathcal{S} \subset \mathcal{D}$. Based on the use of a bounded search space in (27) and (39) and the use of the projection operator in (48) and (51), $\hat{\theta}_{1,i}$ and $\hat{\theta}_{2,i}$ can each be upper-bounded as $2\bar{\theta}$ for all $i \in V$, allowing the user to verify that an initial condition

³Continuous solutions exist over some time interval for systems satisfying Caratheodory existence conditions. According to Caratheodory conditions for the system $\dot{y} = f(y, t)$, f should be locally bounded, continuous in y for each fixed t , and measurable in t for each fixed y [50, Ch. 2, Theorem 1.1]. The dynamics of ζ in (54) satisfy the Caratheodory conditions.

$\zeta(t_0)$ is in \mathcal{S} given $\lambda_1, \lambda_2, \lambda_3, \lambda_4$, and v . The uniform ultimate bound is defined as⁴

$$\mathcal{U} \triangleq \left\{ z \in \mathbb{R}^{N(4n+2p)} : z \leq \sqrt{\frac{\lambda_2 v}{\lambda_1 \lambda_4}} \right\}. \quad (68)$$

The following theorem presents the main result.

Theorem 1. For target and agent dynamics in (13) and (15), respectively, the observer in (33), controller in (45), and the adaptive update law in (48) and (51) guarantee that for any initial condition of the states $\zeta(t_0) \in \mathcal{S}$, ζ exponentially converges to \mathcal{U} , where

$$\|\zeta(t)\| \leq \sqrt{\frac{\lambda_2}{\lambda_1} \left(\frac{v}{\lambda_4} + e^{-\frac{\lambda_4}{\lambda_2}(t-t_0)} \left(\|\zeta(t_0)\|^2 - \frac{v}{\lambda_4} \right) \right)}, \quad (69)$$

for all $t \in [t_0, \infty)$ given that the constants and control gains $\epsilon_3, \epsilon_1, \epsilon_2, k_1$, and k_2 are selected according to the sufficient conditions in (60)-(64), respectively and the sufficient gain condition $\lambda_3 > \lambda_4 + \rho\left(\sqrt{\frac{\lambda_2 v}{\lambda_1 \lambda_4}}\right)$ is satisfied.

Proof: Substituting (36), (47), (50), and (53) into the derivative of (55) yields

$$\begin{aligned} \dot{V} = & \alpha_1 \tilde{q}^T \tilde{q} - \alpha_2 \hat{e}^T \hat{e} - k_1 r_1^T \mathcal{H}^T \mathcal{H} r_1 + \tilde{q}^T r_1 \\ & - (k_2 - \alpha_2) r_2^T r_2 + r_1^T \mathcal{H}^T \nabla_{\hat{\theta}_1} \hat{\Phi}_1 \tilde{\theta}_1 + \hat{e}^T r_2 \\ & - r_2^T \nabla_{\hat{\theta}_2} \hat{\Phi}_2 \tilde{\theta}_2 + \alpha_1 r_1^T \mathcal{H}^T r_1 - \alpha_1^2 r_1^T \mathcal{H}^T \tilde{q} \\ & - \alpha_2^2 r_2^T \hat{e} + r_1^T \mathcal{H}^T \tilde{F} + r_1^T \mathcal{H}^T \chi_1 + r_1^T \mathcal{H} \epsilon_1 - r_2^T \chi_2 - r_2^T \epsilon_2 \\ & - \tilde{\theta}_1^T \Gamma_1^{-1} \left[\text{proj}(\aleph_{1,1}, \hat{\theta}_{1,1}, \bar{\theta})^T, \dots, \text{proj}(\aleph_{1,N}, \hat{\theta}_{1,N}, \bar{\theta})^T \right]^T \\ & - \tilde{\theta}_2^T \Gamma_2^{-1} \left[\text{proj}(\aleph_{2,1}, \hat{\theta}_{2,1}, \bar{\theta})^T, \dots, \text{proj}(\aleph_{2,N}, \hat{\theta}_{2,N}, \bar{\theta})^T \right]^T. \end{aligned} \quad (70)$$

Performing algebraic manipulation and applying [42, Lemma E.1.IV] yields the bound

$$\begin{aligned} & -\tilde{\theta}_1^T \Gamma_1^{-1} \left[\text{proj}(\aleph_{1,1}, \hat{\theta}_{1,1}, \bar{\theta})^T, \right. \\ & \left. \dots, \text{proj}(\aleph_{1,N}, \hat{\theta}_{1,N}, \bar{\theta})^T \right]^T \leq -\tilde{\theta}_1^T \Gamma_1^{-1} \aleph_1, \end{aligned} \quad (71)$$

where $\aleph_1 \triangleq [\aleph_{1,1}^T, \dots, \aleph_{1,N}^T]^T \in \mathbb{R}^{pN}$ and $\aleph_{1,i}$ is defined in (49). Similar to the graph interaction matrix in (35), we define the weight interaction matrix, \mathcal{J} as $\mathcal{J} \triangleq \mathcal{L}_G \otimes I_p$, where \mathcal{L}_G is the graph Laplacian and $\mathcal{J} \in \mathbb{R}^{pN \times pN}$. The ensemble form of $\aleph_{1,i}$ is⁵

$$\aleph_1 = \Gamma_1 \left(k_3 \mathcal{J} \tilde{\theta}_1 - k_3 \hat{\theta}_1 + \nabla_{\hat{\theta}_1} \hat{\Phi}_1^T \mathcal{H} r_1 \right). \quad (72)$$

Once again, we apply [42, Lemma E.1.IV] which yields the bound

$$\begin{aligned} & -\tilde{\theta}_2^T \Gamma_2^{-1} \left[\text{proj}(\aleph_{2,1}, \hat{\theta}_{2,1}, \bar{\theta})^T, \right. \\ & \left. \dots, \text{proj}(\aleph_{2,N}, \hat{\theta}_{2,N}, \bar{\theta})^T \right]^T \leq -\tilde{\theta}_2^T \Gamma_2^{-1} \aleph_2, \end{aligned} \quad (73)$$

⁴The radius of the set \mathcal{U} can be made smaller by setting the observer gain k_1 , controller gain k_2 , and constant ϵ_4 arbitrarily large, thus diminishing the impact of the GNN function approximation error. However, the set \mathcal{U} cannot be made arbitrarily small because it is limited by the size of the σ -modification gains k_3 and k_4 , which also dictate the rate of convergence of $\|\zeta(t)\|$.

⁵The terms featuring the weight interaction matrix \mathcal{J} in (72) and (74) function as a consensus protocol with respect to the GNN weights. Specifically, agents leverage their neighbors' estimates of the ideal GNN weights to refine their own estimates.

where $\aleph_2 \triangleq [\aleph_{2,1}^\top, \dots, \aleph_{2,N}^\top]^\top \in \mathbb{R}^{pN}$ and $\aleph_{2,i}$ is defined in (52). The ensemble form of $\aleph_{2,i}$ is

$$\aleph_2 = \Gamma_2 \left(k_4 \mathcal{J} \tilde{\theta}_2 - k_4 \hat{\theta}_2 - \nabla_{\hat{\theta}_2} \hat{\Phi}_2^\top r_2 \right). \quad (74)$$

Applying the bounds in (71) and (73) and substituting (72) and (74) into (70) gives

$$\begin{aligned} \dot{V} \leq & \alpha_1 \tilde{q}^\top \tilde{q} - \alpha_2 \hat{e}^\top \hat{e} - k_1 r_1^\top \mathcal{H}^\top \mathcal{H} r_1 \\ & - (k_2 - \alpha_2) r_2^\top r_2 - k_3 \tilde{\theta}_1^\top \tilde{\theta}_1 - k_4 \tilde{\theta}_2^\top \tilde{\theta}_2 \\ & + \tilde{q}^\top r_1 + \hat{e}^\top r_2 + \alpha_1 r_1^\top \mathcal{H}^\top r_1 - \alpha_1^2 r_1^\top \mathcal{H}^\top \tilde{q} \\ & - \alpha_2^2 r_2^\top \hat{e} + k_3 \tilde{\theta}_1^\top \theta_1^* - k_3 \tilde{\theta}_1^\top \mathcal{J} \tilde{\theta}_1 + k_4 \tilde{\theta}_2^\top \theta_2^* + r_1^\top \mathcal{H} \varepsilon_1 \\ & - k_4 \tilde{\theta}_2^\top \mathcal{J} \tilde{\theta}_2 + r_1^\top \mathcal{H}^\top \tilde{F} + r_1^\top \mathcal{H}^\top \chi_1 - r_2^\top \chi_2 - r_2^\top \varepsilon_2. \end{aligned} \quad (75)$$

We note that $\lambda_{\min}(\mathcal{J}) = \lambda_{\min}(\mathcal{L}_G) = 0$. Then, $-k_3 \tilde{\theta}_1^\top \mathcal{J} \tilde{\theta}_1 \leq 0$ and $-k_4 \tilde{\theta}_2^\top \mathcal{J} \tilde{\theta}_2 \leq 0$. Using Young's inequality yields the bounds

$$\begin{aligned} \tilde{q}^\top r_1 - \alpha_1^2 r_1^\top \mathcal{H}^\top \tilde{q} & \leq \frac{(1 + \alpha_1^2 \bar{\lambda}_{\mathcal{H}}) \epsilon_1}{2} \|r_1\|^2 \\ & + \frac{(1 + \alpha_1^2 \bar{\lambda}_{\mathcal{H}})}{2\epsilon_1} \|\tilde{q}\|^2, \end{aligned} \quad (76)$$

and

$$\hat{e}^\top r_2 - \alpha_2^2 r_2^\top \hat{e} \leq \frac{(1 + \alpha_2^2) \epsilon_2}{2} \|\hat{e}\|^2 + \frac{(1 + \alpha_2^2)}{2\epsilon_2} \|r_2\|^2, \quad (77)$$

where ϵ_1, ϵ_2 were introduced in (60) and (62), respectively. Using Young's inequality, Assumption 1, and Assumption 2 to upper-bound $r_1^\top \mathcal{H}^\top \tilde{F}$ yields

$$r_1^\top \mathcal{H} \tilde{F} \leq NL \bar{\lambda}_{\mathcal{H}} \|r_1\|^2 + NL \bar{\lambda}_{\mathcal{H}} (1 + \alpha_1) \|r_1\| \|\tilde{q}\|. \quad (78)$$

Using Young's inequality and nonlinear damping yields

$$-k_1 \bar{\lambda}_{\mathcal{H}}^2 \|r_1\|^2 - r_1^\top \mathcal{H}^\top \varepsilon_1 \leq -\frac{k_1}{2} \bar{\lambda}_{\mathcal{H}}^2 \|r_1\|^2 + \frac{\bar{\lambda}_{\mathcal{H}}^2 \bar{\varepsilon}_1^2}{2\lambda_{\mathcal{H}}^2 k_1}, \quad (79)$$

and

$$-k_2 \|r_2\|^2 - r_2^\top \varepsilon_2 \leq -\frac{k_2}{2} \|r_2\|^2 + \frac{\bar{\varepsilon}_2^2}{2k_2}. \quad (80)$$

By Young's inequality, Lemma 5, and Lemma 6, there exists some $\rho_{G,1} : \mathbb{R}_{\geq 0} \rightarrow \mathbb{R}_{\geq 0}$, $\rho_{G,2} : \mathbb{R}_{\geq 0} \rightarrow \mathbb{R}_{\geq 0}$, $\rho_{T,1} : \mathbb{R}_{\geq 0} \rightarrow \mathbb{R}_{\geq 0}$ and $\rho_{T,2} : \mathbb{R}_{\geq 0} \rightarrow \mathbb{R}_{\geq 0}$, such that $\rho_{G,1}, \rho_{G,2}, \rho_{T,1}$ and $\rho_{T,2}$ are strictly increasing functions. Then,

$$\begin{aligned} r_1^\top \mathcal{H} \chi_1 & \leq \frac{N \bar{\lambda}_{\mathcal{H}}}{2\epsilon_4} \\ & + N \bar{\lambda}_{\mathcal{H}} \left(\rho_{T,1}(\|\zeta\|) \|\zeta\| + \frac{\epsilon_4}{2} (\rho_{G,1}(\|\zeta\|))^2 \right) \|\zeta\|^2, \end{aligned} \quad (81)$$

and

$$\begin{aligned} r_2^\top \chi_2 & \leq \frac{N}{2\epsilon_4} \\ & + N \left(\rho_{T,2}(\|\zeta\|) \|\zeta\| + \frac{\epsilon_4}{2} (\rho_{G,2}(\|\zeta\|))^2 \right) \|\zeta\|^2, \end{aligned} \quad (82)$$

where $\epsilon_4 \in \mathbb{R}_{>0}$ is a user-defined constant. Since $\rho_{G,1}, \rho_{G,2}, \rho_{T,1}$ and $\rho_{T,2}$ are strictly increasing functions, there exist some strictly increasing functions $\rho_1 : \mathbb{R}_{\geq 0} \rightarrow \mathbb{R}_{\geq 0}$ and $\rho_2 : \mathbb{R}_{\geq 0} \rightarrow \mathbb{R}_{\geq 0}$ such that

$$N \bar{\lambda}_{\mathcal{H}} \left(\rho_{T,1}(\|\zeta\|) \|\zeta\| + \frac{\epsilon_4}{2} (\rho_{G,1}(\|\zeta\|))^2 \right) \leq \rho_1(\|\zeta\|), \quad (83)$$

and

$$N \left(\rho_{T,2}(\|\zeta\|) \|\zeta\| + \frac{\epsilon_4}{2} (\rho_{G,2}(\|\zeta\|))^2 \right) \leq \rho_2(\|\zeta\|). \quad (84)$$

Lastly, since ρ_1 and ρ_2 are strictly increasing functions, there exists some $\rho : \mathbb{R}_{\geq 0} \rightarrow \mathbb{R}_{\geq 0}$ such that $\rho(\|\zeta\|) > \rho_1(\|\zeta\|) + \rho_2(\|\zeta\|)$. Using (76)-(84) to upper-bound (75) yields

$$\begin{aligned} \dot{V} \leq & - \left(\alpha_1 - \frac{(1 + \alpha_1^2 \bar{\lambda}_{\mathcal{H}})}{2\epsilon_1} - \frac{NL \bar{\lambda}_{\mathcal{H}} (1 + \alpha_1)}{2\epsilon_3} \right) \|\tilde{q}\|^2 \\ & - \left(\alpha_2 - \frac{(1 + \alpha_2^2) \epsilon_2}{2} \right) \|\hat{e}\|^2 - \left(\frac{k_1 \bar{\lambda}_{\mathcal{H}}^2}{2} - \alpha_1 \bar{\lambda}_{\mathcal{H}} \right. \\ & - \frac{(1 + \alpha_1^2 \bar{\lambda}_{\mathcal{H}}) \epsilon_1}{2} - \frac{NL \bar{\lambda}_{\mathcal{H}} (1 + \alpha_1) \epsilon_3}{2} \\ & \left. - NL \bar{\lambda}_{\mathcal{H}} \right) \|r_1\|^2 - \left(\frac{k_2}{2} - \alpha_2 - \frac{(1 + \alpha_2^2)}{2\epsilon_2} \right) \|r_2\|^2 \\ & - \left(\frac{k_3}{2} \right) \|\tilde{\theta}_1\|^2 - \left(\frac{k_4}{2} \right) \|\tilde{\theta}_2\|^2 + \left(\frac{k_3}{2} + \frac{k_4}{2} \right) \bar{\theta}^2 \\ & + \frac{\bar{\lambda}_{\mathcal{H}}^2 \bar{\varepsilon}_1^2}{2\lambda_{\mathcal{H}}^2 k_1} + \frac{\bar{\varepsilon}_2^2}{2k_2} + \frac{N}{2\epsilon_4} (1 + \bar{\lambda}_{\mathcal{H}}) + \rho(\|\zeta\|) \|\zeta\|^2. \end{aligned} \quad (85)$$

Provided constants and control gains $\epsilon_3, \epsilon_1, \epsilon_2, k_1$, and k_2 are selected according to the sufficient conditions in (60)-(64), respectively, then (58) can be used to upper-bound (85) as

$$\dot{V} \leq -(\lambda_3 - \rho(\|\zeta\|)) \|\zeta\|^2 + v, \quad (86)$$

for all $t \in \mathcal{I}$, where v is defined in (65) and λ_3 is defined in (59). Since the solution $t \mapsto \zeta(t)$ is continuous, we have $\zeta(t) \in \mathcal{D}$ for all $t \in \mathcal{I}$. Consequently, applying (58) to (86) yields

$$\dot{V} \leq -\frac{\lambda_4}{\lambda_2} V(\zeta) + v, \quad (87)$$

for all $t \in \mathcal{I}$. Solving the differential inequality in (87) over \mathcal{I} gives

$$V(\zeta(t)) \leq V(\zeta(t_0)) e^{-\frac{\lambda_4}{\lambda_2}(t-t_0)} + \frac{\lambda_2 v}{\lambda_4} \left(1 - e^{-\frac{\lambda_4}{\lambda_2}(t-t_0)} \right). \quad (88)$$

Applying (58) and (88) yields

$$\|\zeta(t)\| \leq \sqrt{e^{-\frac{\lambda_4}{\lambda_2}(t-t_0)} \left(\frac{\lambda_2}{\lambda_1} \|\zeta(t_0)\|^2 - \frac{\lambda_2 v}{\lambda_1 \lambda_4} \right) + \frac{\lambda_2 v}{\lambda_1 \lambda_4}}, \quad (89)$$

for all $t \in \mathcal{I}$. Next, we must show that \mathcal{I} can be extended to $[t_0, \infty)$.

Let $t \mapsto \zeta(t)$ be a solution to the ordinary differential equation (54) with initial condition $\zeta(t_0) \in \mathcal{S}$. By [42, Lemma E.1], the projection operator defined in (4) is locally Lipschitz in its arguments. Then, the right hand side of (54) is piecewise continuous in t and locally Lipschitz in ζ for all $t \geq t_0$ and $\zeta \in \mathbb{R}^{N(4n+2p)}$. Taking the upper-bound of (89) yields

$$\|\zeta(t)\| < \sqrt{\frac{\lambda_2}{\lambda_1}} \|\zeta(t_0)\| + \sqrt{\frac{\lambda_2 v}{\lambda_1 \lambda_4}}, \quad (90)$$

for all $t \in \mathcal{I}$. Since $\zeta(t_0) \in \mathcal{S}$, we have that

$$\|\zeta(t_0)\| < \sqrt{\frac{\lambda_1}{\lambda_2} \bar{\rho}^{-1}} (\lambda_3 - \lambda_4 - \rho(0)) - \sqrt{\frac{v}{\lambda_4}}. \quad (91)$$

Applying (91) to (90) gives $\|\zeta(t)\| < \bar{\rho}^{-1}(\lambda_3 - \lambda_4 - \rho(0))$ for all $t \in \mathcal{I}$, which by the definition of (66), yields $\zeta(t) \in \mathcal{D}$ for all $t \in \mathcal{I}$. Since $\zeta(t)$ remains in the compact set $\mathcal{D} \subset \mathbb{R}^{N(4n+2p)}$ for all $t \in \mathcal{I}$, by [51, Theorem 3.3], a unique solution exists for all $t \geq t_0$. Therefore, $\mathcal{I} = [t_0, \infty)$.

Thus, for $\zeta(t_0) \in \mathcal{S}$, we have

$$\|\zeta(t)\| \leq \sqrt{e^{-\frac{\lambda_4}{\lambda_2}(t-t_0)} \left(\frac{\lambda_2}{\lambda_1} \|\zeta(t_0)\|^2 - \frac{\lambda_2 v}{\lambda_1 \lambda_4} \right) + \frac{\lambda_2 v}{\lambda_1 \lambda_4}}, \quad (92)$$

and $\zeta(t) \in \mathcal{D}$ for all $t \in [t_0, \infty)$. The limit of (92) as $t \rightarrow \infty$ yields $\|\zeta\| \leq \sqrt{\frac{\lambda_2 v}{\lambda_1 \lambda_4}}$, which indicates that $\zeta(t)$ converges to the set \mathcal{U} . For any bounded set $\mathcal{C} \subset \mathbb{R}^{N(4n+2p)}$ with radius $R_{\mathcal{C}} > 0$, selecting $\lambda_3 > \lambda_4 + \rho(\sqrt{\frac{\lambda_2}{\lambda_1}} R_{\mathcal{C}} + \sqrt{\frac{\lambda_2 v}{\lambda_1 \lambda_4}})$ ensures that

$\|\zeta(t)\| \leq \sqrt{e^{-\frac{\lambda_4}{\lambda_2}(t-t_0)} \left(\frac{\lambda_2}{\lambda_1} \|\zeta(t_0)\|^2 - \frac{\lambda_2 v}{\lambda_1 \lambda_4} \right) + \frac{\lambda_2 v}{\lambda_1 \lambda_4}}$. This implies the stability result is semi-global [52, Remark 2], as the set of stabilizing initial conditions can be made arbitrarily large by appropriately adjusting λ_3 to encompass any bounded subset of $\mathbb{R}^{N(4n+2p)}$.

Next, we prove that Assumption 2 holds for all $t \in \mathbb{R}_{\geq 0}$, which states that the unknown drift dynamics modeled by $f(Q_0)$ are Lipschitz on the set $\mathcal{Y}_{1,i}$, where the Lipschitz constant has a known upper bound L . Since $\zeta(t) \in \mathcal{D}$ for all $t \in [t_0, \infty)$, it follows that $\|\zeta(t)\| \leq c_{\zeta}$ for all $t \in [t_0, \infty)$. Applying the triangle inequality, (17), and (20) yields $\|Q_0 - \hat{Q}_{0,i}\| \leq c_{\zeta}(2 + \alpha_1)$ for $\zeta \in \mathcal{D}$. Thus, $Q_0 - \hat{Q}_{0,i} \in \mathcal{Y}_{1,i}$ for all $i \in V$ and Assumption 2 holds everywhere.

We prove that $\hat{Q}_{0,i} \in \mathcal{Y}_{1,i}$ for all $i \in V$ such that Lemma 3 holds by applying (17), (19), and Assumption 1 as above to find $\|\hat{Q}_{0,i}\| \leq \bar{q}_0 + \bar{q}_0 + c_{\zeta}(2 + \alpha_1)$ for $\zeta \in \mathcal{D}$. Thus, $\hat{Q}_{0,i} \in \mathcal{Y}_{1,i}$ for all $i \in V$, $\hat{Q}_0 \in \mathcal{Y}_1$, and the universal function approximation property of the deep Lb-GNN Φ_1 described in Lemma 3 holds everywhere. We repeat this process to show that Lemma 3 holds for the deep Lb-GNN Φ_2 . We upper-bound $\|Q_i\|$ using Assumption 1 and the triangle inequality which yields

$$\|Q_i\| \leq \bar{q}_0 + \bar{q}_0 + c_{\zeta}(3 + \alpha_1 + \alpha_2), \quad (93)$$

for $\zeta \in \mathcal{D}$. Next, we upper-bound $\|R_i\|$. We apply the triangle inequality, (93), and the fact that $\|R_i\|$ is the largest for a fully connected graph, where $\frac{1}{N_i}(m) = 1$ for all $m \in V$, which yields $\|R_i\| \leq N(\bar{q}_0 + \bar{q}_0 + c_{\zeta}(3 + \alpha_1 + \alpha_2))$ for $\zeta \in \mathcal{D}$. Therefore, for $\zeta \in \mathcal{D}$, $R_i \in \mathcal{Y}_{2,i}$ holds for all $i \in V$, $R \in \mathcal{Y}_2$, and the universal function approximation property of the deep GNN Φ_2 described in Lemma 3 holds everywhere.

Since $\|\zeta\| \leq c_{\zeta}$, $\|\tilde{q}\|, \|\hat{e}\|, \|r_1\|, \|r_2\|, \|\hat{\theta}_1\|, \|\hat{\theta}_2\| \leq c_{\zeta}$. Therefore, $\|\tilde{q}\|, \|\hat{e}\|, \|r_1\|, \|r_2\|, \|\hat{\theta}_1\|, \|\hat{\theta}_2\| \in \mathcal{L}_{\infty}$. Since $\|\tilde{q}\|, \|r_1\| \in \mathcal{L}_{\infty}$, then $\|\hat{Q}_0\| \in \mathcal{L}_{\infty}$. Based on the fact that $\|\hat{Q}_0\| \in \mathcal{L}_{\infty}$ and the use of the projection operator in (48), $\|\hat{\Phi}_1\|$ is bounded. Since $\|\hat{e}\|, \|r_2\| \in \mathcal{L}_{\infty}$, then $\|R\| \in \mathcal{L}_{\infty}$. Based on the fact that $\|R\| \in \mathcal{L}_{\infty}$ and the use of the projection operator in (51), $\|\hat{\Phi}_2\|$ is bounded. Based on the fact that $\|\hat{\theta}_1\|, \|\hat{\theta}_2\| \in \mathcal{L}_{\infty}$, the use of the projection operator, and the use of a bounded search space in (27) and (39), $\|\hat{\theta}_1\|, \|\hat{\theta}_2\| \in \mathcal{L}_{\infty}$. Based on the use of activation functions with bounded derivatives and the fact that $\|\hat{Q}_0\|, \|R\|, \|\hat{\theta}_1\|, \|\hat{\theta}_2\| \in \mathcal{L}_{\infty}$, $\|\nabla_{\hat{\theta}_1} \hat{\Phi}_1\|$ and $\|\nabla_{\hat{\theta}_2} \hat{\Phi}_2\|$ are

bounded. Let $\ddot{q}_0 \triangleq [\ddot{q}_{0,i}^T]_{i \in V}^T \in \mathbb{R}^{nN}$. Based on the fact that $\|r_1\|, \|\hat{\theta}_1\| \in \mathcal{L}_{\infty}$ and the boundedness of $\|\hat{\Phi}_1\|$ and $\|\nabla_{\hat{\theta}_1} \hat{\Phi}_1\|$, $\|\ddot{q}_0\|$ is bounded. Let $u \triangleq [u_i^T]_{i \in V}^T \in \mathbb{R}^{nN}$. Based on the fact that $\|r_2\|, \|\hat{\theta}_2\| \in \mathcal{L}_{\infty}$ and the boundedness of $\|\hat{\Phi}_2\|$, $\|\nabla_{\hat{\theta}_2} \hat{\Phi}_2\|$, and $\|\ddot{q}_0\|, \|u\|$ is bounded. Based on the fact that $\|\hat{\theta}_1\|, \|\hat{\theta}_2\|, \|r_1\| \in \mathcal{L}_{\infty}$ and the boundedness of $\|\nabla_{\hat{\theta}_1} \hat{\Phi}_1\|$, $\|\hat{\theta}_1\|$ is bounded. Based on the fact that $\|\hat{\theta}_2\|, \|\hat{\theta}_2\|, \|r_2\| \in \mathcal{L}_{\infty}$ and the boundedness of $\|\nabla_{\hat{\theta}_2} \hat{\Phi}_2\|$, $\|\hat{\theta}_2\|$ is bounded. ■

VII. SIMULATION RESULTS

To demonstrate the performance of the developed GNN and GAT control designs, simulations were performed with a network of $N = 6$ agents tasked with tracking a moving target. Each simulation was performed for a duration of 60 seconds. An all-layer first partial derivative of a DNN with respect to its weights as developed in [2] for DNNs with smooth activation functions was used as a baseline for the adaptive update law in (48). The DNN architectures listed in Table II correspond to Φ_1 and Φ_2 for each simulation, e.g., the GAT + GNN configuration indicates that Φ_1 uses the GAT architecture and Φ_2 uses the GNN architecture. Let $\tilde{\Phi}_1 \triangleq \hat{\Phi}_1 - F(Q_0)$ denote the function approximation error of the DNN Φ_1 and let $\tilde{\Phi}_2 \triangleq \hat{\Phi}_2 - H(R)$ denote the function approximation error of the DNN Φ_2 . The quantities listed in Table II are as follows: e_{RMS} denotes the average RMS position tracking between agents and target, \dot{e}_{RMS} denotes the average RMS velocity tracking between agents and target, $\tilde{\Phi}_{1,\text{RMS}}[X : Y]$ denotes the average RMS function approximation error of Φ_1 from X seconds to Y seconds, $\tilde{\Phi}_{2,\text{RMS}}[X : Y]$ denotes the average RMS function approximation error of Φ_2 from X seconds to Y seconds, and u_{RMS} denotes the average RMS control effort of the agents.

The target has drift dynamics

$$\begin{bmatrix} \ddot{x}_0 \\ \ddot{y}_0 \\ \ddot{z}_0 \end{bmatrix} = \begin{bmatrix} \cos(\dot{x}_0) - \sin(\dot{y}_0) + \cos(2\dot{z}_0) \\ \dot{x}_0 - \dot{y}_0 + \dot{z}_0 + \frac{y_0}{\sqrt{1+|y_0|}} \\ \sin(\dot{y}_0) - \dot{x}_0 \dot{z}_0 \end{bmatrix},$$

where $q_0 \triangleq [x_0, y_0, z_0]^T$ denotes the target's spatial coordinates in \mathbb{R}^3 and $\dot{q}_0 \triangleq [\dot{x}_0, \dot{y}_0, \dot{z}_0]^T$ denotes the target's velocity in \mathbb{R}^3 . The dynamics of the agents are given by

$$\begin{bmatrix} \ddot{x}_i \\ \ddot{y}_i \\ \ddot{z}_i \end{bmatrix} = \begin{bmatrix} \sum_{j \in \mathcal{N}_i} \frac{1}{20,000(y_i - y_j)^2} \\ \sum_{j \in \mathcal{N}_i} (\dot{z}_i - \dot{z}_j) \cos(\dot{x}_i) \\ \sum_{j \in \mathcal{N}_i} \cos(\dot{z}_i \dot{z}_j) \frac{\dot{x}_i - \dot{x}_j}{\sqrt{1+|\dot{x}_i - \dot{x}_j|}} \end{bmatrix} + u_i,$$

where $q_i \triangleq [x_i, y_i, z_i]^T$ denotes the agent's spatial coordinates in \mathbb{R}^3 and $\dot{q}_i \triangleq [\dot{x}_i, \dot{y}_i, \dot{z}_i]^T$ denotes the agent's velocity in \mathbb{R}^3 . The initial conditions of the agents were selected to form an equilateral N -gon around the origin with radius of 10 m . The initial position of the target was selected such that $q_0(t_0) = [-3, 2, 10]^T m$, and the initial velocity of the target was selected such that $\dot{q}_0(t_0) = [-1, 0, -2]^T m/s$. The following communication topologies were considered: path, ring, star, complete, and acyclic. In the star configuration, all agents are connected to a pinned agent where $b_i = 1$. For all

TABLE II

PERFORMANCE COMPARISON RESULTS FOR VARIOUS NN ARCHITECTURES AND COMMUNICATION TOPOLOGIES. FOR A NETWORK OF N AGENTS AND A SIGNAL $s_i(\mathbf{k}) \in \mathbb{R}^n$ WITH $\mathbf{k} \in \mathbb{Z}_{>0}$ SAMPLES, THE AVERAGE ROOT MEAN SQUARE (RMS) VALUE OF THE SIGNAL s_{RMS} IS GIVEN AS $s_{\text{RMS}} \triangleq 1/N \cdot \sum_{i \in V} (1/K \cdot \sum_{\mathbf{k}=1}^K s_i(\mathbf{k})^\top s_i(\mathbf{k}))$.

Path Graph (P_6)							
NN Architecture	e_{RMS}	\dot{e}_{RMS}	$\tilde{\Phi}_{1,\text{RMS}}[0:10]$	$\tilde{\Phi}_{1,\text{RMS}}[10:60]$	$\tilde{\Phi}_{2,\text{RMS}}[0:10]$	$\tilde{\Phi}_{2,\text{RMS}}[10:60]$	u_{RMS}
DNN+DNN	0.4615	0.4207	0.8241	0.5414	0.2755	0.0801	1.088
GNN+GNN	0.3745	0.4008	0.8921	0.4809	2.468	0.0855	1.420
GAT+GNN	0.2826	0.3614	2.289	0.4017	2.698	0.0688	1.621
Ring Graph (R_6)							
NN Architecture	e_{RMS}	\dot{e}_{RMS}	$\tilde{\Phi}_{1,\text{RMS}}[0:10]$	$\tilde{\Phi}_{1,\text{RMS}}[10:60]$	$\tilde{\Phi}_{2,\text{RMS}}[0:10]$	$\tilde{\Phi}_{2,\text{RMS}}[10:60]$	u_{RMS}
DNN+DNN	0.4389	0.4027	0.8243	0.5390	0.2773	0.0800	1.086
GNN+GNN	0.3144	0.3609	0.9347	0.4346	2.131	0.0799	1.399
GAT+GNN	0.2730	0.3415	2.304	0.3737	2.549	0.0632	1.616
Star Graph (S_6)							
NN Architecture	e_{RMS}	\dot{e}_{RMS}	$\tilde{\Phi}_{1,\text{RMS}}[0:10]$	$\tilde{\Phi}_{1,\text{RMS}}[10:60]$	$\tilde{\Phi}_{2,\text{RMS}}[0:10]$	$\tilde{\Phi}_{2,\text{RMS}}[10:60]$	u_{RMS}
DNN+DNN	0.5198	0.4676	0.8230	0.5473	0.3605	0.0831	1.105
GNN+GNN	0.4120	0.4584	0.9971	0.5087	2.549	0.0828	1.556
GAT+GNN	0.2942	0.3968	2.069	0.3879	2.481	0.0645	1.792
Complete Graph (K_6)							
NN Architecture	e_{RMS}	\dot{e}_{RMS}	$\tilde{\Phi}_{1,\text{RMS}}[0:10]$	$\tilde{\Phi}_{1,\text{RMS}}[10:60]$	$\tilde{\Phi}_{2,\text{RMS}}[0:10]$	$\tilde{\Phi}_{2,\text{RMS}}[10:60]$	u_{RMS}
DNN+DNN	0.4267	0.3922	0.8241	0.5378	0.8817	0.0793	1.131
GNN+GNN	0.2680	0.3105	2.070	0.3364	2.220	0.0494	1.430
GAT+GNN	0.2607	0.3161	2.434	0.3281	2.181	0.0614	1.482
Acyclic Graph							
NN Architecture	e_{RMS}	\dot{e}_{RMS}	$\tilde{\Phi}_{1,\text{RMS}}[0:10]$	$\tilde{\Phi}_{1,\text{RMS}}[10:60]$	$\tilde{\Phi}_{2,\text{RMS}}[0:10]$	$\tilde{\Phi}_{2,\text{RMS}}[10:60]$	u_{RMS}
DNN+DNN	0.4836	0.4394	0.8240	0.5436	0.4391	0.0812	1.102
GNN+GNN	0.3952	0.4250	0.9185	0.4919	2.174	0.0834	1.411
GAT+GNN	0.2912	0.3900	2.256	0.4110	2.242	0.0662	1.568

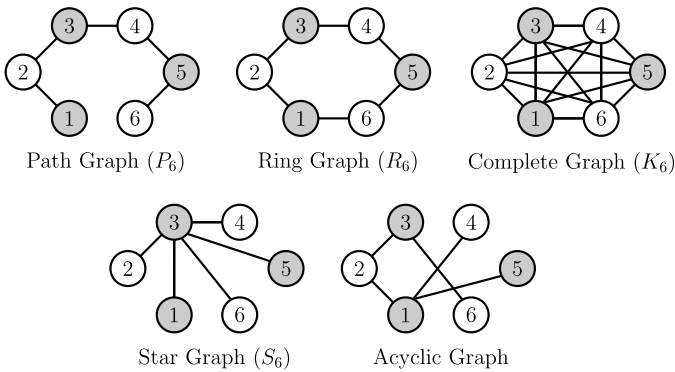


Fig. 3. Visualization of communication topologies examined in Table II. Shaded agents are connected to the target, where $b_i = 1$.

communication topologies, half of the agents are connected to the target such that $b_i = 1$.

The GAT was used only for the approximation of the unknown target dynamics because the updates from agents not connected to the target are less informative than the agents who are connected to the target. The use of attention helps to

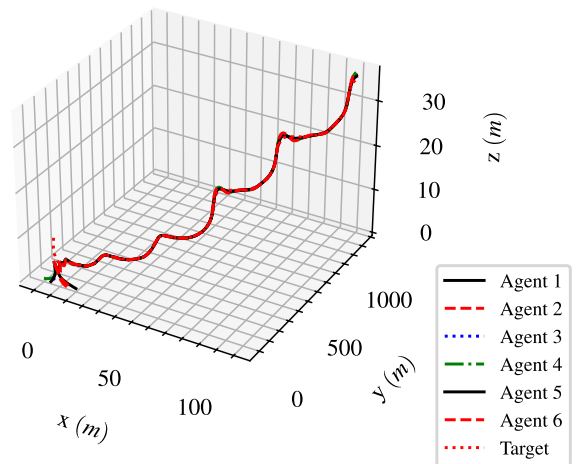


Fig. 4. Trajectory visualization for the GNN+GNN configuration and acyclic graph communication topology.

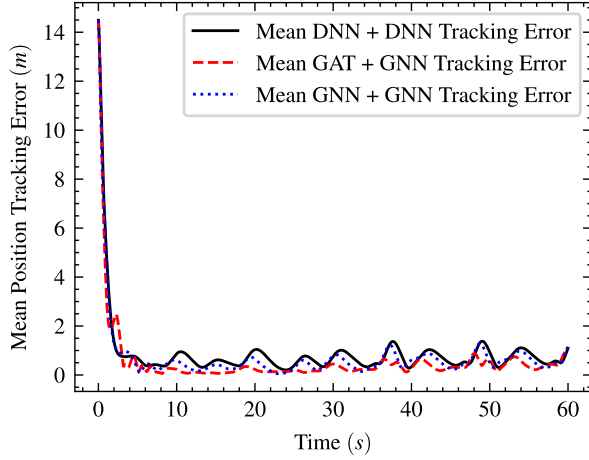


Fig. 5. Mean position tracking error response for each NN architecture with the acyclic graph communication topology.

discern between these updates. However, the updates from all neighbors should be weighted equally to approximate agent interaction dynamics, motivating the use of the standard GNN rather than the GAT to approximate the unknown interaction dynamics.

In all simulations, each agent was initialized using the same set of weights. For all $i \in V$ and $j \in \{0, \dots, k\}$, the weights of the DNN and GNN were initialized from the distribution $W_i^{(j)} \sim \mathcal{N}(0, 0.03)$ and the weights of the GAT were initialized from the distribution $W_i^{(j)} \sim \mathcal{N}(0, 0.3)$, where $W_i^{(j)} \in \mathbb{R}^{(d^{(j-1)}+1) \times d^{(j)}}$. For all $i \in V$ and $j \in \{0, \dots, k-1\}$, the attention weights of the j^{th} layer of the GAT were initialized from the distribution $a_i^{(j)} \sim \mathcal{N}(0, 0.3)$, where $a_i^{(j)} \in \mathbb{R}^{1 \times 2d^{(j)}}$. These distributions were empirically found to yield the best results for each architecture. The $\tanh(\cdot)$ activation function was used for all hidden layers in all architectures.

Gain values were empirically selected and held constant for all NN configurations. For all $i \in V$, the chosen gains are as follows: $\alpha_1 = 0.85, \alpha_2 = 2.45, k_1 = 6.5, k_2 = 3.85, k_3 = 0.01, k_4 = 0.08$, and $\Gamma_1 = \Gamma_2 = 0.875 \cdot I_{p \times p}$. For every agent, the DNN architecture has 6 layers and 24 neurons at each layer while the GNN and GAT architectures have 2 layers and 24 neurons at each layer. The number of GNN layers must be carefully selected for decentralized applications. Due to the message-passing framework of the GNN, the number of required successive communications between neighbors is equivalent to the number of message-passing layers in the network. In the multi-agent control literature, the number of GNN layers is typically limited to between 1 and 4 layers [30], [31], [36].

A three-dimensional visualization of the agents and target for the GNN architecture and the acyclic graph communication topology is given in Fig. 4. As seen in Fig. 5, which shows the mean position tracking error performance of all NN configurations, the transient performance in the first 3 seconds is the same for all NN architectures because the robust state-feedback terms are predominant in the control input, and the

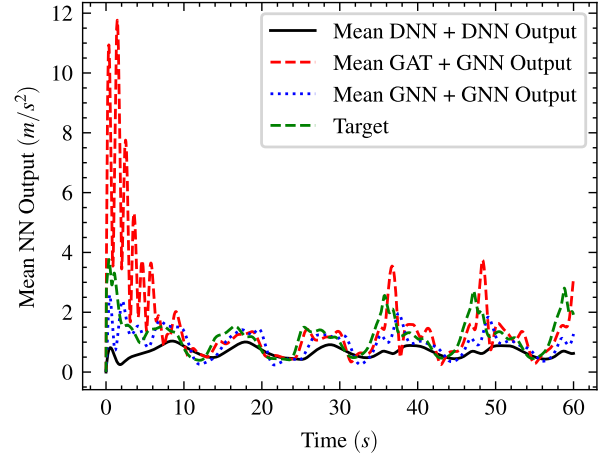


Fig. 6. Mean NN output with the acyclic graph communication topology.

NNs have just started to learn the target dynamics. However, after 3 seconds, the differences in precision of the target tracking are more prevalent. As evidenced in Fig. 6, which shows the mean function approximation capabilities of all NN configurations with respect to the mean drift dynamics of the target agent, the GNN + GNN and GAT + GNN configurations are able to achieve more accurate estimates of the target dynamics than the DNN + DNN configuration.

The initial spike in the function approximation error in Fig. 6 is a consequence of the message-passing framework of the GNN architecture. When the network is initialized, the estimate of the target dynamics is inaccurate for all agents. When these estimates are exchanged among nodes in the forward pass, the initial function approximation error is amplified. The function approximation overshoot is quickly corrected as the GNN learns. The same transient performance is not seen for the DNN + DNN configuration. The lack of compensation for the unknown target and interaction dynamics by the DNN leads to the oscillatory tracking error performance seen in Fig. 5.

The performance improvement offered by the GNN and GAT architectures is most apparent in communication topologies that are less connected. In the path graph communication topology, the GNN + GNN and GAT + GNN configurations yielded a 20.8% and 48.1% improvement over the baseline RMS position tracking error performance of the DNN + DNN configuration, respectively. The improvement in RMS position tracking error performance can be attributed to the GNN and GAT's ability to leverage information from neighboring nodes during the forward pass. Incorporating neighborhood messages in each GNN update allows the network to accurately learn the target dynamics even when few agents are connected to the target and not all agents can communicate. The developed GNN and GAT-based controllers are impactful for implementation in real-world distributed systems, where achieving fully connected communication topologies can be challenging due to onboard hardware constraints.

VIII. CONCLUSION

In this work, a new Lyapunov-based GNN adaptive controller and observer are developed to address the second-order target tracking problem with unknown target dynamics and unknown inter-agent interaction dynamics. Real-time training methods for the GNN and GAT architectures are introduced. Additionally, a new distributed weight adaptation law is developed to ensure exponential convergence of each agent's GNN weights to a neighborhood of the ideal values. A Lyapunov-based stability analysis is conducted to guarantee exponential convergence of the target state estimates and agent states to a neighborhood of the target state. Numerical simulations validate the theoretical findings, revealing that the GNN and GAT architectures achieve 20.8% and 48.1% improvements in position tracking error performance, respectively, compared to a baseline DNN architecture. These results were demonstrated using a network of 6 agents with a path communication topology, indicating that GNN and GAT architectures offer particular advantages for practical distributed systems where complete network connectivity is often constrained by hardware limitations. Future applications of the GNN architecture include distributed state estimation with partial feedback for a target with unknown dynamics as well as consensus and formation control for multi-agent systems with unknown dynamics.

APPENDIX

Proof of Lemma 1: The recursive model of the GNN architecture in (6) is given as

$$\phi_i = W_i^{(k)\top} \sigma^{(k-1)} \left(W_i^{(k-1)\top} \left[\phi_{m^{(k-1)}}^{(k-2)} \right]_{\mathbf{m}^{(k-1)}} \bar{A}_i^\top \right). \quad (94)$$

We begin by taking the partial derivative of (94) with respect to $\text{vec}(W_i^{(j)})$, which yields

$$\begin{aligned} \frac{\partial \phi_i}{\partial \text{vec}(W_i^{(j)})} &= W_i^{(k)\top} \pi_i^{(k-1)} W_i^{(k-1)\top} \\ &\cdot \tau_i^{(k-1)} \left[\left(\frac{\partial}{\partial \text{vec}(W_i^{(j)})} \phi_{m^{(k-1)}}^{(k-2)} \right)^\top \right]_{\mathbf{m}^{(k-1)}}^\top. \end{aligned} \quad (95)$$

Next, we evaluate the partial derivative of $\phi_{m^{(k-1)}}^{(k-2)}$ with respect to $\text{vec}(W_i^{(j)})$. This operation yields

$$\begin{aligned} \frac{\partial \phi_{m^{(k-1)}}^{(k-2)}}{\partial \text{vec}(W_i^{(j)})} &= \pi_{m^{(k-1)}}^{(k-2)} W_{m^{(k-1)}}^{(k-2)\top} \\ &\cdot \tau_{m^{(k-1)}}^{(k-2)} \left[\left(\frac{\partial}{\partial \text{vec}(W_i^{(j)})} \phi_{m^{(k-2)}}^{(k-3)} \right)^\top \right]_{\mathbf{m}^{(k-2)}}^\top. \end{aligned} \quad (96)$$

Equation (96) has the same derivative structure seen in (95), but with a deeper layer index. We continue executing the partial derivatives of $\phi_{m^{(\ell)}}^{(\ell-1)}$ from $\ell = k-1, k-2, \dots, j+1$ until $\ell = j$, where

$$\frac{\partial \phi_{m^{(j+1)}}^{(j)}}{\partial \text{vec}(W_i^{(j)})} = \pi_{m^{(j+1)}}^{(j)} \frac{\partial}{\partial \text{vec}(W_i^{(j)})} l_{m^{(j+1)}}^{(j)} \text{vec}(W_{m^{(j+1)}}^{(j)}).$$

We note that $\frac{\partial}{\partial \text{vec}(W_i^{(j)})} \text{vec}(W_{m^{(j+1)}}^{(j)}) = \mathbf{0}_{d^{(j)} \times (d^{(j-1)+1}}$ if $m^{(j+1)} \neq i$. Therefore,

$$\frac{\partial \phi_{m^{(j+1)}}^{(j)}}{\partial \text{vec}(W_i^{(j)})} = \pi_{m^{(j+1)}}^{(j)} \delta_{i, m^{(j+1)}} l_{m^{(j+1)}}^{(j)}. \quad (97)$$

Next, we leverage a recursive term to capture the nested structure of the partial derivative of ϕ_i with respect to $\text{vec}(W_i^{(j)})$. Recall the definitions of $\Delta_i^{(j)} \in \mathbb{R}^{(d^{(j)+1}) \times N(d^{(j-1)+1)}$ and $\varphi_{m^{(\ell+1)}}^{(\ell)} \in \mathbb{R}^{(d^{(\ell)+1}) \times d^{(\ell)}(d^{(\ell-1)+1)}$ from Table III. We note that $\varphi_{m^{(\ell+1)}}^{(\ell)}$ for $\ell = k-1, \dots, j+1$ captures the structure of the partial derivative in (95) and (96), while $\varphi_{m^{(\ell+1)}}^{(\ell)}$ for $\ell = j$ captures the root partial derivative in (97). Therefore, the partial derivative of ϕ_i with respect to $\text{vec}(W_i^{(j)})$ is equal to

$$\frac{\partial \phi_i}{\partial \text{vec}(W_i^{(j)})} = W_i^{(k)\top} \varphi_i^{(k-1)},$$

where $\frac{\partial \phi_i}{\partial \text{vec}(W_i^{(j)})} \in \mathbb{R}^{d^{(k)} \times d^{(j)}(d^{(j+1)+1)}$. Then, the first partial derivative of the GNN architecture in (6) with respect to (7) is equal to (8). ■

Proof of Lemma 2: We begin by taking the partial derivative of the outer layer of the GAT architecture in (10) with respect to $\text{vec}(W_i^{(j)})$ as

$$\begin{aligned} \frac{\partial \phi_i}{\partial \text{vec}(W_i^{(j)})} &= W_i^{(k)\top} \Delta_i^{(k-1)} \\ &\cdot \left[\left(\frac{\partial}{\partial \text{vec}(W_i^{(j)})} \phi_{m^{(k-1)}}^{(k-2)} \beta_{i, m^{(k-1)}}^{(k-1)} \right)^\top \right]_{\mathbf{m}^{(k-1)}}^\top. \end{aligned} \quad (98)$$

Note that both $\phi_{m^{(k-1)}}^{(k-2)}$ and $\beta_{i, m^{(k-1)}}^{(k-1)}$ are functions of $W_i^{(j)}$. Therefore, we apply the product rule to (98) which gives

$$\begin{aligned} \frac{\partial \phi_i}{\partial \text{vec}(W_i^{(j)})} &= W_i^{(k)\top} \Delta_i^{(k-1)} \left[\left(\frac{\partial \phi_{m^{(k-1)}}^{(k-2)}}{\partial \text{vec}(W_i^{(j)})} \beta_{i, m^{(k-1)}}^{(k-1)} \right. \right. \\ &\left. \left. + \phi_{m^{(k-1)}}^{(k-2)} \frac{\partial \beta_{i, m^{(k-1)}}^{(k-1)}}{\partial \text{vec}(W_i^{(j)})} \right)^\top \right]_{\mathbf{m}^{(k-1)}}^\top. \end{aligned} \quad (99)$$

Evaluating the partial derivative of $\phi_{m^{(k-1)}}^{(k-2)}$ with respect to $\text{vec}(W_i^{(j)})$ yields

$$\Lambda_{m^{(k-1)}}^{(k-2)} \triangleq \frac{\partial \phi_{m^{(k-1)}}^{(k-2)}}{\partial \text{vec}(W_i^{(j)})} = \Delta_{m^{(k-1)}}^{(k-2)}$$

$$\cdot \left[\left(\frac{\partial}{\partial \text{vec}(W_i^{(j)})} \phi_{m^{(k-2)}}^{(k-3)} \beta_{m^{(k-1)}, m^{(k-2)}}^{(k-2)} \right)^\top \right]_{\mathbf{m}^{(k-2)}}^\top.$$

Evaluating the partial derivative of $\beta_{i, m^{(k-2)}}^{(k-1)}$ with respect to $\text{vec}(W_i^{(j)})$ yields

$$\frac{\partial \beta_{i, m^{(k-2)}}^{(k-1)}}{\partial \text{vec}(W_i^{(j)})} = \frac{\partial}{\partial \text{vec}(W_i^{(j)})} \frac{\exp \left(c_{i, m^{(k-2)}}^{(k-1)} \right)}{\exp \left(c_{i, m^{(k-2)}}^{(k-1)} \right) \bar{A}_i^\top}. \quad (100)$$

TABLE III
DEFINITIONS OF TERMS USED IN COMPUTING THE FIRST PARTIAL DERIVATIVES OF THE GNN AND GAT ARCHITECTURES WITH RESPECT TO THEIR WEIGHT VECTORS.

Term	Definition	Term Dimensions
$\pi_i^{(\ell)}$	$\triangleq \frac{\partial \sigma^{(\ell)}(x_i^{(\ell)})}{\partial x_i^{(\ell)}}$	$(d^{(\ell)} + 1) \times d^{(\ell)}$
$\xi_i^{(\ell)}$	$\triangleq I_{d^{(\ell)}} \otimes \phi_i^{(\ell-1)\top}$	$d^{(\ell)} \times d^{(\ell)} (d^{(\ell-1)} + 1)$
$\iota_i^{(\ell)}$	$\triangleq I_{d^{(\ell)}} \otimes (\bar{A}_i \phi^{(\ell-1)\top})$	$d^{(\ell)} \times d^{(\ell)} (d^{(\ell-1)} + 1)$
$\Delta_i^{(\ell)}$	$\triangleq \pi_i^{(\ell)} W_i^{(\ell)\top} \tau_i^{(\ell)}$	$(d^{(\ell)} + 1) \times N (d^{(\ell-1)} + 1)$
$\gamma_{i,m}^{(\ell)}$	$\triangleq \exp(c_{i,m}^{(\ell)})$	1×1
$\epsilon_i^{(\ell)}$	$\triangleq \exp(c_i^{(\ell)}) \bar{A}_i^\top$	1×1
$\eta_i^{(\ell)}$	$\triangleq \frac{1}{(\exp(c_i^{(\ell)}) \bar{A}_i^\top)^2}$	1×1
$\tau_i^{(\ell)}$	$\triangleq \bar{A}_i \otimes I_{(d^{(\ell-1)}+1)}$	$(d^{(\ell-1)} + 1) \times N (d^{(\ell-1)} + 1)$
$\varphi_{m^{(\ell+1)}}^{(\ell)}$	$\triangleq \begin{cases} \Delta_{m^{(\ell+1)}}^{(\ell)} [(\varphi_{m^{(\ell+1)}}^{(\ell-1)})^\top]^\top_{\mathbf{m}^{(\ell)}}, & \ell = k-1, \dots, j+1 \\ \delta_{i,m^{(\ell+1)}}^{(\ell)} \pi_{m^{(\ell+1)}}^{(\ell)} \iota_{m^{(\ell+1)}}^{(\ell)}, & \ell = j. \end{cases}$	$(d^{(\ell)} + 1) \times d^{(j)} (d^{(j-1)} + 1)$
$\Lambda_{m^{(\ell+1)}}^{(\ell)}$	$\triangleq \begin{cases} \Delta_{m^{(\ell+1)}}^{(\ell)} \left[\left(\Lambda_{m^{(\ell+1)}}^{(\ell-1)} \beta_{m^{(\ell+1)},m^{(\ell)}}^{(\ell)} + \phi_{m^{(\ell+1)},m^{(\ell)}}^{(\ell-1)} \Upsilon_{m^{(\ell+1)},m^{(\ell)}}^{(\ell)} \right)^\top \right]^\top_{\mathbf{m}^{(\ell)}}, & \ell = k-1, \dots, j+1 \\ \pi_{m^{(\ell+1)}}^{(\ell)} \delta_{i,m^{(\ell+1)}}^{(\ell)} \iota_{m^{(\ell+1)}}^{(\ell)} + \pi_{m^{(\ell+1)}}^{(\ell)} W_{m^{(\ell+1)}}^{(\ell)\top} \tau_{m^{(\ell+1)}}^{(\ell)} \left[\left(\phi_{m^{(\ell+1)},m^{(\ell)}}^{(\ell-1)} \Upsilon_{m^{(\ell+1)},m^{(\ell)}}^{(\ell)} \right)^\top \right]^\top_{\mathbf{m}^{(\ell)}}, & \ell = j \end{cases}$	$(d^{(\ell)} + 1) \times d^{(j)} (d^{(j-1)} + 1)$
$\Upsilon_{m^{(\ell+1)},m^{(\ell)}}^{(\ell)}$	$\triangleq \eta_{m^{(\ell+1)}}^{(\ell)} \left(\epsilon_{m^{(\ell+1)}}^{(\ell)} \varkappa_{m^{(\ell+1)},m^{(\ell)}}^{(\ell)} - \gamma_{m^{(\ell+1)},m^{(\ell)}}^{(\ell)} \bar{A}_{m^{(\ell+1)}} \left[\left(\varkappa_{m^{(\ell+1)},m^{(\ell)}}^{(\ell)} \right)^\top \right]^\top_{\mathbf{m}^{(\ell)}} \right)$	$1 \times d^{(j)} (d^{(j-1)} + 1)$
$\varkappa_{m^{(\ell+1)},m^{(\ell)}}^{(\ell)}$	$\triangleq \begin{cases} \gamma_{m^{(\ell+1)},m^{(\ell)}}^{(\ell)} a_{m^{(\ell+1)}}^{(\ell)} \left((W_{m^{(\ell+1)}}^{(\ell)\top} \Lambda_{m^{(\ell+1)}}^{(\ell-1)}) \oplus (W_{m^{(\ell+1)}}^{(\ell)\top} \Lambda_{m^{(\ell+1)}}^{(\ell-1)}) \right), & \ell = k-1, \dots, j+1 \\ \gamma_{m^{(\ell+1)},m^{(\ell)}}^{(\ell)} a_{m^{(\ell+1)}}^{(\ell)\top} \delta_{i,m^{(\ell+1)}}^{(\ell)} \left((\xi_{m^{(\ell+1)}}^{(\ell)}) \oplus (\xi_{m^{(\ell+1)}}^{(\ell)}) \right), & \ell = j \end{cases}$	$1 \times d^{(j)} (d^{(j-1)} + 1)$
$\varsigma_{m^{(\ell+1)}}^{(\ell)}$	$\triangleq \begin{cases} \Delta_{m^{(\ell+1)}}^{(\ell)} \left[\left(\varsigma_{m^{(\ell+1)},m^{(\ell)}}^{(\ell-1)} \beta_{m^{(\ell+1)},m^{(\ell)}}^{(\ell)} + \phi_{m^{(\ell+1)},m^{(\ell)}}^{(\ell-1)} \vartheta_{m^{(\ell+1)},m^{(\ell)}}^{(\ell)} \right)^\top \right]^\top_{\mathbf{m}^{(\ell)}}, & \ell = k-1, \dots, j+1 \\ \pi_{m^{(\ell+1)}}^{(\ell)} W_{m^{(\ell+1)}}^{(\ell)\top} \tau_{m^{(\ell+1)}}^{(\ell)} \left[\left(\phi_{m^{(\ell+1)},m^{(\ell)}}^{(\ell-1)} \vartheta_{m^{(\ell+1)},m^{(\ell)}}^{(\ell)} \right)^\top \right]^\top_{\mathbf{m}^{(\ell)}}, & \ell = j \end{cases}$	$(d^{(\ell)} + 1) \times 2d^{(j)}$
$\vartheta_{m^{(\ell+1)},m^{(\ell)}}^{(\ell)}$	$\triangleq \eta_{m^{(\ell+1)}}^{(\ell)} \left(\epsilon_{m^{(\ell+1)}}^{(\ell)} \varrho_{m^{(\ell+1)},m^{(\ell)}}^{(\ell)} - \gamma_{m^{(\ell+1)},m^{(\ell)}}^{(\ell)} \bar{A}_{m^{(\ell+1)}} \left[\left(\varrho_{m^{(\ell+1)},m^{(\ell)}}^{(\ell)} \right)^\top \right]^\top_{\mathbf{m}^{(\ell)}} \right)$	$1 \times 2d^{(j)}$
$\varrho_{m^{(\ell+1)},m^{(\ell)}}^{(\ell)}$	$\triangleq \begin{cases} \gamma_{m^{(\ell+1)},m^{(\ell)}}^{(\ell)} a_{m^{(\ell+1)}}^{(\ell)} \left((W_{m^{(\ell+1)}}^{(\ell)\top} \varsigma_{m^{(\ell+1)}}^{(\ell-1)}) \oplus (W_{m^{(\ell+1)}}^{(\ell)\top} \varsigma_{m^{(\ell+1)}}^{(\ell-1)}) \right), & \ell = k-1, \dots, j+1 \\ \gamma_{m^{(\ell+1)},m^{(\ell)}}^{(\ell)} \delta_{i,m^{(\ell+1)}}^{(\ell)} \left((W_{m^{(\ell+1)}}^{(\ell)\top} \phi_{m^{(\ell+1)}}^{(\ell-1)}) \oplus (W_{m^{(\ell+1)}}^{(\ell)\top} \phi_{m^{(\ell+1)}}^{(\ell-1)}) \right)^\top, & \ell = j \end{cases}$	$1 \times 2d^{(j)}$

We apply the quotient rule to (100) such that

$$\frac{\partial \beta_{i,m^{(k-1)}}^{(k-1)}}{\partial \text{vec}(W_i^{(j)})} = \eta_i^{(k-1)} \left[\epsilon_i^{(k-1)} \frac{\partial \exp(c_{i,m^{(k-1)}}^{(k-1)})}{\partial \text{vec}(W_i^{(j)})} - \gamma_{i,m^{(k-1)}}^{(k-1)} \frac{\partial (\bar{A}_i \text{vec}(c_i^{(k-1)})^\top)}{\partial \text{vec}(W_i^{(j)})} \right]. \quad (101)$$

Next, we briefly prove (3). For two vectors $A(x), B(x) \in \mathbb{R}^n$ and input $x \in \mathbb{R}^m$, let their concatenation be denoted by the vector $C(x) \in \mathbb{R}^{2n}$. Then, the partial derivative of $C(x)$ is applied elementwise. This operation yields

$$\frac{\partial}{\partial x} C(x) = \left[\frac{\partial}{\partial x} A_1(x)^\top, \dots, \frac{\partial}{\partial x} A_n(x)^\top, \frac{\partial}{\partial x} B_1(x)^\top, \dots, \frac{\partial}{\partial x} B_n(x)^\top \right]^\top \quad (102)$$

where $\frac{\partial}{\partial x} C(x) \in \mathbb{R}^{n \times m}$. Equation (102) is equivalent to

$$\frac{\partial}{\partial x} C(x) = \left[\frac{\partial}{\partial x} A(x)^\top, \frac{\partial}{\partial x} B(x)^\top \right]^\top. \quad (103)$$

Equation (103) is the concatenation of the derivative of $A(x)$ with respect to x and the derivative of $B(x)$ with respect to x . Therefore,

$$\frac{\partial}{\partial x} (A(x) \oplus B(x)) = \frac{\partial}{\partial x} C(x) = \left(\frac{\partial}{\partial x} A(x) \oplus \frac{\partial}{\partial x} B(x) \right).$$

Next, we evaluate the partial derivative of $\exp(c_{i,m^{(k-1)}}^{(k-1)})$ with respect to $\text{vec}(W_i^{(j)})$ and apply (3), which gives

$$\frac{\partial \exp(b_{i,m^{(k-1)}}^{(k-1)})}{\partial \text{vec}(W_i^{(j)})} = \gamma_{i,m^{(k-1)}}^{(k-1)} a_i^{(k-1)\top} \cdot \left(\left(W_i^{(k-1)\top} \frac{\partial \phi_i^{(k-2)}}{\partial \text{vec}(W_i^{(j)})} \right) \oplus \left(W_i^{(k-1)\top} \frac{\partial \phi_m^{(k-2)}}{\partial \text{vec}(W_i^{(j)})} \right) \right).$$

Then, evaluating the partial derivative of $\bar{A}_i \text{vec}(\mathbf{c}_i^{(k-1)})^\top$ with respect to $\text{vec}(W_i^{(j)})$ gives

$$\frac{\partial \left(\bar{A}_i \text{vec}(\mathbf{c}_i^{(k-1)})^\top \right)}{\partial \text{vec}(W_i^{(j)})} = \bar{A}_i \left(\gamma_{i,m^{(k-1)}}^{(k-1)} \mathbf{a}_i^{(k-1)\top} \left(W_i^{(k-1)\top} \right. \right. \\ \left. \left. \frac{\partial \phi_i^{(k-2)}}{\partial \text{vec}(W_i^{(j)})} \oplus W_i^{(k-1)\top} \frac{\partial \phi_{m^{(k-1)}}^{(k-2)}}{\partial \text{vec}(W_i^{(j)})} \right) \right)_{\mathbf{m}^{(k-1)}}^\top.$$

For brevity of notation, let $\boldsymbol{\varkappa}_{m^{(\ell+1)},m^{(\ell)}}^{(\ell)} \in \mathbb{R}^{1 \times d^{(j)}(d^{(j-1)}+1)}$ be defined as

$$\boldsymbol{\varkappa}_{m^{(\ell+1)},m^{(\ell)}}^{(\ell)} \triangleq \gamma_{m^{(\ell+1)},m^{(\ell)}}^{(\ell)} \mathbf{a}_{m^{(\ell+1)}}^{(\ell)} \\ \cdot \left(\left(W_{m^{(\ell+1)}}^{(\ell)\top} \frac{\partial \phi_{m^{(\ell+1)}}^{(\ell-1)}}{\partial \text{vec}(W_i^{(j)})} \right) \oplus \left(W_{m^{(\ell+1)}}^{(\ell)\top} \frac{\partial \phi_{m^{(\ell)}}^{(\ell-1)}}{\partial \text{vec}(W_i^{(j)})} \right) \right).$$

Then, the partial derivative of $\exp(\mathbf{c}_{i,m^{(k-1)}}^{(k-1)})$ with respect to $\text{vec}(W_i^{(j)})$ becomes

$$\frac{\partial \exp \left(\mathbf{c}_{i,m^{(k-1)}}^{(k-1)} \right)}{\partial \text{vec}(W_i^{(j)})} = \boldsymbol{\varkappa}_{i,m^{(k-1)}}^{(k-1)}, \quad (104)$$

and the partial derivative of $\bar{A}_i \text{vec}(\mathbf{c}_i^{(k-1)})^\top$ with respect to $\text{vec}(W_i^{(j)})$ becomes

$$\frac{\partial \left(\bar{A}_i \text{vec}(\mathbf{c}_i^{(k-1)})^\top \right)}{\partial \text{vec}(W_i^{(j)})} = \bar{A}_i \left[\boldsymbol{\varkappa}_{i,m^{(k-1)}}^{(k-1)} \right]_{\mathbf{m}^{(k-1)}}^\top. \quad (105)$$

Then, substituting (104) and (105) into (101) gives

$$\frac{\partial \beta_{i,m^{(k-1)}}^{(k-1)}}{\partial \text{vec}(W_i^{(j)})} = \eta_i^{(k-1)} \left(\boldsymbol{\varepsilon}_i^{(k-1)} \boldsymbol{\varkappa}_{i,m^{(k-1)}}^{(k-1)} \right. \\ \left. - \gamma_{i,m^{(k-1)}}^{(k-1)} \bar{A}_i \left[\boldsymbol{\varkappa}_{i,m^{(k-1)}}^{(k-1)} \right]_{\mathbf{m}^{(k-1)}}^\top \right). \quad (106)$$

We continue to analyze the partial derivatives of $\phi_{m^{(\ell+1)}}^{(\ell)}$ with respect to $\text{vec}(W_i^{(j)})$ from $\ell = k-1, k-2, \dots, j+1$ until $\ell = j$. Then, the partial derivative of $\phi_{m^{(\ell+1)}}^{(\ell)}$ with respect to $\text{vec}(W_i^{(j)})$ is

$$\frac{\partial \phi_{m^{(j+1)}}^{(j)}}{\partial \text{vec}(W_i^{(j)})} = \pi_{m^{(j+1)}}^{(j)} \frac{\partial}{\partial \text{vec}(W_i^{(j)})} \cdot W_{m^{(j+1)}}^{(j)\top} \mathbf{B}_{m^{(j+1)}}^{(j)} \bar{A}_{m^{(j+1)}}^\top.$$

We must apply the chain rule because $\mathbf{B}_{m^{(j+1)},m^{(j)}}^{(j)}$ is also a function of $W_i^{(j)}$. Therefore,

$$\frac{\partial \phi_{m^{(j+1)}}^{(j)}}{\partial \text{vec}(W_i^{(j)})} = \pi_{m^{(j+1)}}^{(j)} \left(\frac{\partial \left(W_{m^{(j+1)}}^{(j)\top} \mathbf{B}_{m^{(j+1)}}^{(j)} \bar{A}_{m^{(j+1)}}^\top \right)}{\partial \text{vec}(W_i^{(j)})} \right. \\ \left. + W_{m^{(j+1)}}^{(j)\top} \frac{\partial \left(\mathbf{B}_{m^{(j+1)}}^{(j)} \bar{A}_{m^{(j+1)}}^\top \right)}{\partial \text{vec}(W_i^{(j)})} \right). \quad (107)$$

Evaluating the partial derivative of $W_{m^{(j+1)}}^{(j)\top} \mathbf{B}_{m^{(j+1)}}^{(j)} \bar{A}_{m^{(j+1)}}^\top$ with respect to $\text{vec}(W_i^{(j)})$ yields

$$\frac{\partial \left(W_{m^{(j+1)}}^{(j)\top} \mathbf{B}_{m^{(j+1)}}^{(j)} \bar{A}_{m^{(j+1)}}^\top \right)}{\partial \text{vec}(W_i^{(j)})} = \delta_{i,m^{(j+1)}} \iota_{m^{(j+1)}}^{(j)}.$$

and the partial derivative of $\mathbf{B}_{m^{(j+1)}}^{(j)} \bar{A}_{m^{(j+1)}}^\top$ with respect to $\text{vec}(W_i^{(j)})$ is

$$\frac{\partial \left(\mathbf{B}_{m^{(j+1)}}^{(j)} \bar{A}_{m^{(j+1)}}^\top \right)}{\partial \text{vec}(W_i^{(j)})} = \boldsymbol{\tau}_{m^{(j+1)}}^{(j)} \\ \cdot \left[\left(\phi_{m^{(j)}}^{(j-1)} \frac{\partial \beta_{m^{(j+1)},m^{(j)}}^{(j)}}{\partial \text{vec}(W_i^{(j)})} \right) \right]_{\mathbf{m}^{(j)}}^\top.$$

We evaluate the partial derivative of $\beta_{m^{(j+1)},m^{(j)}}^{(j)}$ with respect to $\text{vec}(W_i^{(j)})$ yielding

$$\Upsilon_{m^{(j+1)},m^{(j)}}^{(j)} \triangleq \frac{\partial \beta_{m^{(j+1)},m^{(j)}}^{(j)}}{\partial \text{vec}(W_i^{(j)})} = \eta_{m^{(j+1)}}^{(j)} \boldsymbol{\varepsilon}_{m^{(j+1)}}^{(j)} \\ \cdot \gamma_{m^{(j+1)},m^{(j)}}^{(j)} \mathbf{a}_{m^{(j+1)}}^{(j)\top} \delta_{i,m^{(j+1)}} \left(\boldsymbol{\xi}_{m^{(j+1)}}^{(j)} \oplus \boldsymbol{\xi}_{m^{(j)}}^{(j)} \right) \\ - \eta_{m^{(j+1)}}^{(j)} \gamma_{m^{(j+1)},m^{(j)}}^{(j)} \bar{A}_{m^{(j+1)}} \\ \cdot \left[\left(\gamma_{m^{(j+1)},m^{(j)}}^{(j)} \mathbf{a}_{m^{(j+1)}}^{(j)\top} \delta_{i,m^{(j+1)}} \right. \right. \\ \left. \left. \cdot \left(\boldsymbol{\xi}_{m^{(j+1)}}^{(j)} \oplus \boldsymbol{\xi}_{m^{(j)}}^{(j)} \right) \right]_{\mathbf{m}^{(j+1)}}^\top. \quad (108)$$

The following terms capture the recursive nature of the partial derivative of ϕ_i with respect to $\text{vec}(W_i^{(j)})$. Recall the definitions of $\Lambda_{m^{(\ell+1)}}^{(\ell)} \in \mathbb{R}^{(d^{(\ell)}+1) \times d^{(j)}(d^{(j-1)}+1)}$, $\Upsilon \in \mathbb{R}^{1 \times d^{(j)}(d^{(j-1)}+1)}$, and $\boldsymbol{\varkappa}_{m^{(\ell+1)},m^{(\ell)}}^{(\ell)} \in \mathbb{R}^{1 \times d^{(j)}(d^{(j-1)}+1)}$ from Table III. The term $\Lambda_{m^{(\ell+1)}}^{(\ell)}$ contains the structure of the partial derivative of $\phi_{m^{(\ell+1)}}^{(\ell)}$ with respect to $\text{vec}(W_i^{(j)})$ seen in (99) and (107). The term $\Upsilon_{m^{(\ell+1)},m^{(\ell)}}^{(\ell)}$ contains the structure of the partial derivative of $\beta_{m^{(\ell+1)},m^{(\ell)}}^{(\ell)}$ with respect to $\text{vec}(W_i^{(j)})$ seen in (106). Finally, the term $\boldsymbol{\varkappa}_{m^{(\ell+1)},m^{(\ell)}}^{(\ell)}$ contains the structure of the partial derivative of $\exp(\mathbf{c}_{m^{(\ell+1)},m^{(\ell)}}^{(\ell)})$ with respect to $\text{vec}(W_i^{(j)})$ seen in (104) and (108). Then, the partial derivative of ϕ_i with respect to $\text{vec}(W_i^{(j)})$ can be written as

$$\frac{\partial \phi_i}{\partial \text{vec}(W_i^{(j)})} = W_i^{(k)\top} \Lambda_i^{(k-1)},$$

where $\frac{\partial \phi_i}{\partial \text{vec}(W_i^{(j)})} \in \mathbb{R}^{d^{(k)} \times d^{(j)}(d^{(j-1)}+1)}$. We repeat this process by taking the partial derivative of the outer layer of the GAT architecture in (10) with respect to $\text{vec}(W_i^{(j)})$ as

$$\frac{\partial \phi_i}{\partial \mathbf{a}_i^{(j)}} = W_i^{(k)\top} \Delta_i^{(k-1)} \\ \cdot \left[\left(\frac{\partial}{\partial \mathbf{a}_i^{(j)}} \phi_{m^{(k-1)}}^{(k-2)} \beta_{i,m^{(k-1)}}^{(k-1)} \right) \right]_{\mathbf{m}^{(k-1)}}^\top \quad (109)$$

Both $\phi_{m^{(k-1)}}^{(k-2)}$ and $\beta_{i,m^{(k-1)}}^{(k-1)}$ are functions of $\mathbf{a}_i^{(j)}$. Therefore,

we apply the product rule to (109) as

$$\frac{\partial \phi_i}{\partial a_i^{(j)}} = W_i^{(k)\top} \Delta_i^{(k-1)} \left[\left(\frac{\partial \phi_{m^{(k-1)}}^{(k-2)}}{\partial a_i^{(j)}} \beta_{i,m^{(k-1)}}^{(k-1)} + \phi_{m^{(k-1)}}^{(k-2)} \frac{\partial \beta_{i,m^{(k-1)}}^{(k-1)}}{\partial a_i^{(j)}} \right) \right]_{\mathbf{m}^{(k-1)}}^\top. \quad (110)$$

Evaluating the partial derivative of $\phi_{m^{(k-1)}}^{(k-2)}$ with respect to $a_i^{(j)}$ yields

$$\zeta_{m^{(k-1)}}^{(k-2)} \triangleq \frac{\partial \phi_{m^{(k-1)}}^{(k-2)}}{\partial a_i^{(j)}} = \Delta_{m^{(k-1)}}^{(k-2)} \left[\left(\frac{\partial \phi_{m^{(k-2)}}^{(k-3)}}{\partial a_i^{(j)}} \beta_{m^{(k-1)},m^{(k-2)}}^{(k-2)} + \phi_{m^{(k-2)}}^{(k-3)} \frac{\partial \beta_{m^{(k-1)},m^{(k-2)}}^{(k-2)}}{\partial a_i^{(j)}} \right) \right]_{\mathbf{m}^{(k-2)}}^\top.$$

Evaluating the partial derivative of $\beta_{i,m^{(k-1)}}^{(k-1)}$ with respect to $a_i^{(j)}$ yields

$$\frac{\partial \beta_{i,m^{(k-1)}}^{(k-1)}}{\partial a_i^{(j)}} = \frac{\partial}{\partial a_i^{(j)}} \frac{\exp(c_{i,m^{(k-1)}}^{(k-1)})}{\exp(c_i^{(k-1)}) \bar{A}_i^\top}. \quad (111)$$

We apply the quotient rule to (111) and find

$$\frac{\partial \beta_{i,m^{(k-1)}}^{(k-1)}}{\partial a_i^{(j)}} = \eta_i^{(k-1)} \left(\epsilon_i^{(k-1)} \frac{\partial \exp(c_{i,m^{(k-1)}}^{(k-1)})}{\partial a_i^{(j)}} - \gamma_{i,m^{(k-1)}}^{(k-1)} \frac{\partial \left(\bar{A}_i \text{vec}(c_i^{(k-1)})^\top \right)}{\partial a_i^{(j)}} \right). \quad (112)$$

Evaluating the partial derivative of $b_{i,m^{(k-1)}}^{(k-1)}$ with respect to $a_i^{(j)}$ gives

$$\frac{\partial \exp(c_{i,m^{(k-1)}}^{(k-1)})}{\partial a_i^{(j)}} = \gamma_{i,m^{(k-1)}}^{(k-1)} a_i^{(k-1)} \left(\left(W_i^{(k-1)\top} \frac{\partial \phi_i^{(k-2)}}{\partial a_i^{(j)}} \right) \oplus \left(W_i^{(k-1)\top} \frac{\partial \phi_{m^{(k-1)}}^{(k-2)}}{\partial a_i^{(j)}} \right) \right). \quad (113)$$

For compactness of notation, let $\varrho_{m^{(\ell+1)},m^{(\ell)}}^{(\ell)} \in \mathbb{R}^{1 \times 2d^{(j)}}$ be defined as

$$\varrho_{m^{(\ell+1)},m^{(\ell)}}^{(\ell)} \triangleq \gamma_{m^{(\ell+1)},m^{(\ell)}}^{(\ell)} a_{m^{(\ell+1)}}^{(\ell)} \left(\left(W_{m^{(\ell+1)}}^{(\ell)\top} \frac{\partial \phi_{m^{(\ell+1)}}^{(\ell-1)}}{\partial a_i^{(j)}} \right) \oplus \left(W_{m^{(\ell+1)}}^{(\ell)\top} \frac{\partial \phi_{m^{(\ell)}}^{(\ell-1)}}{\partial a_i^{(j)}} \right) \right).$$

Then, (112) becomes

$$\frac{\partial \beta_{i,m^{(k-1)}}^{(k-1)}}{\partial a_i^{(j)}} = \eta_i^{(k-1)} \left(\epsilon_i^{(k-1)} \rho_{i,m^{(k-1)}}^{(k-1)} - \gamma_{i,m^{(k-1)}}^{(k-1)} \bar{A}_i \left[\rho_{i,m^{(k-1)}}^{(k-1)} \right]_{\mathbf{m}^{(k-1)}} \right).$$

We continue evaluating partial derivatives of $\phi_{m^{(\ell+1)}}^{(\ell)}$ from $\ell = k-1, \dots, j+1$ until $\ell = j$. Then, the partial derivative of $\phi_{m^{(j+1)}}^{(j)}$ with respect to $a_i^{(j)}$ is

$$\frac{\partial \phi_{m^{(j+1)}}^{(j)}}{\partial a_i^{(j)}} = \pi_{m^{(j+1)}}^{(j)} W_{m^{(j+1)}}^{(j)\top} \tau_{m^{(j+1)}}^{(j)} \cdot \left[\left(\phi_{m^{(j)}}^{(j-1)} \frac{\partial}{\partial \text{vec}(a_i^{(j)})} \beta_{m^{(j+1)},m^{(j)}}^{(j)} \right) \right]_{\mathbf{m}^{(j)}}^\top. \quad (114)$$

Then, the partial derivative of $\beta_{m^{(\ell+1)},m^{(\ell)}}^{(\ell)}$ with respect to $a_i^{(j)}$ is

$$\vartheta_{m^{(j+1)},m^{(j)}}^{(j)} \triangleq \frac{\partial \beta_{m^{(j+1)},m^{(j)}}^{(j)}}{\partial a_i^{(j)}} = \eta_{m^{(j+1)}}^{(j)} \epsilon_{m^{(j+1)}}^{(j)} \frac{\partial \exp(c_{m^{(j+1)},m^{(j)}}^{(j)})}{\partial a_i^{(j)}} - \eta_{m^{(j+1)}}^{(j)} \gamma_{m^{(j+1)},m^{(j)}}^{(j)} \bar{A}_{m^{(j+1)}} \frac{\partial \exp(c_{m^{(j+1)}}^{(j)})}{\partial a_i^{(j)}}. \quad (115)$$

Evaluating the partial derivative of $\exp(c_{m^{(j+1)},m^{(j)}}^{(j)})$ with respect to $a_i^{(j)}$ yields

$$\varrho_{m^{(j+1)},m^{(j)}}^{(j)} \triangleq \frac{\partial \exp(c_{m^{(j+1)},m^{(j)}}^{(j)})}{\partial a_i^{(j)}} = \gamma_{m^{(j+1)},m^{(j)}}^{(j)} \cdot \delta_{i,m^{(j+1)}} \left(\left(W_{m^{(j+1)}}^{(j)\top} \phi_{m^{(j+1)}}^{(j-1)} \right) \oplus \left(W_{m^{(j)}}^{(j)\top} \phi_{m^{(j)}}^{(j-1)} \right) \right)^\top. \quad (116)$$

The following terms capture the recursive nature of the partial derivative of ϕ_i with respect to $a_i^{(j)}$. Recall the definitions of $\zeta_{m^{(\ell+1)}}^{(\ell)} \in \mathbb{R}^{d^{(\ell+1)} \times 2d^{(j)}}$, $\vartheta_{m^{(\ell+1)},m^{(\ell)}}^{(\ell)} \in \mathbb{R}^{1 \times 2d^{(j)}}$, and $\varrho_{m^{(\ell+1)},m^{(\ell)}}^{(\ell)} \in \mathbb{R}^{1 \times 2d^{(j)}}$ from Table III. The term $\zeta_{m^{(\ell+1)}}^{(\ell)}$ contains the structure of the partial derivative of $\phi_{m^{(\ell+1)}}^{(\ell)}$ with respect to $a_i^{(j)}$ seen in (110) and (114). The term $\vartheta_{m^{(\ell+1)},m^{(\ell)}}^{(\ell)}$ captures the structure of the partial derivative of $\beta_{m^{(\ell+1)},m^{(\ell)}}^{(\ell)}$ with respect to $a_i^{(j)}$ seen in (112) and (115). The term $\varrho_{m^{(\ell+1)},m^{(\ell)}}^{(\ell)}$ captures the partial derivative of $\exp(c_{m^{(\ell+1)},m^{(\ell)}}^{(\ell)})$ with respect to $a_i^{(j)}$ seen in (113) and (116). Then, the partial derivative of ϕ_i with respect to $a_i^{(j)}$ can be written as

$$\frac{\partial \phi_i}{\partial a_i^{(j)}} = W_i^{(k)\top} \zeta_i^{(k-1)},$$

where $\frac{\partial \phi_i}{\partial a_i^{(j)}} \in \mathbb{R}^{d^{(k)} \times 2d^{(j)}}$. Therefore, the first partial derivative of (10) with respect to (11) is equal to (12). ■

Proof of Lemma 4: We begin by finding a formula for $\underline{\lambda}_{\mathcal{H}}$ in terms of N , where $\underline{\lambda}_{\mathcal{H}} = \lambda_{\min}(\mathcal{H})$, and $\mathcal{H} = (\mathcal{L}_G + \mathcal{B}) \otimes I_n$. Let $a(G)$ denote the algebraic connectivity of the graph G . Let P_N denote the path graph with $N \in \mathbb{Z}_{>0}$ nodes. By [53, Proposition 1.12], we have that $a(P_N) \leq a(G)$ for all connected G . Therefore, $\lambda_{\min}(\mathcal{L}_G + \mathcal{B})$ is minimized when $\mathcal{L}_G = \mathcal{L}_G(P_N)$.

Let $\mathcal{B}(1, 2, \dots, M) \in \mathbb{R}^{N \times N}$ denote the matrix such that $[b_{11}] = [b_{22}] = \dots = [b_{MM}] = \epsilon$, and all other entries are 0.

We first prove that $\lambda_{\min}(\mathcal{L}_G(P_N) + \mathcal{B}(i)) \leq \lambda_{\min}(\mathcal{L}_G(P_N) + \mathcal{B}(1, 2, \dots, M))$ for any set $\mathcal{R} \triangleq 1, 2, \dots, M$ for $|\mathcal{R}| > 1$ and any $i \in \mathcal{R}$. We employ the first-order perturbation expansion for simple eigenvalues, which states that

$$\lambda_{\min}(\mathcal{L}_G(P_N) + \mathcal{B}(1, 2, \dots, M)) = \lambda_{\min}(\mathcal{L}_G(P_N)) + \frac{x^\top \mathcal{B}(1, 2, \dots, M)x}{x^\top x} + \mathcal{O}(\|\mathcal{B}(1, 2, \dots, M)\|^2), \quad (117)$$

where x is a nonzero eigenvector such that $\mathcal{L}_G(P_N)x = \lambda_{\min}(\mathcal{L}_G(P_N))x$ [54]. Then, let $\Delta_\lambda(\mathcal{B}(1, 2, \dots, M)) \triangleq \lambda_{\min}(\mathcal{L}_G(P_N) + \mathcal{B}(1, 2, \dots, M)) - \lambda_{\min}(\mathcal{L}_G(P_N))$. Then, (117) becomes

$$\Delta_\lambda(\mathcal{B}(1, 2, \dots, M)) = \frac{x^\top \mathcal{B}(1, 2, \dots, M)x}{x^\top x} + \mathcal{O}(\|\mathcal{B}(1, 2, \dots, M)\|^2). \quad (118)$$

For a connected graph G , the eigenvector corresponding to $\lambda_{\min}(\mathcal{L}_G)$ is $\mathbb{1}_N^\top$. Then, (118) simplifies to

$$\Delta_\lambda(\mathcal{B}(1, 2, \dots, M)) = \frac{1}{N} \sum_{m=0}^{|\mathcal{R}|} \epsilon + \mathcal{O}(\epsilon^2),$$

where $|\mathcal{R}|$ is the cardinality of \mathcal{R} . Therefore, $\Delta_\lambda(\mathcal{B}(i)) = \epsilon + \mathcal{O}(\epsilon^2)$ and $\Delta_\lambda(\mathcal{B}(1, 2, \dots, M)) = |\mathcal{R}|\epsilon + \mathcal{O}(\epsilon^2)$. This shows that $\Delta_\lambda(\mathcal{B}(i)) < \Delta_\lambda(\mathcal{B}(1, 2, \dots, M))$.

Define $\mathcal{F}(i) \triangleq \mathcal{L}_G(P_N) + \mathcal{B}(i)$ and let $\lambda_{\min}(\mathcal{F}(i)), \lambda_2(\mathcal{F}(i)), \dots, \lambda_{n-1}(\mathcal{F}(i)), \lambda_{\max}(\mathcal{F}(i))$ denote the eigenvalues of $\mathcal{F}(i)$ indexed from smallest to largest. We will prove that

$$\lambda_{\min}(\mathcal{F}(1)) = \lambda_{\min}(\mathcal{F}(N)) \leq \lambda_{\min}(\mathcal{F}(k)),$$

where $1 < k < N$. Note that $\mathcal{F}(1)$ and $\mathcal{F}(N)$ are similar matrices that can be obtained from one another by using a similarity transformation. The similarity transformation from $\mathcal{F}(1)$ to $\mathcal{F}(N)$ is $\mathcal{F}(N) = P\mathcal{F}(1)P^{-1}$, where P is a permutation matrix that reverses the order of the rows and columns of $\mathcal{F}(1)$. We see that $\mathcal{F}(1)$ and $\mathcal{F}(N)$ are similar, which shows that they have the same eigenvalues. Therefore, $\lambda_{\min}(\mathcal{F}(1)) = \lambda_{\min}(\mathcal{F}(N))$.

Next, we consider $\mathcal{F}(k)$ for $1 < k < N$. We know that $\mathcal{F}(k) = \mathcal{L}_G(P_N) + \mathcal{B}(k)$. Additionally, for $\mathcal{F}(1)$ we have $\mathcal{L}_G(P_N) = \mathcal{F}(1) - \mathcal{B}(1)$. Then, $\mathcal{F}(k) = \mathcal{F}(1) + \mathcal{B}(k) - \mathcal{B}(1)$. Weyl's inequality states that for Hermitian matrices A and B , we have $\lambda_{\min}(A) + \lambda_{\max}(B) \leq \lambda_{\min}(A + B)$. Then,

$$\lambda_{\min}(\mathcal{F}(1)) + \lambda_{\max}(\mathcal{B}(k) - \mathcal{B}(1)) \leq \lambda_{\min}(\mathcal{F}(k)).$$

Note that $1 < k < N$. Then, $\mathcal{B}(k) - \mathcal{B}(1)$ is a matrix where $[b_{kk}] = 1$, $[b_{11}] = -1$, and $[b_{xy}] = 0$ for all $x, y \in [N]$ such that $x \neq y$. Therefore, $\lambda_{\max}(\mathcal{B}(k) - \mathcal{B}(1)) = 1$. We see that $\lambda_{\min}(\mathcal{F}(1)) + 1 \leq \lambda_{\min}(\mathcal{F}(k))$, which yields $\lambda_{\min}(\mathcal{F}(1)) \leq \lambda_{\min}(\mathcal{F}(k))$. Therefore, $\mathcal{L}_G + \mathcal{B}$ has the smallest minimum eigenvalue when $\mathcal{L}_G + \mathcal{B} = \mathcal{L}_G(P_N) + \mathcal{B}(1) = \mathcal{L}_G(P_N) + \mathcal{B}(N)$.

Without loss of generality, consider $\mathcal{L}_G(P_N) + \mathcal{B}(1)$. Next, let [55, Lemma 1] hold. We see that $\mathcal{L}_G(P_N) + \mathcal{B}(1)$ takes the form of a special tridiagonal matrix in [55], where $a = -1, b = 2, c = -1, \alpha = 0$, and $\beta = \sqrt{ac} = 1$. Therefore, by

[55, Theorem 1], the k^{th} largest eigenvalue of $\mathcal{L}_G(P_N) + \mathcal{B}(1)$ is given as

$$\lambda_k \triangleq b + 2\sqrt{ac} \cos\left(\frac{2(N+1-k)\pi}{2N+1}\right),$$

where $1 \leq k \leq N$. The smallest eigenvalue of $\mathcal{L}_G(P_N) + \mathcal{B}(1)$ corresponds to $k = 1$. Therefore,

$$\lambda_{\min}(\mathcal{L}_G(P_N) + \mathcal{B}(1)) = 2 + 2 \cos\left(\frac{2N\pi}{2N+1}\right).$$

Then, recall the definition of \mathcal{H} , where $\mathcal{H} = (\mathcal{L}_G + \mathcal{B}) \otimes I_n$. For two matrices $A \in \mathbb{R}^{m \times m}$ and $B \in \mathbb{R}^{n \times n}$, let λ be an eigenvalue of A with corresponding eigenvector v , and let μ be an eigenvalue of B with corresponding eigenvector y . Then, $\lambda\mu$ is an eigenvalue of $A \otimes B$ with corresponding eigenvector $v \otimes y$, and any eigenvalue of $A \otimes B$ arises as a product of eigenvalues of A and B [56, Theorem 4.2.12]. All eigenvalues of I_n are equal to 1. Therefore, $\lambda_{\min}(\mathcal{H}) = \lambda_{\min}(\mathcal{L}_G + \mathcal{B})$, and $\lambda_{\max}(\mathcal{H}) = \lambda_{\max}(\mathcal{L}_G + \mathcal{B})$. This shows that

$$\lambda_{\mathcal{H}} = 2 + 2 \cos\left(\frac{2N\pi}{2N+1}\right).$$

Next, we upper bound $\bar{\lambda}_{\mathcal{H}}$, where $\bar{\lambda}_{\mathcal{H}} = \lambda_{\max}(\mathcal{H})$. The eigenvalues of \mathcal{H} are maximized when $\mathcal{B} = I_N$. The complete graph with N nodes K_N has the largest maximum eigenvalue of any connected graph. For any square matrix A with eigenvalue λ and corresponding eigenvector v , where $Av = \lambda v$, $\lambda + 1$ is an eigenvalue of $A + I$ with the corresponding eigenvector v , where I is the identity matrix. The largest eigenvalue of the graph Laplacian of the complete graph is $\lambda_{\max}(\mathcal{L}_G(K_N)) = N$ [57, Lemma 2]. Therefore, $\lambda_{\max}(\mathcal{L}_G(K_N) + I_N) \leq N + 1$. Finally, we invoke [56, Theorem 4.2.12] which shows that $\lambda_{\max}(\mathcal{H}) = \lambda_{\max}(\mathcal{L}_G + I_N)$. Therefore, $\bar{\lambda}_{\mathcal{H}} \leq N + 1$. ■

Proof of Lemma 5: The z^{th} component of the GNN's first Lagrange remainder $T_{y,z}$ is expressed as $T_{y,z} = [T_{y,z}(s_1), \dots, T_{y,z}(s_n)]^\top$, where $T_{y,z}(s_m) = \tilde{\theta}_{y,z}^\top \nabla_{\tilde{\theta}_{y,z}}^2 \phi_{y,i}(\kappa_i, \kappa_{j:j \in \mathcal{N}_i^k}, \tilde{\theta}_{y,z} + s_m(\tilde{\theta}_{y,z})\tilde{\theta}_{y,z}, \hat{\theta}_{y,j:j \in \mathcal{N}_i^{k-1} \setminus z})\tilde{\theta}_{y,z}$ for all $m \in [n]$. The use of the projection operator in (48) and (51) ensure that $\tilde{\theta}_{y,z}(t) \in \mathcal{U}_{y,z}$ for all $t \in \mathbb{R}_{\geq 0}$, for $y = 1, 2$, and all $i \in V$, where $\mathcal{U}_{y,z} \triangleq \{\theta \in \mathbb{R}^p : \|\theta\| \leq \bar{\theta}\}$. Additionally, due to the facts that $\mathcal{U}_{y,z}$ is a convex set, $s_m(\hat{\theta}) \in [0, 1]$ for all $m \in [n]$, and $\theta_{y,z}^*, \hat{\theta}_{y,z} \in \mathcal{U}_{y,z}$, the term $\tilde{\theta}_{y,z} \in \mathcal{U}_{y,z}$ for all $z \in V$. Due to the fact that $s_m(\hat{\theta}_{y,z})$ is unknown, we conduct this analysis considering the worst-case bound in which $\|\tilde{\theta}_{y,z} + s_m(\hat{\theta}_{y,z})\tilde{\theta}_{y,z}\| \leq \bar{\theta}$ for all $m \in [n]$. Thus, we consider arbitrary values of $\theta_{y,z} \in \mathcal{U}_{y,z}$ for all $z \in V$. Additionally, in this bound, we consider the complete communication graph as it represents the maximal inter-agent aggregation that can occur at each GNN layer.

Then, we consider $T_{y,z}(s_m) = \tilde{\theta}_{y,z}^\top \nabla_{\tilde{\theta}_{y,z}}^2 \phi_{y,i}(\kappa_i, \kappa_{j:j \in \mathcal{N}_i^k}, \theta_{y,j:j \in \mathcal{N}_i^{k-1}})\tilde{\theta}_{y,z}$. For simplicity of notation, we denote $\phi_{y,i}(\kappa_i, \kappa_{j:j \in \mathcal{N}_i^k}, \theta_{y,j:j \in \mathcal{N}_i^{k-1}})$ as $\phi_{y,i}$. For $\kappa_i \in \mathbb{R}^n$, let $\kappa = [\kappa_i^\top]_{i \in V}^\top \in \mathbb{R}^{nN}$. Then, the norm of $T_{y,z}$ can be upper-bounded as

$$\|T_{y,z}\| \leq \|\tilde{\theta}_{y,z}\|^2 \left\| \nabla_{\tilde{\theta}_{y,z}}^2 \phi_{y,i} \right\|_F, \quad (119)$$

where $\|\cdot\|_F$ denotes the Frobenius norm. The tensor of the second partial derivative of $\phi_{y,i}$ with respect to $\text{vec}(W_z^{(p)})$ and $\text{vec}(W_z^{(q)})$ is composed of blocks of the form $\frac{\partial^2 \phi_{y,i}}{\partial \text{vec}(W_z^{(p)}) \text{vec}(W_z^{(q)})}$ for $p, q \in [k]$. To bound the norm of the second partial derivatives of $\phi_{y,i}$ with respect to $\text{vec}(W_z^{(p)})$ and $\text{vec}(W_z^{(q)})$, we must first bound the norm of the first partial derivative of $\phi_{y,i}$ with respect to $\theta_{y,z}$ in terms of the norm of the ensemble input κ . By the triangle inequality,

$$\|\nabla_{\theta_{y,z}} \phi_{y,i}\|_F \leq \sum_{q=0}^k \left\| \frac{\partial \phi_{y,i}}{\partial \text{vec}(W_z^{(q)})} \right\|_F. \quad (120)$$

The use of bounded activation function ensures that the GNN input κ appears in (120) only for the term with $q = 0$. This is a direct result of the formula for $\varphi_{m^{(\ell+1)}}^{(\ell)}$ in Table I, in which κ only explicitly appears for $j = 0$. Otherwise, the base case for $\varphi_{m^{(\ell+1)}}^{(\ell)}$ when $\ell = j$ contains $\phi^{(\ell-1)}$, whose Frobenius norm is upper-bounded by $N(\sqrt{d^{(\ell-1)}}\bar{\sigma}^{(\ell-1)} + 1)$. Thus, we examine how the norm of the partial derivative of $\phi_{y,i}$ with respect to $\text{vec}(W_z^{(q)})$ scales according to the norm of the ensemble GNN input κ when $q = 0$.

Let $\boldsymbol{\rho}^{(w)}$ denote the set of w^{th} -order strictly increasing polynomials with coefficients $c_w, c_{w-1}, \dots, c_0 \in \mathbb{R}_{\geq 0}$, where at least one coefficient c_i is strictly positive for $i \in \{1, \dots, w\}$. We find that $\|\pi_{m^{(\ell+1)}}^{(\ell)}\|_F \leq \sqrt{d^{(\ell)}}\bar{\sigma}^{(\ell)}$, where $\bar{\sigma}^{(\ell)}$ denotes the upper bound of the derivative of the activation function at the ℓ^{th} layer. Then, when $q = 0$, $\|\varphi_{m^{(1)}}^{(0)}\|_F \in \boldsymbol{\rho}^{(1)}$ for all $m^{(1)} \in V$, where $\boldsymbol{\rho}^{(1)}$ is the set of strictly increasing linear functions of the norm of the ensemble GNN input. The term $\|\varphi_{m^{(1)}}^{(0)}\|_F$ is upper-bounded by a first-order polynomial of the GNN input which has leading coefficient upper-bounded by $d^{(0)}\sqrt{N}\bar{\sigma}^{(0)}$.

We find that $\|W_z^{(\ell)}\|_F \leq \bar{\theta}$ and $\|\Delta_{m^{(\ell)}}^{(\ell-1)}\|_F \leq \bar{\theta}\bar{\sigma}^{(\ell)}\sqrt{N(d^{(\ell)})(d^{(\ell-1)} + 1)}$ for all $\ell \in [k-1]$ and all $m^{(\ell)} \in V$. Then, $\|\varphi_{m^{(2)}}^{(1)}\|_F \in \boldsymbol{\rho}^{(1)}$ holds for all $m^{(2)} \in V$. We bound the term $\|\varphi_{m^{(\ell+1)}}^{(\ell)}\|_F$ for each layer of the GNN, and find that $\|\varphi_{m^{(\ell+1)}}^{(\ell)}\|_F \in \boldsymbol{\rho}^{(1)}$ holds for all $\ell \in [k-1]$ and all $m^{(\ell+1)} \in V$. For brevity of notation, let $\mathbf{g}^{(\ell)} \triangleq \bar{\theta}^\ell N^{\frac{1}{2} + \frac{3\ell}{2}} (d^{(0)})^{\frac{1}{2}} \prod_{i=0}^{\ell} (\bar{\sigma}^{(i)} (d^{(i)})^{\frac{1}{2}}) \prod_{i=0}^{\ell-2} (d^{(i)} + 1)^{\frac{1}{2}}$. The term $\|\varphi_{m^{(\ell+1)}}^{(\ell)}\|_F$ is upper-bounded by a first-order polynomial of the GNN input which has leading coefficient upper-bounded by $\mathbf{g}^{(\ell)}$. We reach the highest level of the partial derivative of $\phi_{y,i}$ with respect to $\text{vec}(W_z^{(q)})$, where

$$\left\| \frac{\partial \phi_{y,i}}{\partial \text{vec}(W_z^{(q)})} \right\|_F \leq \|W_z^{(k)}\|_F \|\Delta_{m^{(k)}}^{(k-1)}\|_F \sum_{m^{(k-1)}} \|\varphi_{m^{(k-1)}}^{(k-2)}\|_F.$$

By the use of bounded activation functions with bounded first derivatives and the use of a bounded search space in (27) and (39), we find that

$$\left\| \frac{\partial \phi_{y,i}}{\partial \text{vec}(W_z^{(q)})} \right\|_F \in \boldsymbol{\rho}^{(1)}. \quad (121)$$

Then, the first-order polynomial of the GNN input which upper-bounds (121) has a leading coefficient upper-bounded by $\theta \mathbf{g}^{(k-1)}$. Next, using (120) and (121) yields

$\|\nabla_{\theta_{y,z}} \phi_{y,i}\|_F \in \boldsymbol{\rho}^{(1)}$. Therefore, the norm of the first partial derivative of the GNN $\phi_{y,i}$ with respect to the weights $\theta_{y,z}$ is linear in the ensemble input.

We return to bounding the blocks of the tensor of the second partial derivative of $\phi_{y,i}$ with respect to $\theta_{y,z}$, where by the submultiplicity of the Frobenius norm and the triangle inequality, it follows that

$$\left\| \nabla_{\theta_{y,z}}^2 \phi_{y,i} \right\|_F \leq \sum_{p=0}^k \sum_{q=0}^k \left\| \frac{\partial \phi_{y,i}}{\partial \text{vec}(W_z^{(p)}) \text{vec}(W_z^{(q)})} \right\|_F. \quad (122)$$

By the use of bounded activation functions with bounded first and second derivatives, the GNN input only appears in (122) when $p = 0$ or $q = 0$. Once again, this is a result of the formula for $\varphi_{m^{(\ell+1)}}^{(\ell)}$ in Table I, in which κ only explicitly appears for $j = 0$. Thus, we will consider the double derivative tensor block in which $p = q = 0$. The norm of all other blocks of the second partial derivative of $\phi_{y,i}$ with respect to $\theta_{y,z}$ will scale in terms of $\|\kappa\|$ at an order less than or equal to the case when $p = q = 0$. By the use of bounded activation functions with bounded first and second derivatives and the use of a bounded search space in (27) and (39), we find that

$$\left\| \frac{\partial \pi_{m^{(\ell)}}^{(\ell-1)}}{\partial \text{vec}(W_z^{(0)})} \right\|_F \in \boldsymbol{\rho}^{(1)}, \quad (123)$$

holds for all $\ell \in [k-1]$ and $m^{(\ell)} \in V$. Then, using (123), we find that

$$\left\| \frac{\partial \varphi_{m^{(1)}}^{(0)}}{\partial \text{vec}(W_z^{(0)})} \right\|_F \in \boldsymbol{\rho}^{(2)}, \quad (124)$$

holds for all $m^{(1)} \in V$. Next, we examine

$$\left\| \frac{\partial \varphi_{m^{(2)}}^{(1)}}{\partial \text{vec}(W_z^{(0)})} \right\|_F = \left\| \frac{\partial}{\partial \text{vec}(W_z^{(0)})} \Delta_{m^{(2)}}^{(1)} \left[\left(\varphi_{m^{(1)}}^{(0)} \right)^\top \right]_{m^{(1)}}^\top \right\|_F.$$

By the use of bounded activation functions with bounded second derivatives, (123), (121), and the use of a bounded search space in (27) and (39), we find that

$$\left\| \frac{\partial \Delta_{m^{(\ell+1)}}^{(\ell)}}{\partial \text{vec}(W_z^{(0)})} \right\|_F \in \boldsymbol{\rho}^{(1)}, \quad (125)$$

holds for all $\ell \in [k-1]$ and $m^{(\ell+1)} \in V$. Then, we find that

$$\left\| \frac{\partial \varphi_{m^{(2)}}^{(1)}}{\partial \text{vec}(W_z^{(0)})} \right\|_F \in \boldsymbol{\rho}^{(2)}, \quad (126)$$

holds for all $m^{(2)} \in V$. We repeat this analysis from (125) and (126) for each layer of the GNN, showing that

$$\left\| \frac{\partial \varphi_{m^{(\ell+1)}}^{(\ell)}}{\partial \text{vec}(W_z^{(0)})} \right\|_F \in \boldsymbol{\rho}^{(2)}, \quad (127)$$

holds for $\ell = 0, 1, \dots, k-1$ and for all $m^{(\ell+1)} \in V$. Then, we reach the outermost term in the second partial derivative of the GNN with respect to its layer weights, where

$$\left\| \frac{\partial^2 \phi_{y,i}}{\partial \text{vec}(W_z^{(0)}) \partial \text{vec}(W_z^{(0)})} \right\|_F = \left\| \frac{\partial}{\partial \text{vec}(W_z^{(p)})} W_z^{(k)} \Delta_{m^{(k)}}^{(k-1)} \left[\left(\varphi_{m^{(k-1)}}^{(k-2)} \right)^\top \right]_{m^{(k-1)}}^\top \right\|_F.$$

Based on the use of bounded activation functions with bounded first and second derivatives, (125), (127), and the use of a bounded search space in (27) and (39), we find that

$$\left\| \frac{\partial^2 \phi_{y,i}}{\partial \text{vec}(W_z^{(0)}) \partial \text{vec}(W_z^{(0)})} \right\|_F \in \boldsymbol{\rho}^{(2)}. \quad (128)$$

Since the norm of all other blocks of the second partial derivative of $\phi_{y,i}$ with respect to $\text{vec}(W_z^{(0)})$ and $\text{vec}(W_z^{(0)})$ will scale in terms of $\|\kappa\|$ at an order less than or equal to the case when $p = q = 0$, we use (128) to conclude that

$$\left\| \nabla_{\theta_{y,z}}^2 \phi_{y,i} \right\|_F \in \boldsymbol{\rho}^{(2)}.$$

Additionally, since $\|T_{y,z}\| \leq \|\tilde{\theta}_{y,z}\|^2 \|\nabla_{\theta_{y,z}}^2 \phi_{y,i}\|_F$, then

$$\|T_{y,z}\| \leq \rho(\|\kappa\|) \|\tilde{\theta}_{y,z}\|^2,$$

where $\rho(\|\kappa\|)$ is a strictly increasing, quadratic polynomial in the norm of the ensemble GNN input $\|\kappa\|$. ■

Proof of Lemma 6: This analysis is conducted considering the worst-case bound in which $\|\hat{\theta}_{y,z} + s_m(\tilde{\theta}_{y,z})\tilde{\theta}_{y,z}\| \leq \bar{\theta}$ for all $m \in [n]$. Thus, we consider arbitrary values of $\theta_{y,z} \in \mathcal{U}_{y,z}$ for all $z \in V$. In this bound, we consider the complete communication graph as it represents the maximal inter-agent aggregation that can occur at each GAT layer. The norm of $T_{y,z}$ can be upper-bounded as

$$\|T_{y,z}\| \leq \|\tilde{\theta}_{y,z}\|^2 \left\| \nabla_{\theta_{y,z}}^2 \phi_{y,i} \right\|_F. \quad (129)$$

The tensor of the second partial derivative of $\phi_{y,i}$ with respect to $\theta_{y,z}$ is composed of blocks of the form $\frac{\partial^2 \phi_{y,i}}{\partial \text{vec}(W_z^{(p)}) \partial \text{vec}(W_z^{(q)})}$ for $p, q \in [k]$, $\frac{\partial^2 \phi_{y,i}}{\partial \text{vec}(a_z^{(p)}) \partial \text{vec}(W_z^{(q)})}$ for $p \in [k-1], q \in [k]$, $\frac{\partial^2 \phi_{y,i}}{\partial \text{vec}(a_z^{(p)}) \partial \text{vec}(a_z^{(q)})}$ for $p, q \in [k-1]$, and $\frac{\partial^2 \phi_{y,i}}{\partial \text{vec}(W_z^{(p)}) \partial \text{vec}(a_z^{(q)})}$ for $p \in [k]$ and $q \in [k-1]$. To bound the norm of the second partial derivatives of $\phi_{y,i}$, we must bound the norm of the first partial derivatives of $\phi_{y,i}$ with respect to its layer weights and its attention weights, respectively. By the triangle inequality,

$$\begin{aligned} \|\nabla_{\theta_{y,z}} \phi_{y,i}\|_F &\leq \sum_{q=0}^k \left\| \frac{\partial \phi_{y,i}}{\partial \text{vec}(W_z^{(q)})} \right\|_F \\ &+ \sum_{q=0}^{k-1} \left\| \frac{\partial \phi_{y,i}}{\partial \text{vec}(a_z^{(q)})} \right\|_F. \end{aligned} \quad (130)$$

Once again, the input of the GNN κ appears explicitly in (130) only for the term with $q = 0$, and all other terms will scale at an order less than or equal to the case when $q = 0$. Thus, we begin by quantifying how the Frobenius norm of the first derivative of the GAT with respect to its base layer weights scales according to the norm of the ensemble GAT input. Based on the fact that $\|\beta_{x,y}^{(z)}\|_F \leq 1$ for all $x, y \in V$ and all $z \in [k-1]$ and the use of a bounded search space in (27) and (39), we find that

$$\left\| \frac{\partial \beta_{m^{(1)}, m^{(0)}}^{(0)}}{\partial \text{vec}(W_z^{(0)})} \right\|_F \in \boldsymbol{\rho}^{(1)}, \quad (131)$$

holds for all $m^{(0)}, m^{(1)} \in V$. Then, by the use of activation functions with bounded first derivatives, (131), and the use of a bounded search space in (27) and (39),

$$\left\| \frac{\partial \phi_{m^{(1)}}^{(0)}}{\partial \text{vec}(W_z^{(0)})} \right\|_F \in \boldsymbol{\rho}^{(2)}, \quad (132)$$

holds for all $m^{(1)} \in V$.

Next, we examine the Frobenius norm of the partial derivative of $\beta_{m^{(2)}, m^{(0)}}^{(1)}$ with respect to $\text{vec}(W_z^{(0)})$. Based on the fact that $\|\beta_{x,y}^{(z)}\|_F \leq 1$ for all $x, y \in V$ and all $z \in [k-1]$, (132), and the use of a bounded search space in (27) and (39), we find that

$$\left\| \frac{\partial \beta_{m^{(2)}, m^{(1)}}^{(1)}}{\partial \text{vec}(W_z^{(0)})} \right\|_F \in \boldsymbol{\rho}^{(2)}, \quad (133)$$

holds for all $m^{(1)}, m^{(2)} \in V$. Then, for the Frobenius norm of the corresponding partial derivative of $\phi_{m^{(2)}}^{(1)}$ with respect to $\text{vec}(W_z^{(0)})$, we have

$$\left\| \frac{\partial \phi_{m^{(2)}}^{(1)}}{\partial \text{vec}(W_z^{(0)})} \right\|_F \in \boldsymbol{\rho}^{(3)}, \quad (134)$$

which holds for all holds for all $m^{(2)} \in V$. We repeat the analysis from (133) and (134) for each layer of the GAT, finding that $\left\| \frac{\partial \beta_{m^{(\ell+1)}, m^{(\ell)}}^{(\ell)}}{\partial \text{vec}(W_z^{(0)})} \right\|_F \in \boldsymbol{\rho}^{(\ell+1)}(\|\kappa\|)$ and $\left\| \frac{\partial \phi_{m^{(\ell+1)}}^{(\ell)}}{\partial \text{vec}(W_z^{(0)})} \right\|_F \in \boldsymbol{\rho}^{(\ell+2)}$ holds for $\ell = 0, 1, \dots, k-1$ and all $m^{(\ell)}, m^{(\ell+1)} \in V$. Then, we reach the outermost term, where

$$\begin{aligned} \left\| \frac{\partial \phi_{y,z}}{\partial \text{vec}(W_z^{(0)})} \right\|_F &= \left\| \frac{\partial}{\partial \text{vec}(W_z^{(0)})} W_z^{(k)} \Delta_{m^{(k)}}^{(k-1)} \right. \\ &\left. \left[\left(\Lambda_{m^{(k-1)}}^{(k-2)} \beta_{m^{(k)}, m^{(k-1)}}^{(k-1)} + \phi_{m^{(k-1)}}^{(k-2)} \Upsilon_{m^{(k)}, m^{(k-1)}}^{(k-1)} \right)^\top \right]^\top \right\|_F. \end{aligned}$$

Based on the use of bounded activation functions with bounded derivatives, the fact that $\|\beta_{x,y}^{(z)}\|_F \leq 1$ for all $x, y \in V$ and all $z \in [k-1]$, and the use of a bounded search space in (27) and (39), we find that

$$\left\| \frac{\partial \phi_{y,z}}{\partial \text{vec}(W_z^{(0)})} \right\|_F \in \boldsymbol{\rho}^{(k)}, \quad (135)$$

A structurally identical argument can be conducted to show that $\left\| \frac{\partial \phi_{y,z}}{\partial \text{vec}(a_z^{(0)})} \right\|_F \in \boldsymbol{\rho}^{(k)}$ and thus, $\|\nabla_{\theta_{y,z}} \phi_{y,i}\|_F \in \boldsymbol{\rho}^{(k)}$.

We now return to the scaling analysis of the second partial derivative of $\phi_{y,i}$ with respect to $\theta_{y,z}$. By the submultiplicity of the Frobenius norm and the triangle inequality,

$$\begin{aligned} \|\nabla_{\theta_{y,z}}^2 \phi_{y,i}\|_F &\leq \sum_{p=0}^k \sum_{q=0}^k \left\| \frac{\partial^2 \phi_{y,i}}{\partial \text{vec}(W_z^{(p)}) \partial \text{vec}(W_z^{(q)})} \right\|_F \\ &+ \sum_{p=0}^{k-1} \sum_{q=0}^k \left\| \frac{\partial^2 \phi_{y,i}}{\partial \text{vec}(a_z^{(p)}) \partial \text{vec}(W_z^{(q)})} \right\|_F \\ &+ \sum_{p=0}^{k-1} \sum_{q=0}^{k-1} \left\| \frac{\partial^2 \phi_{y,i}}{\partial \text{vec}(a_z^{(p)}) \partial \text{vec}(a_z^{(q)})} \right\|_F \\ &+ \sum_{p=0}^k \sum_{q=0}^{k-1} \left\| \frac{\partial^2 \phi_{y,i}}{\partial \text{vec}(W_z^{(p)}) \partial \text{vec}(a_z^{(q)})} \right\|_F. \end{aligned}$$

We first compute how the norm of the second partial derivative of $\phi_{y,i}$ with respect to $\text{vec}(W_z^{(p)})$ and $\text{vec}(W_z^{(q)})$ scales according to the norm of the ensemble GAT input $\|\kappa\|$. Once again, we consider the case in which $p = q = 0$, as all other cases will scale at a rate less than or equal to that of $p = q = 0$ with respect to $\|\kappa\|$. Based on (135) and the use of a bounded search space in (27) and (39), we find that

$$\left\| \frac{\partial^2 \beta_{m^{(1)}, m^{(0)}}^{(0)}}{\partial \text{vec}(W_z^{(0)}) \partial \text{vec}(W_z^{(0)})} \right\|_F \in \rho^{(k+1)}, \quad (136)$$

holds for all $m^{(0)}, m^{(1)} \in V$. Then, based on the use of bounded activation functions with bounded first and second derivatives, (135), (136), and the use of a bounded search space in (27) and (39),

$$\left\| \frac{\partial^2 \phi_{m^{(1)}}^{(0)}}{\partial \text{vec}(W_z^{(0)}) \partial \text{vec}(W_z^{(0)})} \right\|_F \in \rho^{(2k)}, \quad (137)$$

holds for all $m^{(1)} \in V$.

Next, we examine the norm of the partial derivative of $\Upsilon_{m^{(2)}, m^{(1)}}^{(1)}$ with respect to $\text{vec}(W_z^{(0)})$. Based on the use of bounded activation functions with bounded first and second derivatives, (135), (137), and the use of a bounded search space in (27) and (39),

$$\left\| \frac{\partial^2 \beta_{m^{(2)}, m^{(1)}}^{(1)}}{\partial \text{vec}(W_z^{(0)}) \partial \text{vec}(W_z^{(0)})} \right\|_F \in \rho^{(2k)}, \quad (138)$$

and

$$\left\| \frac{\partial^2 \phi_{m^{(2)}}^{(1)}}{\partial \text{vec}(W_z^{(0)}) \partial \text{vec}(W_z^{(0)})} \right\|_F \in \rho^{(2k)}, \quad (139)$$

holds for all $m^{(1)}, m^{(2)} \in V$. We repeat the analysis from (138) and (139) for each layer of the GAT, finding that

$$\left\| \frac{\partial^2 \beta_{m^{(\ell+1)}, m^{(\ell)}}^{(\ell)}}{\partial \text{vec}(W_z^{(0)}) \partial \text{vec}(W_z^{(0)})} \right\|_F \in \rho^{(2k)},$$

and

$$\left\| \frac{\partial^2 \phi_{m^{(\ell+1)}}^{(\ell)}}{\partial \text{vec}(W_z^{(0)}) \partial \text{vec}(W_z^{(0)})} \right\|_F \in \rho^{(2k)}$$

holds for $\ell = 0, 1, \dots, k-1$ and for all $m^{(\ell)}, m^{(\ell+1)} \in V$. Then, we reach the outermost term, where

$$\left\| \frac{\partial^2 \phi_{y,i}}{\partial \text{vec}(W_z^{(0)}) \partial \text{vec}(W_z^{(0)})} \right\|_F = \left\| \frac{\partial}{\partial \text{vec}(W_z^{(0)})} W_i^{(k)\top} \Delta_{m^{(k)}}^{(k-1)} \left[\left(\Lambda_{m^{(k-1)}}^{(k-2)} \beta_{m^{(k)}, m^{(k-1)}}^{(k-1)} + \phi_{m^{(k-1)}}^{(k-2)} \Upsilon_{m^{(k)}, m^{(k-1)}}^{(k-1)} \right)^\top \right]^\top \right\|_F.$$

Based on the use of bounded activation functions with bounded first and second derivatives, (135), and the use of a bounded search space in (27) and (39),

$$\left\| \frac{\partial^2 \phi_{y,i}}{\partial \text{vec}(W_z^{(0)}) \partial \text{vec}(W_z^{(0)})} \right\|_F \in \rho^{(2k)}.$$

Structurally identical arguments can be carried out to prove that $\left\| \frac{\partial^2 \phi_{y,i}}{\partial \text{vec}(a_z^{(0)}) \partial \text{vec}(W_z^{(0)})} \right\|_F \in \rho^{(2k)}$, $\left\| \frac{\partial^2 \phi_{y,i}}{\partial \text{vec}(a_z^{(0)}) \partial \text{vec}(a_z^{(0)})} \right\|_F \in \rho^{(2k)}$, and $\left\| \frac{\partial^2 \phi_{y,i}}{\partial \text{vec}(W_z^{(0)}) \partial \text{vec}(a_z^{(0)})} \right\|_F \in \rho^{(2k)}$, and thus,

$$\|\nabla_{\theta_{y,z}} \phi_{y,i}\|_F \in \rho^{(2k)}. \quad (140)$$

Additionally, since $\|T_{y,z}\| \leq \|\tilde{\theta}_{y,z}\|^2 \|\nabla_{\theta_{y,z}}^2 \phi_{y,i}\|_F$, then

$$\|T_{y,z}\| \leq \rho(\|\kappa\|) \|\tilde{\theta}_{y,z}\|^2,$$

where $\rho(\|\kappa\|)$ is a strictly increasing, polynomial of degree $2k$ in the norm of the ensemble GNN input $\|\kappa\|$, where k is the number of GAT layers. ■

REFERENCES

- [1] Y. LeCun, Y. Bengio, and G. Hinton, "Deep learning," *Nature*, vol. 521, no. 436444, 2015.
- [2] O. Patil, D. Le, M. Greene, and W. E. Dixon, "Lyapunov-derived control and adaptive update laws for inner and outer layer weights of a deep neural network," *IEEE Control Syst. Lett.*, vol. 6, pp. 1855–1860, 2022.
- [3] D. M. Le, O. S. Patil, C. Nino, and W. E. Dixon, "Accelerated gradient approach for neural network-based adaptive control of nonlinear systems," in *Proc. IEEE Conf. Decis. Control*, 2022, pp. 3475–3480.
- [4] O. S. Patil, D. M. Le, E. Griffis, and W. E. Dixon, "Deep residual neural network (ResNet)-based adaptive control: A Lyapunov-based approach," in *Proc. IEEE Conf. Decis. Control*, 2022, pp. 3487–3492.
- [5] E. Vacchini, N. Sacchi, G. P. Incremona, and A. Ferrara, "Design of a deep neural network-based integral sliding mode control for nonlinear systems under fully unknown dynamics," *IEEE Control Syst. Lett.*, 2023.
- [6] E. Griffis, O. Patil, Z. Bell, and W. E. Dixon, "Lyapunov-based long short-term memory (Lb-LSTM) neural network-based control," *IEEE Control Syst. Lett.*, vol. 7, pp. 2976–2981, 2023.
- [7] R. Hart, O. Patil, E. Griffis, and W. E. Dixon, "Deep Lyapunov-based physics-informed neural networks (DeLb-PINN) for adaptive control design," in *Proc. IEEE Conf. Decis. Control*, 2023, pp. 1511–1516.
- [8] I. Ganie and S. Jagannathan, "Lifelong reinforcement learning tracking control of nonlinear strict-feedback systems using multilayer neural networks with constraints," *Neurocomputing*, vol. 600, p. 128139, 2024.
- [9] D. M. Le, O. S. Patil, C. F. Nino, and W. E. Dixon, "Accelerated gradient approach for deep neural network-based adaptive control of unknown nonlinear systems," *IEEE Trans. Neural Netw. Learn. Syst.*, 2024.
- [10] O. S. Patil, E. J. Griffis, W. A. Makumi, and W. E. Dixon, "Composite adaptive Lyapunov-based deep neural network (Lb-DNN) controller," *arXiv preprint arXiv:1306.3432*, 2023.
- [11] H. Lu, J. Wu, and W. Wang, "Adaptive deep neural network optimized control for a class of nonlinear strict-feedback systems with prescribed performance," *Int. J. Adapt. Control Signal Process.*, pp. 1–24, 2024.
- [12] J. Wu, H. Lu, and W. Wang, "Adaptive deep neural network optimized backstepping control for a class of nonlinear strict-feedback systems," *Int. Conf. Intell. Control Inf. Process.*, pp. 172–181, 2024.
- [13] J. Mei, H. Jian, Y. Li, W. Wang, and D. Lin, "Deep neural networks-based output-dependent intermittent control for a class of uncertain nonlinear systems," *Chaos Solitons Fractals*, vol. 185, p. 114999, 2024.
- [14] W. Makumi, Z. Bell, and W. E. Dixon, "Approximate optimal indirect regulation of an unknown agent with a Lyapunov-based deep neural network," *IEEE Control Syst. Lett.*, vol. 7, pp. 2773–2778, 2023.
- [15] M. Ryu and K. Choi, "CNN-based end-to-end adaptive controller with stability guarantees," *arXiv preprint arXiv:2403.03499*, 2024.
- [16] H. M. Sweatland, O. S. Patil, and W. E. Dixon, "Adaptive deep neural network-based control barrier functions," *arXiv preprint arXiv:2406.14430*, 2024.
- [17] S. Li and C. C. Cheah, "An analytic end-to-end collaborative deep learning algorithm," *IEEE Control Syst. Lett.*, vol. 7, pp. 3024–3029, 2023.
- [18] S. Li, H. T. Nguyen, and C. C. Cheah, "A theoretical framework for end-to-end learning of deep neural networks with applications to robotics," *IEEE Access*, vol. 11, pp. 21992–22006, 2023.
- [19] L. Cheng, Z.-G. Hou, M. Tan, Y. Lin, and W. Zhang, "Neural network-based adaptive leader-following control for multiagent systems with uncertainties," *IEEE Trans. Neural Netw.*, vol. 21, no. 8, pp. 1351–1358, 2010.

- [20] D. Chen, X. Liu, W. Yu, L. Zhu, and Q. Tang, "Neural-network based adaptive self-triggered consensus of nonlinear multi-agent systems with sensor saturation," *IEEE Trans. Netw. Sci. Eng.*, vol. 8, no. 2, pp. 1531–1541, 2021.
- [21] P. Wang, H. Tian, D. Huang, and T. Huang, "A continuous neural network adaptive controller for consensus of uncertain multi-agent systems," *IEEE Trans. Emerg. Top. Comput. Intell.*, vol. 8, no. 2, pp. 1280–1289, 2024.
- [22] W. L. Hamilton, *Graph Representation Learning*. Morgan & Claypool Publishers, 2020.
- [23] S. Hochreiter and J. Schmidhuber, "Long short-term memory," *Neural computation*, vol. 9, pp. 1735–80, 12 1997.
- [24] A. Vaswani, N. Shazeer, N. Parmar, J. Uszkoreit, L. Jones, A. N. Gomez, L. Kaiser, and I. Polosukhin, "Attention is all you need," in *Adv. Neural Inf. Process. Syst.*, I. Guyon, U. V. Luxburg, S. Bengio, H. Wallach, R. Fergus, S. Vishwanathan, and R. Garnett, Eds., vol. 30, 2017.
- [25] F. Scarselli, M. Gori, A. C. Tsoi, M. Hagenbuchner, and G. Monfardini, "The graph neural network model," *IEEE Trans. Neural Netw.*, vol. 20, no. 1, pp. 61–80, 2008.
- [26] P. Veličković, G. Cucurull, A. Casanova, A. Romero, P. Lio, and Y. Bengio, "Graph attention networks," *Int. Conf. Learn. Represent.*, 2018.
- [27] S. Xiao, S. Wang, Y. Dai, and W. Guo, "Graph neural networks in node classification: survey and evaluation," *Mach. Vis. Appl.*, vol. 33, no. 1, p. 4, 2022.
- [28] F. Errica, M. Podda, D. Bacciu, and A. Micheli, "A fair comparison of graph neural networks for graph classification," in *Int. Conf. Learn. Represent.*, 2020.
- [29] M. Zhang and Y. Chen, "Link prediction based on graph neural networks," in *Adv. Neural Inf. Process. Syst.*, S. Bengio, H. Wallach, H. Larochelle, K. Grauman, N. Cesa-Bianchi, and R. Garnett, Eds., vol. 31. Curran Associates, Inc., 2018.
- [30] F. Gama, E. Tolstaya, and A. Ribeiro, "Graph neural networks for decentralized controllers," *IEEE Int. Conf. Acoust. Speech Signal Process.*, pp. 5260–5264, 2021.
- [31] Q. Li, F. Gama, A. Ribeiro, and A. Prorok, "Graph neural networks for decentralized multi-robot path planning," *Int. Conf. Intell. Robot. Syst.*, pp. 11 785–11 792, 2020.
- [32] S. Muthusamy, D. Owerko, C. I. Kanatsoulis, S. Agarwal, and A. Ribeiro, "Generalizability of graph neural networks for decentralized unlabeled motion planning," *arXiv preprint arXiv:2409.19829*, 2024.
- [33] E. S. Lee, L. Zhou, A. Ribeiro, and V. Kumar, "Graph neural networks for decentralized multi-agent perimeter defense," *Front. Control Eng.*, vol. 4, 2023.
- [34] S. Chen, J. Dong, P. Ha, Y. Li, and S. Labi, "Graph neural network and reinforcement learning for multi-agent cooperative control of connected autonomous vehicles," *Comput.-Aided Civ. Infrastruct. Eng.*, vol. 36, no. 7, pp. 838–857, 2021.
- [35] H. Riess, M. Veveakis, and M. M. Zavlanos, "Path signatures and graph neural networks for slow earthquake analysis: better together?" *arXiv preprint arXiv:2402.03558*, 2024.
- [36] L. Zhou, V. D. Sharma, Q. Li, A. Prorok, A. Ribeiro, P. Tokekar, and V. Kumar, "Graph neural networks for decentralized multi-robot target tracking," in *IEEE Int. Symp. Saf. Secur. Rescue Robot.*, 2022, pp. 195–202.
- [37] Z. Peng, D. Wang, H. Zhang, and G. Sun, "Distributed neural network control for adaptive synchronization of uncertain dynamical multiagent systems," *IEEE Trans. Neural Netw. Learn. Syst.*, vol. 25, no. 8, pp. 1508–1519, 2013.
- [38] A. Raj, S. Jagannathan, and T. Yucelen, "Distributed adaptive state estimation and tracking scheme for nonlinear systems using active passive sensor networks," *Am. Control Conf.*, pp. 2587–2592, 2020.
- [39] K. Aryankia and R. R. Selmic, "Neural network-based formation control with target tracking for second-order nonlinear multiagent systems," *IEEE Trans. Aerosp. Electron. Syst.*, vol. 58, no. 1, pp. 328–341, 2021.
- [40] C. F. Nino, O. S. Patil, S. C. Edwards, Z. I. Bell, and W. E. Dixon, "Distributed target tracking under partial feedback using Lyapunov-based deep neural networks," *Proc. IEEE Conf. Decis. Control*, 2025.
- [41] D. S. Bernstein, *Matrix Mathematics*. Princeton University Press, 2009.
- [42] M. Krstic, I. Kanellakopoulos, and P. V. Kokotovic, *Nonlinear and Adaptive Control Design*. New York: John Wiley & Sons, 1995.
- [43] W. Azizian and M. Lelarge, "Expressive power of invariant and equivariant graph neural networks," *Proc. Int. Conf. Learn. Represent.*, 2020.
- [44] C. Merkwirth and T. Lengauer, "Automatic generation of complementary descriptors with molecular graph networks," *J. Chem. Inf. Model.*, vol. 45, no. 5, pp. 1159–1168, 2005.
- [45] Y. Zeng and J. Tang, "RLC-GNN: An improved deep architecture for spatial-based graph neural network with application to fraud detection," *Appl. Sci.*, vol. 11, no. 12, p. 5656, 2021.
- [46] F. Zegers, P. Deptula, J. Shea, and W. E. Dixon, "Event/self-triggered approximate leader-follower consensus with resilience to byzantine adversaries," *IEEE Trans. Autom. Control*, vol. 67, no. 3, pp. 1356–1370, Mar. 2022.
- [47] I. Goodfellow, Y. Bengio, A. Courville, and Y. Bengio, *Deep Learning*. MIT press Cambridge, 2016, vol. 1.
- [48] P. Fitzpatrick, *Advanced Calculus*. American Mathematical Society, 2009, vol. 5.
- [49] Z. Qu, *Cooperative Control of Dynamical Systems: Applications to Autonomous Vehicles*. New York: Springer-Verlag, 2009.
- [50] E. A. Coddington and N. Levinson, *Theory of Ordinary Differential Equations*. McGraw-Hill, 1955.
- [51] H. K. Khalil, *Nonlinear Systems*, 3rd ed. Prentice Hall, 2002.
- [52] K. Y. Pettersen, "Lyapunov sufficient conditions for uniform semiglobal exponential stability," *Automatica*, vol. 78, pp. 97–102, 2017.
- [53] S. Belhaiza, N. M. M. De Abreu, P. Hansen, and C. S. Oliveira, "Variable neighborhood search for extremal graphs. XI. bounds on algebraic connectivity," in *Graph Theory Comb. Optim.* Springer, 2005, pp. 1–16.
- [54] Y. Nakatsukasa, "Off-diagonal perturbation, first-order approximation and quadratic residual bounds for matrix eigenvalue problems," in *Algorithms Softw. Appl. Petascale Comput.* Springer, 2017, pp. 233–249.
- [55] W.-C. Yueh, "Eigenvalues of several tridiagonal matrices," *Appl. Math.*, vol. 5, pp. 66–74, 2005.
- [56] R. A. Horn and C. R. Johnson, *Topics in Matrix Analysis*. Cambridge University Press, 1991.
- [57] W. N. Anderson and T. D. Morley, "Eigenvalues of the Laplacian of a Graph," *Linear Multilinear Algebra*, vol. 18, no. 2, pp. 141–145, 1985.



Brandon Fallin received his Bachelor of Science degree in Aerospace Engineering at the University of Florida in May 2022. He subsequently earned his Master of Science degree in Aerospace Engineering, also from the University of Florida. He is currently pursuing a Ph.D. in Aerospace Engineering at the University of Florida under the supervision of Dr. Warren Dixon. His research interests include privacy and obfuscation with application to nonlinear control systems.



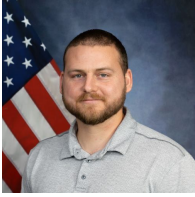
Cristian F. Nino received the B.S. degrees in Mathematics and Mechanical Engineering from the University of Florida, Gainesville, FL, USA. He subsequently earned the M.S. degree in Mechanical Engineering, also from the University of Florida, with a focus on control systems. He is currently pursuing the Ph.D. degree in Mechanical Engineering at the University of Florida under the guidance of Dr. Warren Dixon. Mr. Nino is a recipient of the SMART Scholarship, the NSF Fellowship, and the Machen Florida Opportunity Scholarship. His

research interests include robust adaptive nonlinear control, multi-agent target tracking, distributed state estimation, reinforcement learning, Lyapunov-based deep learning, and geometric mechanics and control.



Omkar Sudhir Patil received his Bachelor of Technology (B.Tech.) degree in production and industrial engineering from Indian Institute of Technology (IIT) Delhi in 2018, where he was honored with the BOSS award for his outstanding bachelor's thesis project. In 2019, he joined the Nonlinear Controls and Robotics (NCR) Laboratory at the University of Florida under the guidance of Dr. Warren Dixon to pursue his doctoral studies. Omkar received his Master of Science (M.S.) degree in mechanical engineering in 2022 and Ph.D. in mechanical engineering

in 2023 from the University of Florida. During his Ph.D. studies, he was awarded the Graduate Student Research Award for outstanding research. In 2023, he started working as a postdoctoral research associate at NCR Laboratory, University of Florida. His research focuses on the development and application of innovative Lyapunov-based nonlinear, robust, and adaptive control techniques.



Zachary I. Bell received his Ph.D. from the University of Florida in 2019 and is a researcher for the Air Force Research Lab. His research focuses on cooperative guidance and control, computer vision, adaptive control, and reinforcement learning.



Prof. Warren Dixon received his Ph.D. in 2000 from the Department of Electrical and Computer Engineering from Clemson University. He worked as a research staff member and Eugene P. Wigner Fellow at Oak Ridge National Laboratory (ORNL) until 2004, when he joined the University of Florida in the Mechanical and Aerospace Engineering Department. His main research interest has been the development and application of Lyapunov-based control techniques for uncertain nonlinear systems. His work has been recognized by the 2019 IEEE Control

Systems Technology Award, (2017-2018 & 2012-2013) University of Florida College of Engineering Doctoral Dissertation Mentoring Award, 2015 & 2009 American Automatic Control Council (AACC) O. Hugo Schuck (Best Paper) Award, the 2013 Fred Ellersick Award for Best Overall MILCOM Paper, the 2011 American Society of Mechanical Engineers (ASME) Dynamics Systems and Control Division Outstanding Young Investigator Award, the 2006 IEEE Robotics and Automation Society (RAS) Early Academic Career Award, an NSF CAREER Award (2006-2011), the 2004 Department of Energy Outstanding Mentor Award, and the 2001 ORNL Early Career Award for Engineering Achievement. He is an ASME Fellow (2016) and IEEE Fellow (2016), was an IEEE Control Systems Society (CSS) Distinguished Lecturer (2013-2018), served as the Director of Operations for the Executive Committee of the IEEE CSS Board of Governors (BOG) (2012-2015), and served as an elected member of the IEEE CSS BOG (2019-2020). His technical contributions and service to the IEEE CSS were recognized by the IEEE CSS Distinguished Member Award (2020). He was awarded the Air Force Commander's Public Service Award (2016) for his contributions to the U.S. Air Force Science Advisory Board. He is currently or formerly an associate editor for ASME Journal of Journal of Dynamic Systems, Measurement and Control, Automatica, IEEE Control Systems, IEEE Transactions on Systems Man and Cybernetics: Part B Cybernetics, and the International Journal of Robust and Nonlinear Control.